Electrochemical Micro- and Nanostructuring by Cathodic Deposition on Solid Electrolytes

Fachbereich Biologie und Chemie
Justus-Liebig-Universität Gießen

zur Erlangung des
Doktorgrades der Naturwissenschaften
- Dr. rer. nat. -

genehmigte
Dissertation
von

Dipl.-Chem. Klaus Peppler
geboren am 26. Dezember 1977 in Gießen

Gießen 2009

Dean / Dekan	Prof. Dr. Volkmar Wolters
1st Reviewer / 1. Gutachter	Prof. Dr. Jürgen Janek
2nd Reviewer / 2. Gutachter	Prof. Dr. Herbert Over

submitted 8th April 2009 / eingereicht 8. April 2009
day of oral defense (viva voce) 13th July 2009 / Tag der mündlichen Prüfung 13. Juli 2009
published / veröffentlicht in Gießener Elektronische Bibliothek (GEB)

This thesis was prepared in the period of 1st January 2004 to 8th April 2009 at the Institute of Physical Chemistry of the Justus-Liebig-University Giessen under the supervision and guidance of Prof. Dr. Jürgen Janek. The preparation of this Ph. D. Thesis, experimentally and theoretically, is my own work. Except the advices in the context of the supervision I have not used other sources or assistances than the ones referred to.

Die vorliegende Arbeit wurde im Zeitraum vom 1. Januar 2004 bis zum 8. April 2009 am Physikalisch-Chemischen Institut der Justus-Liebig-Universität Gießen unter Betreuung von Prof. Dr. Jürgen Janek angefertigt. Hiermit erkläre ich, dass die vorgelegte Dissertation im experimentellen und theoretischen Teil selbstständig angefertigt wurde und außer den Ratschlägen im Rahmen der Betreuung keine anderen als in der Arbeit angegebenen Quellen und Hilfsmittel verwendet wurden.

This picture is a scanning electron microscopic image of non-equilibrium silver sulfide structures grown during the reaction of silversulfide with sulfur (details see chapter 2.3.1).

Danksagung

Mein Dank geht zuerst an meine Eltern, die mir das Chemiestudium finanziell ermöglich haben und somit den Grundstein zu dieser Dissertation gelegt haben.

Bei Prof. Jürgen Janek bedanke ich mich für die sehr interessante Themenstellung und die Möglichkeit, diese mit dem nötigen Freiraum eigenständig zu bearbeiten. Auch bin ich für seine zahlreichen Anregungen und Hinweise dankbar. Die Ermunterung zur Teilnahme an verschiedenen nationalen und internationalen Tagungen möchte ich auch dankend erwähnen. Diese Tagungsteilnahmen haben z. T. für einen anderen Blickwinkel auf meine Arbeit gesorgt, eine Erfahrung, die ich nicht missen möchte.

Ebenso möchte ich mich bei Prof. Herbert Over bedanken für die Übernahme des Koreferats.

Dr. Bjoern Luerßen danke ich für seine stets vorhandene Hilfsbereitschaft. Vor allem danke ich ihm für das Korrekturlesen von großen Teilen dieser Arbeit und seine Anmerkungen dazu.

Bei Dr. Ilia Valov möchte ich mich für die vielen Diskussionen zu Beginn meiner Arbeit bedanken. Sie haben mir den Einstieg in die Materie erleichtert.

Zuletzt möchte ich mich auch noch bei allen Mitarbeiterinnen und Mitarbeitern der Arbeitsgruppe von Prof. Janek bedanken, es war eine angenehme Zeit am Physikalisch-Chemischen Institut.

Zusammenfassung

In der vorliegenden Arbeit wurde der Einfluss experimenteller Parameter (Temperatur, Stromdichte, Kathodengeometrie, Elektrolytgeometrie) auf die kathodische Abscheidung von Silber auf festen Silberelektrolyten untersucht. Hierzu wurden zwei Überführungszellen (−)Ag|AgBr(Einkristall)|Ag(+) und (−)Ag|Ag_2S(polykristallin)|Ag(+) in verschiedenen Konfigurationen verwendet. Bei diesen elektrochemischen Zellen handelt es sich um relativ einfache Modellsysteme. Die Verwendung von einkristallinem Silberbromid hat mehrere Vorteile: Zum einen ist es stabil unter normalen Laborbedingungen, auch einige Zeit gegen die Einwirkung von Licht. Zum anderen ist seine elektronische Leitfähigkeit vernachlässigbar klein, d. h. es ist bei höheren Temperaturen nahezu ein reiner Kationenleiter. Somit wird eine elektronischer Strom an der Ag|AgBr-Grenzfläche (fast) vollständig in einen Silberionenstrom umgewandelt. Die Überführungszelle vom Typ (−)Ag|Ag_2S(polykristallin)|Ag(+) wurde verwendet, um den Elektrolyten in ein Templat einzubringen. Silbersulfid hat den Vorteil, dass es relativ einfach herzustellen ist und somit ein Befüllen von Poren ohne großen Aufwand möglich ist. Es hat jedoch den Nachteil, dass es ein gemischter Leiter mit elektronischer und ionischer Leitfähigkeit ist. Im Gleichgewicht mit Silber (was in einer elektrochemischen Zelle mit Silberelektroden bei höheren Temperaturen der Fall ist) ist die Überführungszahl für Elektronen wesentlich größer als die für Silberionen. Deshalb wird an der Phasengrenze Ag|Ag_2S nur ein kleiner Teil des elektrischen Stroms in einen Silberionenstrom überführt.

Im Wesentlichen ist diese Arbeit aus drei Teilen zusammengesetzt:

In Kapitel 2.1 (Seite 27) wird die kathodische Abscheidung von Silber an Mikroelektroden auf festem Silberbromid abgehandelt. Um eine konstante Abscheidungsrate von Silber zu gewährleisten, wurden die Experimente unter galvanostatischen Bedingungen durchgeführt. Es konnten zwei unterschiedliche Morphologien beobachtet werden: Bei „niedrigen“ Stromdichten ($j < 0{,}1$ A/cm^2; $I < 0{,}5$ µA, d(Ag-Mikroelektrode) = 25 µm) wurde ein Wachstum in die Höhe (d. h. senkrecht zur Elektrolytoberfläche) in Form von Silberwhiskern beobachtet. Die Mikroelektroden, die aus flexiblen Silberdrähten bestanden, wurden dabei von den wachsenden Whiskern nach oben weggedrückt. Bei „hohen“ Stromdichten ($j > 0{,}6$ A/cm^2; $I > 3{,}0$ µA, d(Ag-Mikroelektrode) = 25 µm) wurde ein Wachstum parallel zur Oberfläche in Form von Dendriten beobachtet. Eine Änderung der Temperatur hatte eine beachtliche Änderung der Morphologie zur Folge. Der Durchmesser der Whisker nahm bei einer Temperaturerniedrigung von $\theta = 300$ °C zu $\theta = 150$ °C von wenigen Mikrometern auf einige Hundert Nanometer ab. Im Fall der Dendri-

ten wurde eine Änderung von isotropem zu anisotropem Wachstum bevorzugt in zwei Raumrichtungen (vermutlich entlang ausgewiesener kristallographischer Ausrichtungen des Elektrolyten) beobachtet. Diese Temperaturabhängigkeit kann mit der Nukleationsrate in Zusammenhang gebracht werden.

In Kapitel 2.2 (Seite 43) wird über die Stabilität von elektronisch (aber nicht ionisch) isolierten Metallpartikeln, die sich in einem externen elektrischen Feld befinden, berichtet. In den letzten Jahren wurden neue Ansätze für zukünftige Speichermedien basierend auf Konzepten der Festkörperelektrochemie verfolgt. So wurde z. B. das Hin- und Herschalten zwischen zwei Zuständen mit unterschiedlich hohen Widerständen durch das Abscheiden und Auflösen von Metallen in oder auf Festelektrolyten untersucht. Hierbei spielt also die Stabilität des abgeschiedenen Metalls eine wichtige Rolle für die Erhaltung der gespeicherten Daten. Es konnte gezeigt werden, dass sich elektronisch (aber nicht ionisch) isolierte Silberpartikel auf einem festen Silberionenleiter wie bipolare Elektroden verhielten, wenn ein externes elektrisches Feld angelegt wird. Folglich wurden sie an ihrer anodischen Seite aufgelöst, und an ihrer kathodischen Seite wurde Silber abgeschieden. Die Abscheidung erfolgte dabei in keiner der bisher beobachteten Morphologien, sondern in Form von dünnen Silberfilmen, also weder in Form von Whiskern noch Dendriten.

In Kapitel 2.3 (Seite 49) wird über die Abscheidung von Silber in Form von Silberdrähten mit vorgegebenem Durchmesser berichtet. Wie schon berichtet erhält man bei der Abscheidung von Silber an Mikroelektroden auf Silberbromid Whisker mit unterschiedlichen Durchmessern in Abhängigkeit der experimentellen Parameter. Allerdings konnte im Vorfeld nicht vorhergesagt werden, welchen Durchmesser die Whisker haben werden. Um Silbermikrodrähte (d. h. Whisker) mit vorgegebenen Durchmessern zu erhalten, ist es deshalb nötig, den Elektrolyten in ein Templat mit geraden zylindrischen Poren einzubetten. Dadurch wird die Abscheidung von Silber räumlich begrenzt und die Silberdrähte haben den gleichen Durchmesser wie die Poren. Als Template wurden poröses Aluminiumoxid und poröses Silizium verwendet. Die Poren wurden durch eine einfache chemische Reaktion zwischen Silber und Schwefel gefüllt, die dazu führt, dass sich das Silbersulfid in den Poren abscheidet.

Abgeschlossen wird diese Arbeit mit einer Einordnung der eigenen Ergebnisse (Kapitel 3.1, Seite 59) und einem Ausblick (Kapitel 3.2, Seite 91).

Contents

1 Introduction

1.1 Motivation

In the present work the "electrochemical micro- and nanostructuring by cathodic deposition on solid electrolytes" is investigated. The understanding of how experimental parameters (i. e. temperature, current density, electrode geometry, preparation of samples, etc.) influence the morphology of the metal deposition is sought.

1.1.1 Electrochemical Micro- and Nanostructuring

In the 1970ies Ohachi and Taniguchi [Ohachi1972, Ohachi1974a, Ohachi1974b] and Corish et al. [Corish1972, Corish1978] reported on the growth of fine silver filaments from silver chalcogenides by supersaturation. The cathodic deposition of silver in form of whiskers from solid silver iodide is also briefly mentioned in a contribution to the anodic dissolution of silver at the Ag|AgI interface by Janek and Majoni [Majoni1995]. From following work in the research group of Prof. Janek by Best [Best2001] and Sickenius [Sickenius2003] (see also Rohnke et. al [Rohnke2005]) it is well known that the cathodic deposition of silver from solid silver ion conductors at spatially extended planar electrodes leads to the formation of arrays of silver whiskers, see fig. (1.1).

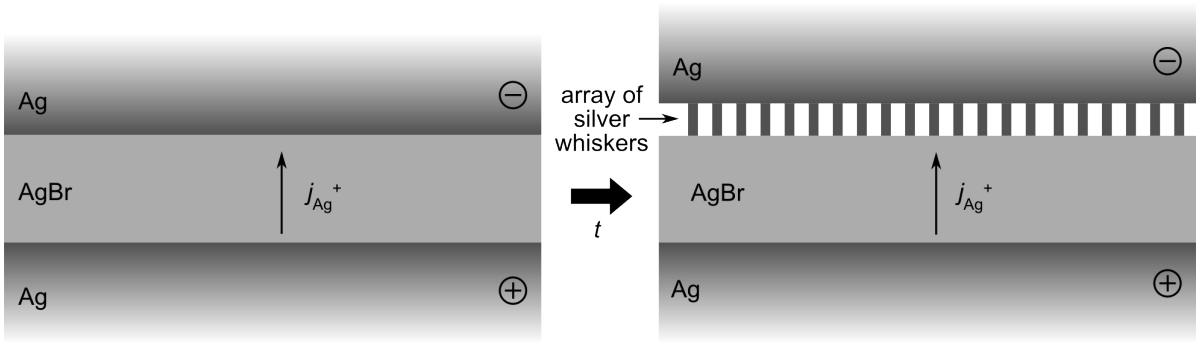

Figure 1.1: Sketch of a cross section through a Ag|AgBr|Ag electrochemical cell: Cathodic deposition of silver from solid silver ion conductors at spatially extended planar electrodes as cathodes results in the formation of arrays of silver whiskers

Starting from this knowledge the question is what happens when microelectrodes instead of spatially extended electrodes are employed as cathodes, i. e. when the electrode geometry is changed. Is it possible to obtain single silver whiskers instead of arrays of whiskers? Are there other morphologies to appear? Concerning the question of the influence of electrode geometry on deposition morhology works from Spangenberg et al. [Spangenberg2001a, Spangenberg2001b] and Schroeder [Schroeder2004] showed that at rigid tungsten microelectrodes as cathodes on silver chloride crystal surfaces deposition in form of dendrites occurred under potentiostatic conditions.

1.1.2 Cathodic Metal Deposition at Solid|Solid Interfaces

Cathodic metal deposition is one of the most important electrochemical processes. It plays a central role in a number of technological processes. But, whereas the electrodeposition at solid|liquid interfaces was intensively studied during the last century, the electrodeposition at solid|solid interfaces is still insufficiently investigated. The investigation of the electrochemistry at solid|solid interfaces started some 30 to 40 years ago. Early works are from Armstrong and co-workers [Armstrong1971, Armstrong1973, Armstrong1975]. But these interfaces have been rarely studied with respect to mechanistic aspects.

Several reasons may be considered to explain the lack of fundamental data. Obviously, there has simply been less time compared to the investigation of solid|liquid interfaces. The number of solid|solid interfaces which can be investigated concerning the cathodic metal deposition is limited because only few cation conducting solid materials with sufficient chemical stability exist. The preparation of well defined model solid|solid interfaces is complicated. For instance, at solid|liquid interfaces only the electrode surface has to be prepared because the liquid electrolyte adapts to the surface. Whereas at solid|solid interfaces the roughness of the electrode leads to bad contact with the solid electrolyte. Thus, in reality the real contact area at solid|solid interfaces prepared by mechanical contacting is always smaller than the apparent (or geometrical) contact area.[1] Even when electrode and electrolyte surfaces are both atomically smooth, the interfacial properties depend on the crystallographic details, i. e. on the degree of coherency of both lattices. Upon electrodeposition formation of nucleii might lead to a separation of the electrode and the electrolyte, depending on their mechanical properties and the applied mechanical load (pressure). Thus, the contact area is altered during experiments. So there are many problems at solid|solid interfaces which hinder the measurement of reproducible and quantitative data.

In order to investigate fundamental processes at solid|solid interfaces it is therefore necessary to use simple and well defined model systems, for instance, the employment of single crystals as solid electrolytes to get well defined surfaces without grain boundaries.

[1] This is exactly the other way around as for solid|liquid interfaces. In case of a rough surface of the electrode the real contact area is always greater then the apparent one because the solid electrode is normally wetted completely by the liquid electrolyte.

An introduction to the electrodeposition of metals at all possible interfaces between solid, liquid and gaseous phases is given in the article "*Electrodeposition of Metals for Micro- and Nanostructuring at Interfaces between Solid, Liquid and Gaseous Conductors: Dendrites, Whiskers and Nanoparticles*" (chapter 1.1.4) published in "*Zeitschrift für Physikalische Chemie*" [Peppler2006a][2] which concludes this introduction.

1.1.3 Structure of the Present Thesis

The experimental part of this thesis is divided into three main parts. The core of each part is based on published articles or manuscripts. They are always briefly put in a wider context. In case of collaborative work, the contribution of the author of this thesis is pointed out. Some topics are augmented by short subsections of supplementary information or discussions of additional aspects.

The first part is based on the article "*Cathodic Deposition of Silver on Silver Bromide at Microelectrodes*" (chapter 2.1.2, page 27) published in "*Solid State Ionics*" [Peppler2006b][2]. In this section the influence of the experimental parameters (temperature, current density, electrode geometry, preparation of samples, etc.) on the evolving morphology during cathodic silver metal deposition is described.

The second part deals with the stability of electronically but not ionically isolated metal particles on solid cation conductors in external electric fields and is based on the article "*Field-driven Migration of Bipolar Metal Particles on Solid Electrolytes*" (chapter 2.2.1, page 43) published in "*Applied Physics Letters*" [Peppler2008][2]. The migration of these particles in external electric fields is described.

The third part deals with the formation of silver micro- and nanowires with predefined diameters and is based on the article "*Template assisted Solid State Electrochemical Growth of Silver Micro- and Nanowires*" (chapter 2.3.1, page 43) published in "*Electrochimica Acta*" [Peppler2007][2]. The basic concept is the spatial confinement of a solid electrolyte into the pores of a given template with straight cylindrical pores throughout the material. Thus, cathodic deposition leads to the growth of silver wires with the diameter of the pores because the formation of other morphologies (like dendrites) is hindered (even at high current densities).

1.1.4 Article: Electrodeposition of Metals for Micro- and Nanostructuring at Interfaces between solid, liquid and gaseous Conductors: Dendrites, Whiskers and Nanoparticles [Peppler2006a]

This article is a joint paper with Manuel Pölleth, Sebastian Meiß, Marcus Rohnke and Jürgen Janek. My contribution to this article are partly found in sections "1. Introduction", "2.1 Theoretical aspects" and "3. Discussion and conclusions". Sections "2.2

[2]Reprinted with permission of the respective journals.

Solid|liquid interfaces" and "2.3 Solid|solid interfaces" were written by myself and co-edited by the other authors.

Reprinted with permission from K. Peppler, M. Pölleth, S. Meiss, M. Rohnke, J. Janek, Electrodeposition of Metals for Micro- and Nanostructuring at Interfaces between solid, liquid and gaseous Conductors: Dendrites, Whiskers and Nanoparticles, Zeitschrift für Physikalische Chemie, Vol. 220, Page 1507, 2006, Oldenbourg Wissenschaftsverlag.

Synopsis

The following article is a review on the electrodeposition of metals at all possible types of interfaces, i. e. solid|solid, solid|liquid, solid|gas (plasma), liquid|gas (plasma) and liquid|liquid. According to the background of the authors the solid|solid interface is discussed in much more depth than the other interfaces. Examples from own work are also provided, cf. figs. 4 and 5. An experiment concerning an internal electrochemical reaction between two phases with different ionic transference numbers has been carried out especially for this article, cf. figs. 6 and 7.

Z. Phys. Chem. **220** (2006) 1507–1527 / **DOI** 10.1524/zpch.2006.220.10.1507

Electrodeposition of Metals for Micro- and Nanostructuring at Interfaces between Solid, Liquid and Gaseous Conductors: Dendrites, Whiskers and Nanoparticles

By Klaus Peppler, Manuel Pölleth, Sebastian Meiss, Marcus Rohnke, and Jürgen Janek*

Institute of Physical Chemistry, Heinrich-Buff-Ring 58, D-35392 Gießen, Germany

(Received August 8, 2006; accepted September 6, 2006)

Electrodeposition / Electrode Processes / Interfaces / Cathodes / Cathodic Reduction

Electrodeposition of a metal requires the reduction of metal ions by electrons and can in principle occur at any interface or in any boundary region between two electrically conducting phases with different ionic transference numbers. Here we summarize and review metal deposition at all possible five interfaces: solid|solid (short s|s), liquid|liquid (l|l), solid|liquid (s|l), solid|gas (s|g), liquid|gas (l|g), emphasizing processes at less studied interfaces. Cathodic deposition of a metal from a liquid electrolyte (s|l interface) is the most typical case and forms the basis of numerous applied galvanic processes. The equivalent deposition of a metal on a solid electrolyte (s|s interface) is much less usual, but phenomenologically identical. The deposition processes of a metal at the interface between two liquid electrolytes, or between a gaseous conductor and either a solid or a liquid conductor form three other possible situations. Examples for these five general cases (the s|l interface is only briefly treated) are reviewed and discussed with respect to the growth kinetics and the product morphology. Nano-sized memory devices, switches, electron beam induced formation of metals on solid electrolytes and plasma-cathodic metal deposition from ionic liquids, where in the first place the very low vapour pressure of ionic liquids facilitates the application of low-temperature plasmas, are discussed as possible new and unusual applications of electrochemical metal deposition.

1. Introduction

The electrodeposition of a metal is one of the most important electrochemical processes and plays a crucial role in a number of well established technological

* Corresponding author. E-mail: juergen.janek@phys.chemie.uni-giessen.de

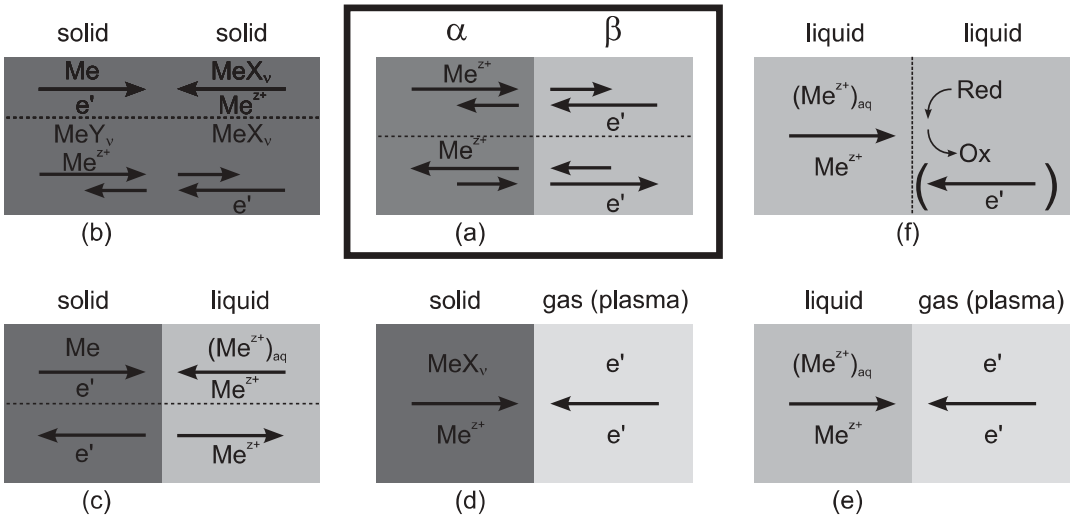

Fig. 1. Electrochemical deposition of a metal at different interfaces. (a) General case of metal deposition/dissolution at an interface $\alpha \mid \beta$; (b) solid|solid interface, *e.g.* metal|solid electrolyte or solid electrolyte 1|solid electrolyte 2; (c) conventional metal|liquid electrolyte interface; (d) solid electrolyte|gas(plasma) interface; (e) liquid electrolyte|gas (plasma) interface; (f) interface between two immiscible liquid electrolytes.

processes. A classical application concerns the electrolytic deposition of precious or protecting metals on solid surfaces. More recent applications deal with the deposition of nanoscale metals or alloys for preparative purpose, the cyclic deposition of lithium in rechargeable batteries [1–4] or of other metals in solid electrolyte capacitors. In many of these cases the metal is deposited on a solid electrode from a liquid electrolyte, and thus, driven by its practical relevance the cathodic deposition of a metal from a liquid electrolyte is also experimentally and theoretically well investigated. However, the cathodic deposition under less conventional conditions – *e.g.* on solid electrolytes or at l|l interfaces – appears to play an increasing role in nanotechnology. For example, Terabe *et al.* developed nano-sized switches on the basis of metal nuclei formation on silver sulfide solid electrolytes [5–7], and Sone *et al.* formed ordered arrays of nanoscale silver deposits on a solid electrolyte surface by reduction with an electron beam in a high resolution scanning electron microscope [8]. The aim of this paper is to point out some general aspects of electrochemical metal deposition at different interfaces, emphasizing processes at less studied interfaces, but also showing commonalities and distinctions – in particular with respect to morphology.

From the general point of view, electrodeposition of a metal can take place at any interface or in any region of an electrically conducting system, where a transition from predominant electronic conduction to predominant ion conduction takes place, and where the metal formation is either thermodynamically and/or kinetically enforced. In Fig. 1, all possible experimental situations at different interfaces are depicted, combining the three essential states of

matter (gaseous (plasma or electron beam), liquid, solid). In addition to the classical s|l interface, four other interfaces exist and may be used for metal deposition. But whereas we know much about the kinetics of metal growth and the morphology of the metal deposit at the s|l interface, we know less about the same process at other types of interfaces. The current short review summarizes the current state of research at these less typical interfaces and tries to extract major differences.

We find that the s|s interface is by far less well studied than the s|l interface, despite the recent activities in nanoscale metal deposition on solid electrolytes. Only a small number of fundamental studies yet exist. The l|l interface, *i.e.* the interface between two immiscible liquids, has become again a subject in electrodeposition since a few years, and interesting experimental studies have been published. The s|g and the l|g interfaces (of course including an ionised gas, *i.e.* a plasma) have rarely been studied, and only very few experimental examples exist.

Discussing electrochemical metal deposition, we have to include inhomogeneous or graded systems without a discrete interface. Such systems with gradients of the electronic and ionic partial conductivities, *i.e.* with gradients of the ionic transference numbers, may be subject to internal electrochemical reduction or oxidation processes under sufficiently high current load. These processes have been analyzed so far only by a few authors, see [9, 10] for reports on field-driven internal reduction and oxidation, but an internal metal deposition has so far not been reported. As inhomogeneous systems with gradients of transport properties can only be maintained in the solid state, they are discussed together with s|s interfaces.

2. Electrodeposition at different interfaces

In the following we summarize briefly some theoretical aspects of electrochemical metal deposition in different environments. Secondly, we review existing experimental studies for the different possible cases, including inhomogeneous systems.

2.1 Theoretical aspects

A comprehensive treatment of all theoretical aspects of metal deposition is beyond the scope of this paper. Three main problems have in principle to be considered: (a) The thermodynamics of metal deposition, including the influence of metal–substrate interaction (*e.g.* underpotential deposition, UPD) and the role of the surface energy (capillarity); (b) The kinetics, *i.e.* the overvoltage for the deposition process and its dependence on the thermodynamic variables and other experimental boundary conditions, and the growth rate; (c) The development of the morphology and the microstructure of the metal deposit as

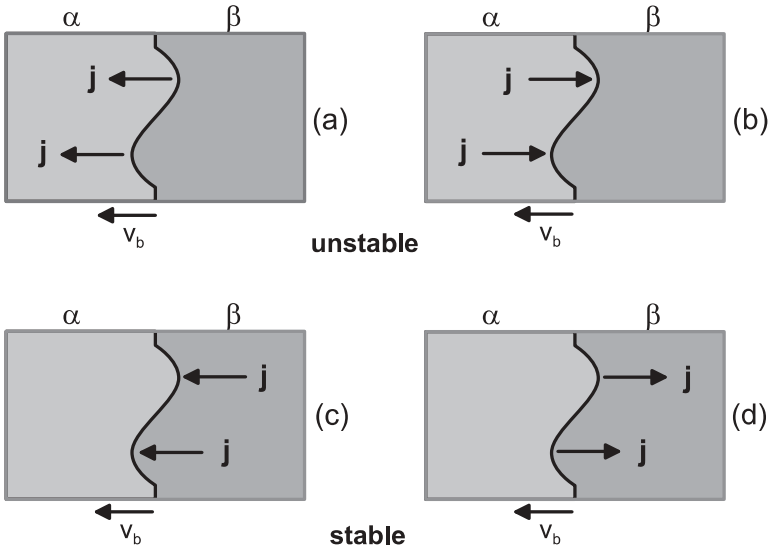

Fig. 2. Morphological evolution of interfaces under the influence of a driving force: (a, b) Unstable interfaces, (c, d) stable interfaces (v_b: advancement of boundary).

a function of all experimental parameters (including thermodynamic variables and driving force). Here we chose the morphology and microstructure of the deposits in different environments as one of the most important aspects for the technological use of any kind of electrochemical process.

The growth of any solid phase relies on nucleation and subsequent growth, and both phenomena are important for its morphology. The nucleation rate, the spatial distribution of nuclei and the orientation of nuclei relative to a solid substrate are primarily responsible for the microstructure of a solid deposit, and thus, the control of the nucleation rate is highly relevant. Here we ignore the initial nucleation phase (see [11] for an early work) and consider a later state, when a macroscopic deposit with dimensions beyond the size of a nucleus already exists. In Fig. 2, the general macroscopic stability criterion for the non-equilibrium growth of a phase is visualized, as worked out by Schmalzried [12]. A phase is growing by the advancement of its interfaces. And we can predict stable and unstable growth of a solid phase if we are able to identify that flux which controls the rate of advancement of the moving interfaces. In all cases a) to d) the interface of the growing phase moves to the left. If the rate-controlling flux occurs to or from the interface within the growing phase, the moving interface is kinetically stable. If the rate-controlling flux occurs to or from the interface in the phase ahead of it, then the moving interface is a priori kinetically unstable.

This simple kinetic and macroscopic criterion does only predict whether an interface is subjected to unstable development, if we ignore all those forces which counteract the development of non-equilibrium interface structures and the related increase of the interface area. Viscous forces and mechanical effects, spatial anisotropies of the phases, as also surface tension and

surface-active compunds, influence the morphological development strongly (see *e.g.* [13]). A first-order theoretical approach to morphological instability is often based on a linear stability analysis [14], including restoring effects like surface tension. One main result of such analysis is the wave length of the fastest growing interface mode (sinusoidal disturbance) and its velocity. Another important result concerns the relation between the magnitude of the driving force and the morphological instability. The predictions of the shape and form of the real instabilities cannot be achieved by this approach. These require nonlinear stability analyses or computer simulations.

In essence, in cases where a growing phase is a priori subject to unstable growth (according to the analysis in Fig. 2), the balance between the driving force and the restoring forces decides whether the real system grows stable or unstable. Perhaps the most obvious example is the cathodic metal deposition from liquid electrolytes: The metal deposit has a much higher electrical conductivity than the electrolyte, and the flux of metal ions to the cathode is rate-controlling. Thus, cathodic metal deposition in liquid electrolytes corresponds to Fig. 2b, and the metal deposit should develop an unstable surface with time. Indeed, dendrite and whisker formation occurs frequently, and special measures have to be undertaken in order to prevent them (see *e.g.* [15]). Special surface-active compunds and optimized deposition rates are required for the growth of smooth surfaces.

The situation becomes more complicate in the case of l|l interfaces, as discussed below. Metal growth at a liquid metal|electrolyte interface is subject to morphological instability, once the product does not dissolve in the liquid metal (*e.g.* mercury). Metal growth at the the interface between two immiscible electrolytes is also subject to morphological instability. If we neglect in a first order approximation possible orientational effects of the interface itself, the growth towards the phase with the less mobile charge carrier should lead to the development of a morphological instability. And – as observed in practice – needle-type morphologies might be created from the initial nuclei under the influence of the electric driving force. Virtually the same arguments are valid for the case of a g(plasma)|l electrode, see discussion below.

S|s and s|g(plasma) electrodes differ considerably from their liquid counterparts, as the rigity of the solid phases also controls the morphology of the metal deposits. Only under extreme conditions the deposit grows into the solid electrolyte, and thus, the product morphologies are quite different, see discussion below and Fig. 3.

We conclude that cathodic metal deposition at all five possible interfaces (gas|gas interfaces do not exist) bears always the possibility of morphological instability. A clear difference is found between electrodes on a solid electrolyte and a liquid electrolyte: Liquid electrolytes do not hinder the growth of metal deposits (*e.g.* dendrites) towards the anode, and the distance between anode and deposit can change. Solid electrolytes, being rigid and not plastic under normal conditions, do not allow the growth of cathodic deposits towards the

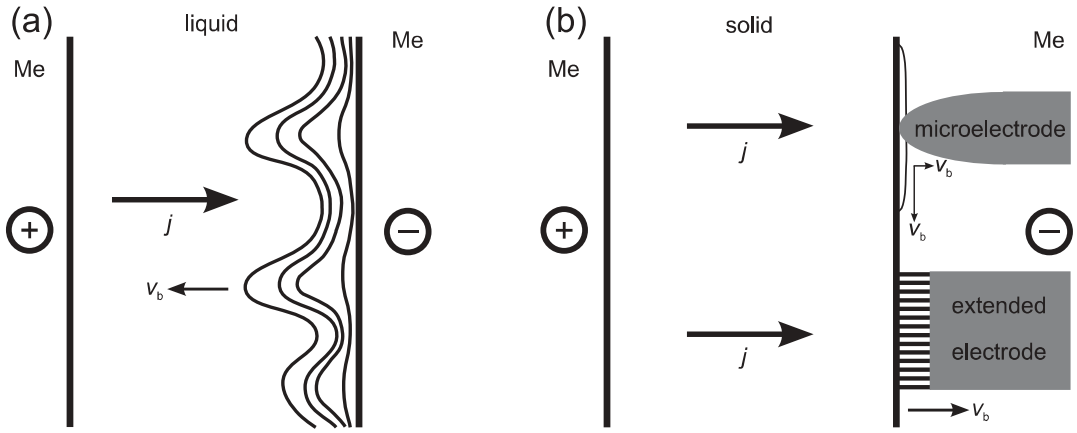

Fig. 3. Morphological evolution of cathodic metal deposits at electrodes on (a) liquid and (b) solid electrolytes.

anode. Therefore, other growth modes like whiskers, surface dendrites and whisker/dendrite hybrids form. In addition, the microstructure of the solid electrolyte and the interface plays an important role for the growth process. Whereas liquid electrolytes are isotropic and homogeneous, solid electrolyte include non-equilibrium defects (sites of repeatable growth) like dislocations and grain boundaries, which may act as nucleation centers for the metal deposit.

2.2 Solid|liquid interfaces

Since the beginning of electrochemistry the s|l interface always played a major role in scientific research, in particular with respect to the kinetics of metal deposition. Several methods and techniques have been developed to investigate the thermodynamics and the kinetics of electrode reactions, see [16, 17] for a survey. All standard electrochemical techniques give no direct information of the microscopic processes which take place at the s|l interface. Either a coupling with spectroscopy, scattering or microscopic techniques is required for a less phenomenological study. It was the STM [18] which revived the research on electrode kinetics in liquid electrolytes at the beginning of the 1980's. Further developments led to the *atomic force microscope* (AFM) [19], and the *electrochemical scanning tunneling microscope* (ESTM) [20]. The ESTM offers the possibility to observe reactions at electrode surfaces in electrolyte solutions in situ. Detailed descriptions of these scanning probe methods can be found in Refs. [21], [22] and [23].

Kolb [22, 23] uses ESTM to deposit nanoclusters on surfaces, *e.g.* arrays of copper clusters on gold surfaces. Schuster and coworkers [24, 25] use ultrashort voltage pulses between a "tool electrode" and a "workpiece" for machining conducting materials with submicrometer precision. The work by Schultze and others [26, 27] aims for the development of "electrochemical micro- and nano-

system technology" (EMST) by optimizing anode and cathode processes in respect to spatial and temporal resolution.

The morphology and microstructure of metal deposits from liquid electrolytes – and more recently – from ionic liquids [28], has long been the subject of intensive experimental and theoretical work. The reader is referred to the comprehensive literature (see *e.g.* [29–31]). Quite recently, electrochemical growth of dendrites has been excavated as a route towards nanoscale metal particles with large surface area [32, 33].

2.3 Solid|solid interfaces

Whereas s|l electrodes have been intensively studied, s|s electrodes have rarely been studied at all with respect to fundamental aspects (except early works by *e.g.* Armstrong *et al.* [34]). The reasons are manifold: Firstly, solid state electrochemistry has only become popular some 25 years ago, and there has simply been less time for a comprehensive study compared to the s|l interface. Secondly, only a few parent metal|solid electrolyte interfaces can be investigated in practice, as only a few cation conducting solid electrolytes with sufficient chemical stability exist. Among these are silver, copper, lithium and sodium electrolytes. To date mainly silver and lithium electrodes have been studied.

Perhaps the most significant difference between s|l and s|s interfaces concerns the ratio of the geometrical and the electroactive interface area. Because of the roughness of an electrode material (at least on the nanoscale) the contact area of a solid electrode with a liquid electrolyte is usually larger than its geometrical area. In the case of a solid electrolyte the contact area is usually much smaller than the geometrical area, due to the rigidity of the two lattices, and only under severe mechanical pressure the contact area can be increased by plastic deformation. Thus, a serious problem in the study of s|s electrodes is the preparation of reproducible contact areas. Even a single half cycle of a sinusoidal voltage signal in AC impedance spectroscopy may already cause a change in the contact area. Accordingly, there are numerous papers on the influence of electrode imperfections on electrode kinetics, *e.g.* Fleig and Maier [35, 36] analyse the influence of imperfect electrode contacts on the AC impedance response. As a model contact area they consider point contacts between the electrode and the electrolyte. Motivated by the results, the authors employed microelectrodes as working electrodes which offer spatial resolution. With such microelectrodes it was possible to measure the surface conductivity of silver ion conductors [37, 38] or the conductivity of grain boundaries [38–40]. Earlier work with less spatial resolution aimed for the determination of profiles of (electro-)chemical potentials [41].

The morphology of cathodic metal deposits has almost exclusively been studied in silver systems (*e.g.* AgCl, AgBr and Ag_2S, see [42] for a short experimental report on the Cu|CuBr electrode). It depends primarily on the driving force, *i.e.* the applied overvoltage (potentiostatic conditions) or the applied

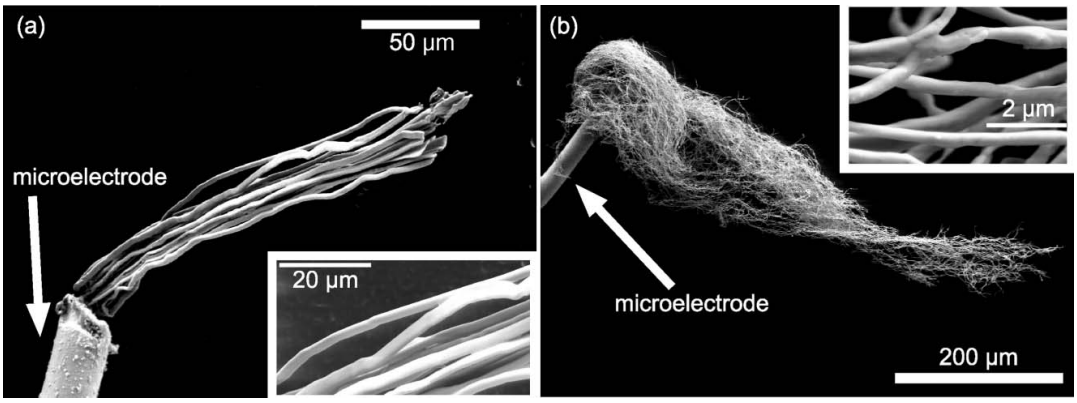

Fig. 4. HSEM picture of silver whisker grown on AgBr at Ag-microelectrodes ($\varnothing = 25\,\mu m$): (a) $\vartheta = 275\,^{\circ}C$, $I = 0.5\,\mu A$, $t = 300\,s$; (b) $\vartheta = 200\,^{\circ}C$, $I = 0.5\,\mu A$, $t = 630\,s$.

current (galvanostatic conditions), but also significantly on the electrode geometry (point electrode or geometrically extended electrode). Thermodynamic variables (pressure, temperature) influence the growth, mainly by controlling the transport properties, the surface energy and the mechanical boundary conditions at the interface. The influence of the electrode geometry, *i.e.* of the electric field distribution in the electrolyte, has been studied in detail by Best and Peppler [43, 44]. Generally, the deposition of silver at planar extended electrodes leads primarily to arrays of metal whiskers, whereas the deposition at a microelectrode usually results in the growth of dendrites on the surface of the electrolyte. However, by choice of the experimental conditions one can control the morphology and can either deposit whisker-shaped or dendrite-shaped silver metal. In Fig. 4 two bunches of silver whiskers are depicted which adhered to the microelectrode (cathode) rather than to the electrolyte (for details on the experiments *cf.* [44]). The only experimental difference was the temperature at which the experiments where conducted. In one case silver wires with a diameter of about 2 µm were obtained (*cf.* Fig. 4a), $\vartheta = 275\,^{\circ}C$), in another case silver wires with a diameter of about 350 nm (*cf.* Fig. 4b, $\vartheta = 200\,^{\circ}C$). At higher currents (galvanostatic setup) the morphology of the silver deposits changes from whisker-type to dendritic. Upon further temperature change, the form of the dendrites itself changes. In one case the dendrite is compact (*cf.* Fig. 5a, $\vartheta = 200\,^{\circ}C$), in another case the dendrite spreads mainly along two directions (*cf.* Fig. 5b, $\vartheta = 150\,^{\circ}C$). Further work is going on, in order to develop a model for the morphology control during metal deposition on solid electrolytes.

Microelectrodes have also been used for the thermodynamic and kinetic study of the deposition process of silver on silver halide surfaces, aiming for a better understanding of nucleation and crystallisation [44–48]. Maier and coworkers find that the unique transport properties of metal|electrolyte interfaces play a crucial role for structure formation. They emphasize that a metal|electrolyte interface is a extremely fast transport path for metal, as

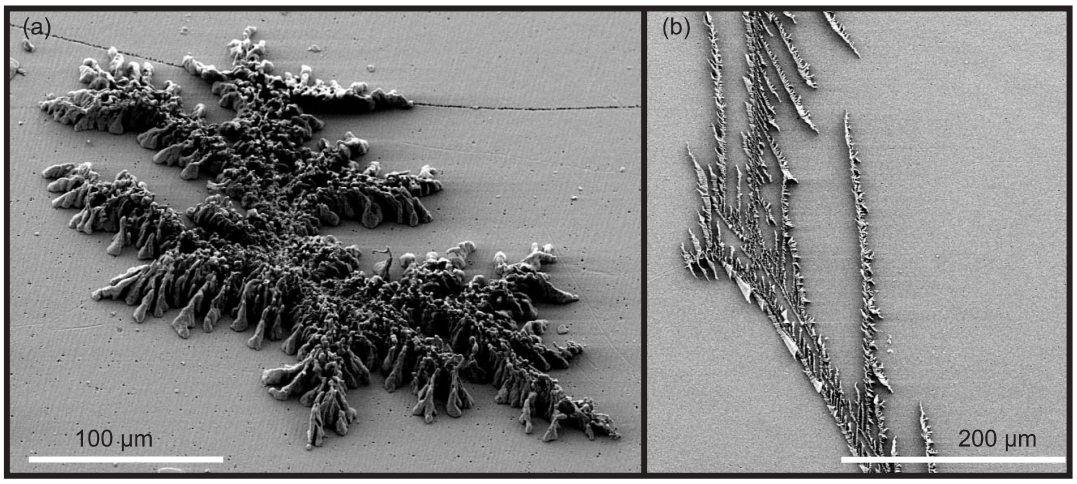

Fig. 5. HSEM picture of silver dendrites on AgBr at Ag-microelectrodes ($\varnothing = 25\,\mu m$): (a) $\vartheta = 200\,^{\circ}C$, $I = 5\,\mu A$, $t = 300\,s$; (b) $\vartheta = 150\,^{\circ}C$, $I = 5\,\mu A$, $t = 90\,s$.

ions can move easily in the electrolyte and electrons in the metal (chemical diffusion by coupled flow of ions and electrons). Thus, spatial differences in the chemical potential of the metal by the size effect on the nanoscale lead to metal diffusion along the surface and to a fast electrochemical Ostwald ripening. It is therefore concluded that electrochemical measurements of nanoparticular electrodes are a priori unstable, due to the instationary character of the metal|electrolyte interface. Thus, with the growth of the larger particles at the expense of the smaller particles (the smaller particles have a higher chemical potential) the nanocrystalline silver electrode converts to a microcrystalline silver electrode. Accordingly the excess emf of about 1 mV of the cell (–)Mo|Ag(nanocryst.)|$RbAg_4I_5$|Ag(microcryst.)|Mo(+) relaxes steadily from about 1 mV towards zero [46, 49]. Electrochemical Ostwald ripening does also take part in the occurence of periodic potential oscillations at s|s electrodes under anodic conditions [50–53].

Electrochemical metal deposition can also take place at interfaces between two different ionic conductors with different ionic transference number. The change of the transference number at the interface enforces a partial switch of the ionic and electronic currents, which leads either to a reduction or an oxidation – depending on the current direction. This internal electrochemical reaction is the origin of certain failure mechanisms of oxygen solid electrolytes in chemical potential gradients under current load [10]. Here we present an own example of an internal electrochemical reaction: In a cell Ag|Ag_2S|AgBr|Ag, both silver ions and electrons are transferred across the Ag_2S|AgBr interface. But Ag_2S and AgBr show different ionic transference numbers, which causes a discontinuity in the transport properties at the interface. If a cathodic potential (galvanostatic setup) is applied to the left silver electrode, see Fig. 6 for a sketch of the cell Ag|Ag_2S|AgBr|Ag, ions move from the right electrode to the left, whereas electrons move from the left to the right. Because of the lower

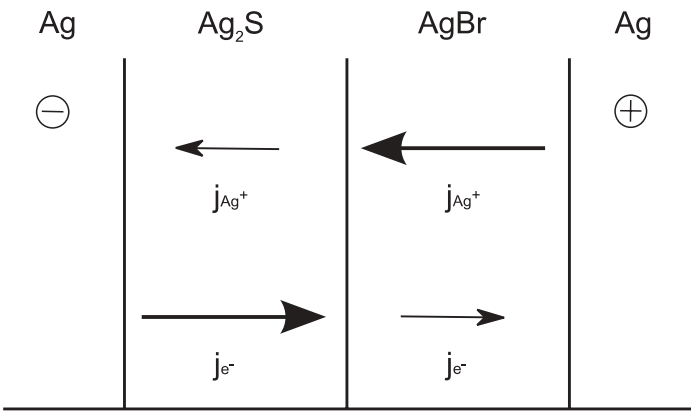

Fig. 6. Schematic representation of the cell $Ag|Ag_2S|AgBr|Ag$.

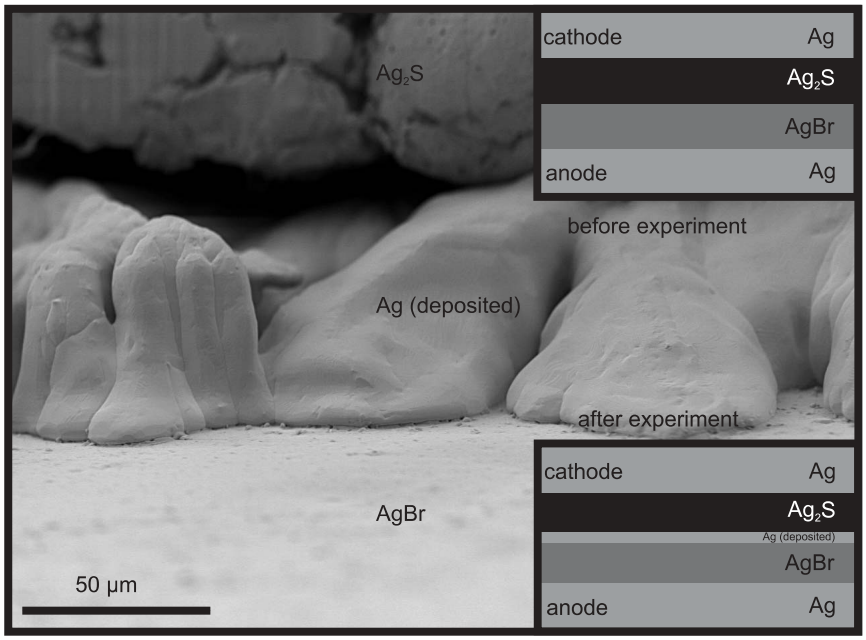

Fig. 7. HRSEM picture of silver deposited between two mixed condutors with different ionic and electronic transference numbers, $\vartheta = 150\,^{\circ}\mathrm{C}$, $I = 100\,\mu\mathrm{A}$.

ionic transference number of Ag_2S, silver deposition occurs at the $Ag_2S|AgBr$ interface. In Fig. 7 the result of this experiment is depicted: Silver was deposited between a silver bromide single crystal and a silver sulfide polycrystal.

2.4 Solid|gas interfaces

S|g electrodes can either be formed by contacting a solid electrolyte with a low temperature plasma (usually a radiofrequency (rf) or direct current (dc) discharge) or with an electron beam, preferably in an electron microscope. The latter method has long been known to solid state electrochemists as an experimentally unavoidable disturbance during the electron microscopical study of

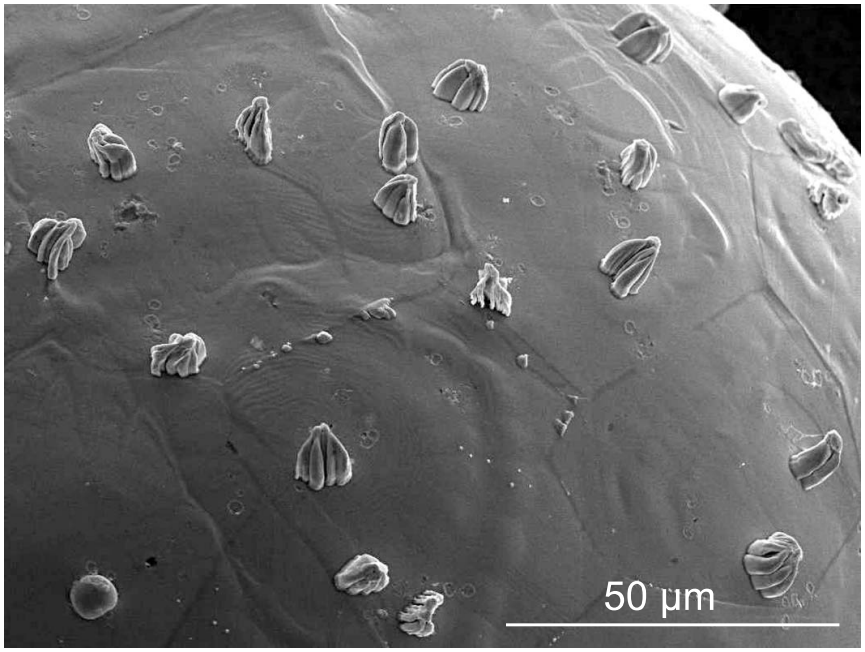

Fig. 8. Small silver deposits of whisker-shape on a silver sulfide surface which has been investigated at room temperature in a scanning electron microscope.

silver or copper halides and chalcogenides, see Fig. 8. But recently Sone *et al.* [8] use a field emission electron microscope with high spatial resolution for a well defined cathodic deposition of silver nuclei with diameters as small as 10 nm. Employing electron beam lithography they were able to write silver clusters on the surface of silver sulfide with desired distance and size. However, they do not give any information on the stability of these nanostructures. In any case, the direct reduction of a metal on the surface of a solid electrolyte with an electron beam is an interesting route to the preparation of metal nanostructures without mechanical contact.

Plasmas represent a powerful tool in modern surface and material engineering sciences and provide a second route towards the reduction of a metal at the free surface of an electrolyte. Examples of processes using plasmas are plasma enhanced chemical vapor deposition (PECVD), also called plasma assisted chemical vapor deposition (PACVD), plasma etching and cathode sputtering. It has been shown in recent years that plasmas are also beneficial as gaseous electrodes for the mechanically contact-free electrical polarisation of solid electrolytes [54–58], however, no direct observation of a plasma-cathodic metal deposition from a solid electrolyte has been reported. The influence of the plasma state on the reduction of metal ions to a metal has been demonstrated by He *et al.*, who synthesized metal nanoparticles embedded into a titanium dioxide gel film by means of a hydrogen gas plasma treatment [59]. In a first step the authors prepared several ultrathin TiO_2-films from titanium butoxide mixed with different amounts of magnesium ethoxide utilizing a sol-gel pro-

cess. Secondly, the magnesium ions were replaced by sodium ions, which were then exchanged by silver or other noble metal cations. In the third and last step the metal cations were reduced by a radiofrequency (rf) H_2 plasma, for a comparison conventional photochemical and chemical reduction routes were also tested. The obtained films were investigated via UV–VIS spectroscopy, XPS/Auger spectroscopy, transmission electron microscopy (TEM) and electron diffraction. In the UV–VIS spectrum the surface plasmon resonance peak of the resulting silver nanoparticles was red-shifted probably due to the high refractive index of the titania matrix [60, 61] or/and due to the close contact of neighboring silver particles [62]. Bigger particles broadened and red-shifted the surface plasmon peaks [59]. Additionally, also a broader size distribution led to wider peaks. With an increasing silver concentration bigger particles were obtained and their size was distributed over a wider range. In general, the obtained films were colorless, transparent and smooth. Films with a very high silver concentration became black and no plasmon band could be observed in the UV–VIS spectrum, because bulk silver metal was formed. A low-energetic rf plasma resulted in smaller nanoparticles [59].

We expect that plasma-cathodic treatment of solid electrolyte surfaces leads to the creation of a high and homogeneous concentration of metal nuclei, even in cases where an irradiation with UV light will not cause a reduction. Whether this plasma-cathodic treatment will be of any practical use, has to remain an open question.

2.5 Liquid|gas interfaces

In contrast to the solid|plasma electrode, the liquid electrolyte|plasma electrode is a surprisingly old subject. Already in 1887, the first electrochemical deposition of silver from an aqueous silver salt solution by means of a direct current (dc) gas discharge was reported by Gubkin [63]. One electrode was immersed in an aqueous silver nitrate solution, the second one was located in the gas phase above the solution. Applying a voltage of 1000 V led to a stable glow discharge and silver was formed cathodically at the interface between the aqueous solution and the gas phase.

In 2005, Lee and co-workers reported the synthesis of platinum nanoparticles [64] in an almost identical experimental arrangement. A He–H_2 plasma was burnt over an aqueous solution of H_2PtCl_6. The flowing He–H_2 mixture was kept almost at atmospheric pressure, and an AC discharge of about 1 kV voltage (60 Hz) and 10 mA current was applied. The distance between the upper electrode and the surface of the solution was as short as 5 mm. Irregular shaped nanoparticles with a narrow diameter distribution between 1 nm and 4 nm were obtained. The selected area electron diffraction (SAED) pattern revealed the face-centred cubic structure of the nanocrystalline platinum particles. According to the authors, no coalescence or aggregation occurred whilst the experiment but during the drying process, when the sample was pre-

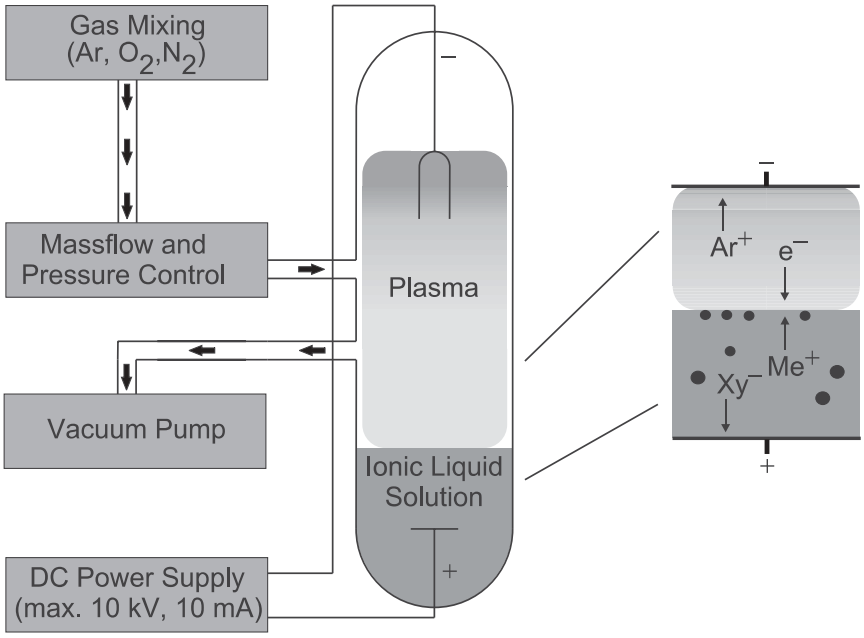

Fig. 9. Setup of the plasma-electrochemical experiment. A platinum hollow electrode served as cathode and a quadratic platinum plate was used as anode.

pared for the transmission electron microscopic (TEM) investigation. Thus, it appears that some inherent aspect of this plasma method prevents particle aggregation during growth – making stabilizers unnecessary. In order to elucidate the process Lee *et al.* assumed that the nanoparticles are charged during the formation process, so that Coulomb repulsion prevents aggregation. In addition, the authors assume that the small particle size is a result of the small area which is affected by the corona discharge. Nanoparticles might rapidly move out and metal ions would move into the reaction area. As a further argument the authors propose that plasmas in general lead to a high nucleation rate. Finally it has to be noted that H_2 gas is required for the plasma-cathodic reduction process. When a pure He plasma was used, no platinum metal deposit was formed [64].

Recently, Meiss *et al.* applied a direct current (dc) argon plasma to silver nitrate and silver trifluoromethylsulfonate dissolved in 1-butyl-3-methylimidazolium trifluoromethylsulfonate as an ionic liquid (*cf.* Fig. 9) [65]. The pressure of the flowing argon gas was held constant at approximately 100 Pa and a voltage of 500 V to 600 V with current densities in the order of $1\,\mathrm{mA\,cm^{-2}}$ was applied. As ionic liquids have extremely low vapor pressures they render possible to employ a low gas pressure under low plasma power conditions. This leads to very homogenous, spatially extended and stable plasmas, whereas Lee and co-workers obtained a localized corona discharge with high power density. The distance between the two electrodes in this experiment was chosen as 10 cm. The silver nanoparticles where formed mainly at the edge of the plasma|ionic liquid interface close to the glass wall of the reaction chamber (*cf.* Fig. 10). The resulting nanoparticles were about one order of mag-

Fig. 10. Formation process of the silver nanoparticles in the ionic liquid.

nitude larger than the nanoparticles obtained by the Lee group, which seems to support their hypothesis that a small reaction area results in smaller nanoparticles. Additionally, the size distribution was still quite narrow. The nanoparticles were characterized via scanning electron microscopy (SEM) (*cf.* Fig. 11), high resolution transmission electron microscopy (HRTEM) (*cf.* Fig. 12), selected area electron diffraction (SAED) and energy dispersive X–ray analysis (EDX) [65]. Information on the surface composition of the particles is yet not available.

In summary, plasmas appear to have a potential as gaseous electrodes for the reduction of metal ions which are dissolved in stable solvents. In contrast to conventional solvents ionic liquids offer the possibility of low pressure conditions in the plasma chamber, thus providing a means for the application of spatially homogeneous plasmas. In order to explore the opportunities of plasma electrodes in metal deposition from ionic liquid electrolytes, systematic studies are on their way.

2.6 Liquid|liquid interfaces

Finally, the l|l interface – often denoted as ITIE (interface between two immiscible electrolytes) – has to be considered. Two cases can be distinguished

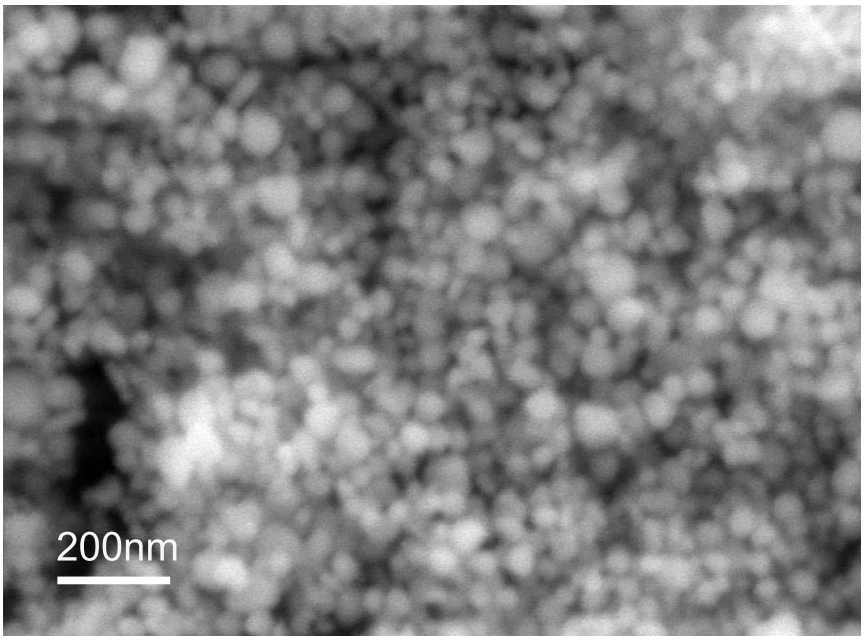

Fig. 11. HSEM picture of the deposited silver nanoparticles.

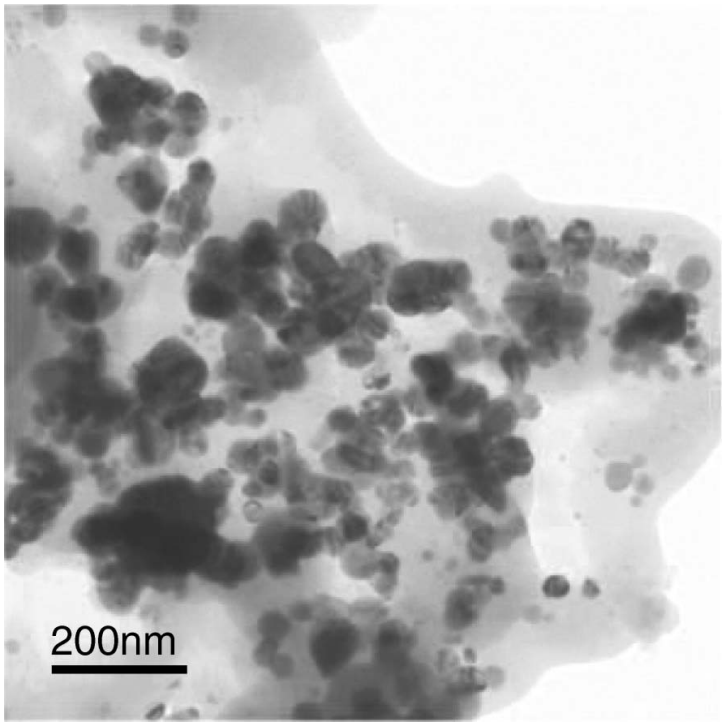

Fig. 12. TEM picture of the deposited silver nanoparticles.

referring to the interface constitution at the beginning of an experiment. Firstly, the metal deposition at a bare, pristine l|l interface is discussed. Secondly, the processes at a modified l|l interface are considered. As the bare l|l interface

loses it pristine character immediately after the precipitation of the first small metal particles, this is merely a formal classification. One general feature of a l|l interface in comparison with a s|l interface is that there are no localized surface defects which serve as nucleation sites in the solid state [66]. We can safely assume that the energy barrier for nucleation is lower at surface defect sites than at regular surface sites [67].

2.6.1 The bare, pristine liquid|liquid interface

As in the case of the l|g interface the very first experimental observations have been reported more than a century ago. Mylius and Fromm [68] and Freundlich and Novikow [69, 70] observed the formation of leaf-like deposits during an electrolysis at the interface between natural oil and an electrolyte solution. The deposits were called "Metallblätter" (metal leaves). Several years thereafter Guainazzi *et al.* deposited a thin copper film at an organic|aqueous interface [71]. The organic phase consisted of either 1,2-dichloroethane or dichloromethane and contained tetrabutylammonium hexacarbonylvanadate ($[Bu_4N][V(CO)_6]$) as reducing agent. The aqueous phase contained copper sulfate. They observed a irregular dependence of the reduction products upon experimental conditions. Furthermore, the efficiency of this method was lower in comparison with ordinary cathodic deposition of copper. Concerning the morphology of the copper films the authors stated that the thickness of the copper layer was affected by the non uniformity of current density at the interface. Some films with shapes similar to the adjacent cathode as well as only partly covered interfaces were obtained. Unfortunately Guainazzi *et al.* did not describe their experimental setup [71].

Recently, Tada *et al.* resumed growing thin copper films at the interface between two immiscible liquids [72]. A copper ring anode was placed at the bottom of a beaker which was filled with a copper sulfate aqueous solution. Above the aqueous phase a *n*-heptane layer was added. The tip of the cathode was placed at the centre of the interface. The distance between the ring anode and the l|l interface amounted to 5 mm. A saturated silver–silver chloride electrode served as reference. Film growth started after applying an electrode potential that was less than normally required for the reduction of copper(II). Generally, branching morphologies of the metal leaves were always observed when the diffusion field affects the growth of the films (DLA, diffusion limited aggregation) [73]. Along the interface the growth velocity decreased not much upon decreasing the copper sulfate concentration [72]. By contrast, the growth velocity perpendicular to the l|l interface (causing the thickness of the leaves) was reduced much more. The deposits comprised two layers, a very thin film along the l|l interface and a layer of many branched hairs which grew perpendicular out of the thin film into the aqueous phase. During the deposition process the thin film grew first, and then the development of the hairs followed. With decreasing electrolyte concentration, the thin films grew to smaller thick-

nesses. However, the overall thickness decrease was much less as one would expect by estimations of a constant material density. Hence, the main effect of a reduced copper salt concentration is that the array of silver "hairs" grew less denser, or its development was even completely suppressed [72]. The two different microstructures of the deposit suggest that there are also two different types of growing mechanism. The authors consider the growth perpendicular to the l|l interface as diffusion controlled because the hair lengths are of the same order of magnitude as the diffusion length [72, 74], whereas the growing mechanism along the l|l interface exhibits the Marangoni effect [75]. At far distances from the growing frontier the copper salt concentration is in equilibrium with the bulk phases, whereas the concentration of Cu^{2+} is reduced to zero right ahead of the growing frontier. As a consequence a gradient develops, which causes a gradient in interfacial tension and leads to a convective stream. This convective flow accelerates mass transport compared to normal diffusion and surface diffusion and has a significant influence on the product morphology [72]. For the case of silver deposits the morphology control at a l|l interface has recently been dicussed by Scholz [76].

2.6.2 The liquid|liquid interface in microstructured templates

Dryfe *et al.* investigated the deposition of palladium and platinum at the interface of an organic and an aqueous phase, where the interface was templated in a porous γ-alumina membrane. 1,2-Dichloroethane served as organic electrolyte containing either bis(triphenylphosphoranylidene)ammonium tetraphenylborate (BTPPA TPB) or bis(triphenylphosphoranylidene)ammonium tetrakis(pentafluoro)phenylborate (BTPPA $TPBF_{20}$) as conducting salt and either bis(pentamethylcyclopentadienyl)iron (DmFc) or butylferrocene (BuFc) as reducing agent. The aqueous solution contained lithium chloride and lithium sulfate as conducting salt and either ammonium tetrachloropalladate or ammonium tetrachloroplatinate as metal cation source. Due to the higher reactivity of the palladium compound it was necessary to use BTPPA $TPBF_{20}$ and BuFc in order to prevent a spontaneous reaction [77]. Using a γ-alumina membrane as a template has several serious effects. Mass transport through the pores of the membrane is increased compared to the mass flow through a pristine l|l interface due to a reduced interface area, where the two liquids are in contact with each other. The l|l interface is stabilized against shear effects resulting from mass flow [78]. If the interface of the two immiscible liquids is located in the interior of the pores the particle growth should be constrained to the pore size. Dryfe and co-workers obtained nanoparticles with mean diameters in the range of 3–5 nm, but these nanoparticles again formed larger aggregates. Although these aggregates were not formed in the interior of the pore but at their openings they exhibit the same diameter as the pores. Thus, the size of a particle aggregate depends on the pore size. As γ-alumina is hydrophilic it is wetted with water much better than with 1,2-di-

chloroethane, hence, the l|l interface was always located at the openings of the pores [77].

Finally, Dryfe *et al.* report that tetrachloropalladate is electrochemically much more reactive than tetrachloroplatinate, which is in contradiction with the standard potential values E^0 (*versus* NHE) for the two redox systems [79].

$$PdCl_4^{2-}(aq.) + 2e^- \rightarrow Pd(s) + 4Cl^-(aq.) \quad E^0 = 0.62\,V$$

$$PtCl_4^{2-}(aq.) + 2e^- \rightarrow Pt(s) + 4Cl^-(aq.) \quad E^0 = 0.80\,V$$

Platinum should be easier reduced in comparison to palladium. This alludes to kinetic effects which influence the formation of the particles. Dryfe *et al.* propose two possible factors which may influence the deposition process [77]: Firstly, if the loss of the chloride ligands takes place prior to reduction, it is suggested that decomplexation occurs much slower for tetrachloroplatinate than for tetrachloropalladate [80, 81], although the reported formation constants are quite similar [82, 83]. But it is not clear which species actually is at hand during reduction. It could be also a MCl_2 species, which is in equilibrium with its dimer [77]. As the second factor the authors propose that the lower surface energy of the solution containing the palladium complex facilitates the deposition compared to platinum. This is of particular importance at the l|l interface, where no stabilizing interactions can occur as it is the case on a solid substrate [77].

These two factors elucidate the alleviated palladium deposition but they do not explain the observation that the platinum nanoparticles are slightly smaller than the palladium particles. Additionally, there is still the question of which phenomenon constrains the growth of the nanoparticles [77]. In an previous article Dryfe *et al.* suggested that due to the weak interaction between pore walls and particles the surface of the γ-alumina is less important and that nucleation starts at the l|l interface [84].

3. Discussion and conclusions

Combining liquid and solid electrolytes with plasmas, we can define five basic types of interfaces: s|s, l|l, s|l, l|g, s|g. Electrochemically driven metal deposition can occur at each of these interface, but so far only the conventional s|l electrolyte interface has been studied in great detail. Whereas this interface is essential for the modification of surfaces by any kind of electrochemical overlayer deposition, the s|s interface plays a role in rechargeable solid state batteries and capacitors. And more recently, the nucleation of silver crystallites on solid electrolytes is tested in ionic memory devices and switches. The metal deposition on solid electrolytes by employing a plasma electrode or an electron beam has not yet found an application, and we believe that it will be critical to overcome stability problems.

The metal deposition in fluid systems (l|l, l|g) might be interesting for the synthesis of free metal nanoparticles with special morphology. First attempts of silver deposition at an ITIE have been reported, but the silver deposition at the free surface of an ionic liquid has not been reported before. Whether this electrochemical route to nanoparticles will be used in practice will depend on its reproducibility and tunability.

Acknowledgement

Financial support by the DFG (projects Ja648/4-2 and Ja648/11-1) is gratefully acknowledged. We thank Prof. Frank Endres for stimulating discussions and a fruitful cooperation in a project on processes at the plasma|ionic liquid interface. We thank Dr. Lorenz Kienle and Viola Duppel (MPI for Solid State Research, Stuttgart) for support in electron microscopy (Fig. 8).

References

1. Z. Takehara, J. Power Sources **68** (1997) 82.
2. R. Mogi, M. Inaba, Y. Iriyama, T. Abe, and Z. Ogumi, J. Electrochem. Soc. **149** (2002) A385.
3. P. C. Howlett, D. R. MacFarlane, A. F. Hollenkamp, and M. Forsyth, *High Lithium Metal Cycling Efficiency in a Room Temperature Ionic Liquid*. Abstracts of Papers, 226th ACS National Meeting, New York, NY, September 7–11, 2003.
4. J.-I. Yamaki, S.-I. Tobishima, K. Hayashi, K. Saito, Y. Nemoto, and M. Arakawa, J. Power Sources **74** (1998) 219.
5. C. Liang, K. Terabe, T. Hasegawa, R. Negishi, T. Tamura, and M. Aono, Small **1** (2005) 971.
6. K. Terabe, T. Hasegawa, T. Nakayama, and M. Aono, Nature **433** (2005) 47.
7. K. Terabe, T. Nakayama, T. Hasegawa, and M. Aono, J. Appl. Phys. **91** (2002) 10 110.
8. H. Sone, T. Tamura, K. Miyazaki, and S. Hosaka, Microelectron. Eng. **83** (2006) 1487.
9. S. Smolin and H. Schmalzried, Phys. Chem. Chem. Phys. **5** (2003) 2248.
10. A. V. Virkar, J. Nachlas, A. V. Joshi, and J. Diamond, J. Am. Ceram. Soc. **73** (1990) 3382.
11. H. Gerischer, Z. Elektrochem. **62** (1958) 256.
12. H. Schmalzried, *Chemical Kinetic of Solids*. VCH-Wiley, Weinheim (1995).
13. C. Monroe and J. Newman, J. Electrochem. Soc. **152** (2005) A396.
14. R. Aoagaki, K. Kitazawa, K. Koichi, and K. Fueki, Electrochim. Acta **25** (1980) 965.
15. K. P. Doyle, C. M. Lang, K. Kim, and P. A. Kohl, J. Electrochem. Soc. **153** (2006) A1353.
16. A. J. Bard and L. R. Faulkner, *Electrochemical Methods – Fundamentals and Applications*. John Wiley & Sons Inc., New York (2001).
17. R. C. Alkire and D. M. Kolb, *Advances In Electrochemical Sciences And Engineering*. Wiley-VCH (2001).
18. G. Binnig and H. Rohrer, Helv. Phys. Acta **55** (1982) 726.
19. G. Binnig, C. F. Quate, and C. Gerber, Phys. Rev. Lett. **56** (1985) 930.

20. K. Itaya and E. Tomita, Surf. Sci. **201** (1988) L507.
21. E. Budevski, G. Staikov, and W. J. Lorenz, *Electrochemical Phase Formation and Growth.* VCH, Weinheim (1996).
22. D. M. Kolb, Angew. Chem. Int. Ed. **40** (2001) 1162.
23. D. M. Kolb, Surf. Sci. **500** (2002) 722.
24. V. Kirchner, X. Xinghua, and R. Schuster, Acc. Chem. Res. **34** (2001) 371.
25. R. Schuster and G. Ertl, *Electrochemical nanostructuring*, in: A. Wieckowski, E. R. Savinova, and C. G. Vayenas (Eds.), Catalysis and Electrocatalysis at Nanoparticle Surfaces. Marcel Dekker, Inc. (2003).
26. J. W. Schultze and V. Tsakova, Electrochim. Acta **44** (1999) 3605.
27. J. W. Schultze and A. Bressel, Electrochim. Acta **47** (2001) 3.
28. S. Z. El Abedin and F. Endres, ChemPhysChem **7** (2006) 58.
29. D. Grier, E. Ben-Jacob, R. Clarke, and L. M. Sander, Phys. Rev. Lett. **56** (1986) 1264.
30. Y. Sawada, A. Dougherty, and J. P. Gollub, Phys. Rev. Lett. **56** (1986) 1260.
31. F. Oberholtzer, D. Barkey, and Q. Wu, Phys. Rev. E **57** (1998) 6955.
32. X. Wen, Y.-T. Xie, M. W. C. Mak, K. Y. Cheung, X.-Y. Li, R. Renneberg, and S. Yang, Langmuir **22** (2006) 4836.
33. T. Qui, X. L. Wu, Y. F. Mei, P. K. Chu, and G. G. Siu, Appl. Phys. A **81** (2005) 669.
34. R. D. Armstrong, T. Dickinson, and P. M. Willis, J. Electroanal. Chem. Interfac. Electrochem. **59** (1975) 281.
35. J. Fleig and J. Maier, Electrochim. Acta **41** (1995) 1003.
36. J. Fleig and J. Maier, Solid State Ion. **85** (1996) 17.
37. J. Fleig, F. Noll, and J. Maier, Ber. Bunsenges. Phys. Chem. **100** (1996) 607.
38. J. Fleig, Solid State Ion. **161** (2003) 279.
39. J. Fleig and J. Maier, Phys. Chem. Chem. Phys. **1** (1999) 3315.
40. J. Fleig, S. Rodewald, and J. Maier, Solid State Ion. **136** (2000) 905.
41. C. Rosenkranz and J. Janek, Solid State Ion. **82** (1995) 95.
42. C. Lambert, P. Lauque, J.-L. Seguin, G. Albinet, M. Bendahan, J.-M. Debierre, and P. Knauth, ChemPhysChem **1** (2002) 107.
43. M. Rohnke, T. Best, and J. Janek, J. Solid State Electrochem. **9** (2005) 239.
44. K. Peppler and J. Janek, Solid State Ion., in print, available online January 23, 2006.
45. A. Spangenberg, J. Fleig, and J. Maier, Adv. Mater. **13** (2001) 1466.
46. A. Schroeder, *Electrochemical Investigations of Silvernanostructures*. Dissertation, Montanuniversity Leoben (2004).
47. M. N. Kozicki, M. Mitkova, and J. P. Aberouette, Physica E **19** (2003) 161.
48. M. N. Kozicki and M. Mitkova, J. Non-Cryst. Solids **352** (2006) 567.
49. A. Schroeder, J. Fleig, H. Drings, R. Wuerschum, J. Maier, and W. Sitte, Solid State Ion. **173** (2004) 95.
50. H. Schmalzried and J. Janek, Ber. Bunsenges. Phys. Chem. **102** (1998) 127.
51. J. Janek, Solid State Ion. **131** (2000) 129.
52. J. Janek and S. Majoni, Ber. Bunsenges. Phys. Chem. **99** (1995) 14.
53. S. Majoni and J. Janek, Ber. Bunsenges. Phys. Chem. **102** (1998) 756.
54. J. Janek and C. Rosenkranz, J. Phys. Chem. B **101** (1997) 5909.
55. M. Vennekamp and M. Janek, Solid State Ion. **141**/**142** (2001) 71.
56. M. Vennekamp and M. Janek, J. Electrochem. Soc. **150** (2003) C723.
57. M. Vennekamp and M. Janek, Z. Anorg. Allg. Chem. **629** (2003) 1851.
58. M. Vennekamp and M. Janek, Phys. Chem. Chem. Phys. **7** (2005) 666.
59. J. He, I. Ichinose, T. Kunitake, and A. Nakao, Langmuir **18** (2002) 10 005.
60. I. Pastoriza-Santos, D. S. Koktysh, A. A. Mamedov, M. Giersig, N. A. Kotov, and L. M. Liz-Marzan, Langmuir **16** (2000) 2731.
61. P. Mulvaney, Langmuir **12** (1996) 788.
62. H. Fujiwara, S. Yanagida, and P. V. Kamat, J. Phys. Chem. B **103** (1999) 2589.

63. J. Gubkin, Ann. Phys. Chem., Neue Folge **32** (1887) 114.
64. I. G. Koo, M. S. Lee, J. H. Shim, J. H. Ahn, and W. M. Lee, J. Mater. Chem. **15** (2005) 4125.
65. S. A. Meiss, M. Rohnke, L. Kienle, S. Zein El Abedin, F. Endres, and J. Janek, ChemPhysChem, in print (2006).
66. M. Platt, R. A. W. Dryfe, and E. P. L. Roberts, Chem. Commun. (2002) 2324.
67. R. M. Penner, J. Phys. Chem. B **106** (2002) 3339.
68. F. Mylius and O. Fromm, Wiedemanns Ann. Phys. **51** (1894) 593.
69. H. Freundlich and W. Novikow, Z. Elektrochem. Angew. Phys. Chem. **15** (1909) 374.
70. H. Freundlich and W. Novikow, Z. Elektrochem. Angew. Phys. Chem. **16** (1910) 394.
71. M. Guainazzi, G. Silvestri, and G. Serravalle, J. C. S. Chem. Comm. (1975) 200.
72. E. Tada, Y. Oishi, and H. Kaneko, Electrochem. Solid-State Lett. **8** (2005) C26.
73. M. Matsushita, M. Sano, Y. Hayakawa, H. Honjo, and Y. Sawada, Phys. Rev. Lett. **53** (1984) 286.
74. T. A. Witten and L. M. Sander, Phys. Rev. Lett. **47** (1981) 1400.
75. C. V. Sternling and L. E. Scriven, AIChE J. **5** (1959) 514.
76. F. Scholz and U. Hasse, Electrochem. Comm. **7** (2005) 541.
77. M. Platt, R. A. W. Dryfe, and E. P. L. Roberts, Electrochim. Acta **49** (2004) 3937.
78. R. A. W. Dryfe, Phys. Chem. Chem. Phys. **8** (2006) 1869.
79. J. F. Llopis and F. Colom, *Encyclopaedia of Electrochemistry of the Elements*, Vol. 6. Marcel Dekker, New York (1976).
80. A. J. Gregory, W. Leavson, R. E. Noftle, R. Le Penven, and D. Pletcher, J. Electroanal. Chem. **399** (1995) 105.
81. J. M. Cosden and R. H. Byrne, Geochim. Cosmochim. Acta **67** (2003) 1331.
82. Y. Gimeno, A. Hernández Creus, P. Carro, S. González, R. C. Salvarezza, and A. J. Arvia, J. Phys. Chem. B **106** (2002) 4232.
83. F. A. Cotton, G. Wilkinson, C. A. Murillo, and M. Bochmann, *Advanced Inorganic Chemistry*, 6th edn. John Wiley & Sons, New York (1999).
84. M. Platt, R. A. W. Dryfe, and E. P. L. Roberts, Electrochim. Acta **48** (2003) 3037.

2 Experimental section

2.1 The System Ag-Microelectrode|AgBr

In order to simplify the system under investigation as much as possible silver bromide single crystals were used as solid silver ion conductors. The main reason is to avoid influences from e. g. grain boundaries as mentioned already in section 1.1.2. Silver bromide single crystals are commercially available and stable under ambient conditions. Additionally, silver bromide is a pure cation conductor with negligible electronic transference number at elevated temperatures. For further details and preparation of the samples see the following article [Peppler2006b] in chapter 2.1.2.

2.1.1 Microelectrodes in Solid State Electrochemistry

Prior to the presentation of the results in the article it is pertinent to briefly discuss the employment of microelectrodes as cathodes in solid state electrochemistry. In contrast to liquid electrochemistry where microelectrodes are rather common the employment of microelectrodes in solid state ionics is seldom the case. Fleig reported on the advantages of microelectrodes in a review article [Fleig2003]. One of the main advantages of microelectrodes is that a reference electrode is not necessarily needed. The reason is a negligible voltage drop at the counter electrode compared to the overpotential at the microelectrode. Another advantage is the possible employment of high current densities at low currents.

In this work microelectrodes were employed for additional reasons. One reason was the observation of the surface during cathodic metal deposition. But the main reason was the atempt to obtain single whiskers instead of arrays of whiskers.

2.1.2 Article: Cathodic Deposition of Silver on Silver Bromide at Microelectrodes [Peppler2006b]

This article is based on own experimental research and was written by myself and coedited by Prof. Jürgen Janek. It was published in a special issue of the journal "Solid State Ionics" and is based on an oral presentation given at the conference "Solid State Ionics 15" (17th-22nd July 2005 in Baden-Baden, Germany).

with permission from Elsevier.

Synopsis

In this article the cathodic metal deposition on solid electrolytes introduced in the previous article [Peppler2006a] in section "2.3 Solid|solid interfaces" is discussed at the example of the system Ag-microelectrode|AgBr. Two distinct morphologies were observed as a result of cathodic deposition. During the application of "high" current densities ($j > 0.6$ A/cm^2; $I > 3.0$ µA, d(Ag-microelectrode) = 25 µm) the growth of dendrites along the surface was observed, at "low" current densities ($j < 0.1$ A/cm^2; $I < 0.5$ µA, d(Ag-microelectrode) = 25 µm) the growth of whiskers perpendicular to the surface. Experiments were conducted at a temperature of $\theta \approx 300$ °C. In chapter 2.1.3 (on page 35) supplementary information from further experiments at other temperatures is given.

Available online at www.sciencedirect.com
ScienceDirect
Solid State Ionics 177 (2006) 1643 – 1648
SOLID STATE IONICS
www.elsevier.com/locate/ssi

Cathodic deposition of silver on silver bromide at microelectrodes

K. Peppler, J. Janek *

Institute of Physical Chemistry, Justus-Liebig University Giessen, Heinrich-Buff-Ring 58, D-35392 Giessen, Germany

Received 29 June 2005; received in revised form 9 December 2005; accepted 12 December 2005

Abstract

The cathodic deposition of silver metal on single crystalline silver bromide leads to deposits with different morphologies depending on the cathode geometry and the current density. The deposition at an extended planar electrode results in the growth of silver whiskers. The deposition at a point (micro-)electrode results in dendritic deposits on the surface of the solid electrolyte. The morphological development of the deposits is studied with microelectrodes of different diameters. A characteristic change from dendritic to whisker growth at microelectrodes upon time is always found. As the reason for the change of the growth mode from dendritic to whisker-type, the changing electric field distribution around a growing surface deposit is discussed.

Keywords: Dendrite; Whisker; Microelectrode; Morphological instability; Electrocrystallization

1. Introduction

Cathodic metal deposition (electrocrystallization) is a fundamental process at electrodes in liquid electrolytes but is still insufficiently investigated in the case of solid electrolytes. Different morphologies of deposits are described in the literature, varying from dendrites on the electrolyte surface [1,2], precipitation in the bulk of the electrolyte crystal [1,3,4] to the formation of single crystalline whiskers [5–7].

Cathodic metal deposition by whisker growth on solid electrolytes has scarcely been investigated. Ohachi and Taniguchi [5] showed that the supersaturation of nonstochiometric silver chalcogenides with silver leads to the spontaneous growth of whiskers on free surfaces of the chalcogenide crystal. Corish and O'Briain [6] where the first to study whisker growth on silver sulfide more quantitatively by relating the growth rate with the silver supersaturation, i. e. the chemical overpotential. A first report on the growth of silver whiskers on silver bromide and the dependence of the number of whiskers per area, their length and diameter on the experimental parameters current (I) and time (t) has been presented by Rohnke et al. [7]. Only few papers deal with the reduction kinetics and thermodynamics at electrodes on solid silver ion conducting electrolytes [8,9]. Yet quantitative and mechanistic information on the growth is still scarce, and compared to the present understanding of electrocrystallization in liquid electrolytes, the level of understanding in the solid state is poor.

Silver bromide is a suitable substrate for cathodic deposition, as it exhibits a high silver ion conductivity (Frenkel disorder) and a negligible electronic conductivity at moderate temperatures around $\theta = 300$ °C. It is available as single crystals and is also stable under ambient conditions. Growth experiments can be performed in a simple cell of the type Ag(anode)|AgBr|Microelectrode(cathode). At the anode the silver metal is oxidized and dissolved, and the silver ions transport the electric charge across the cell. At the cathode, which in our case is usually silver metal too, silver ions from the solid electrolyte are reduced and form the cathodic metal deposit.

2. Experimental setup

2.1. Materials and preparation

Silver bromide single crystals were purchased from Korth Kristall GmbH, cut into small cubes (typically $6 \times 6 \times 3$ mm^3), polished with a fine grained emery paper (particle size 15 μm)

* Corresponding author.
E-mail address: juergen.janek@phys.chemie.uni-giessen.de (J. Janek).
URL: http://www.chemie.uni-giessen.de/home/janek/ (J. Janek).

0167-2738/$ - see front matter © 2005 Elsevier B.V. All rights reserved.
doi:10.1016/j.ssi.2005.12.012

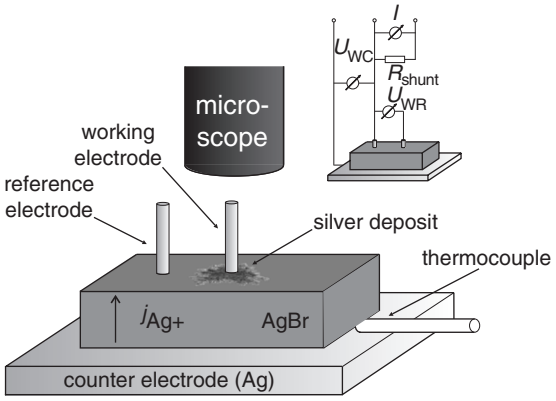

Fig. 1. Experimental setup (schematically) for the electrochemical deposition of silver on silver bromide; (inset) circuit diagram.

and subsequently etched with a $Na_2S_2O_3$ solution. Silver anodes were cut from silver foil with a thickness of 0.5 mm (Chempur, 99.9%) and prepared by grinding and polishing down to 0.25 μm with SiC suspension. The silver microelectrodes with diameters of 100 and 25 μm were prepared by cutting of silver wires with a pair of scissors.

2.2. Cell arrangement

Experiments were performed in a cell arrangement as depicted in Fig. 1. The transference cell Ag|AgBr|Ag was placed on top of a small heating stage mounted on a commercially available Probe Station (PM8 from SUSS MicroTec) used in the semiconductor industry. The cathode is constructed as a microelectrode on the upper side of the silver bromide single crystal. The microelectrode was held in place by a micromanipulator (PH150 from SUSS MicroTec). The reference electrode was also placed on the single crystal surface with a second micromanipulator. The temperature was measured with a thermocouple close to the sample. During silver deposition the temperature was kept constant at about $\theta = 300$ °C. Positioning of the microelectrodes and cathodic deposition of silver on the surface was observed in situ with an optical microscope with its optical axis being perpendicular to the single crystal surface (see Fig. 1). The silver deposits were characterized ex situ with a High Resolution Scanning Electron Microscope (HRSEM, Leo Gemini 982) and by energy-dispersive X-ray (EDX) analysis.

2.3. Experiments

The morphology of the silver deposits was primarily examined as a function of the applied current and the cathode size. The current was varied between 100 nA and 100 μA with a potentiostat (T-1000 from Jaissle) by using a specified ohmic shunt resistance, see inset in Fig. 1. The data acquisition was carried out with a multimeter and a PC (2700 multimeter with 7700 multiplexer from Keithley Instruments). The voltages between the working electrode and the reference electrode (U_{WR}) and between the counter electrode and the working electrode (U_{WC}) were recorded during each experiment as a function of time, together with the temperature.

3. Experimental results

The plasticity of the silver bromide solid electrolyte caused experimental problems in the quantitative reproducibility, but the general features are well reproducible. The cell arrangement under the microscope (in combination with the heating from the bottom side of the cell) always resulted in a large temperature difference between the bottom and the top side of the cell in the range of 20 to 30 K, depending on the thickness of the electrolyte. Thus, a thermovoltage of about $U_{WC} = 20$ mV was measured, which corresponds well with the Seebeck coefficient ε(AgBr, $T = 556$ K) = 882 μV/K of silver bromide as reported by Patrick and Lawson [10]. Under short-circuit conditions, this thermovoltage already led to a current across the cell, resulting in the deposition of silver metal (in the form of dendrites) at the cold upper side. Between the working electrode and the reference electrode, which are both placed on the upper side of the ion conductor, a thermovoltage in the

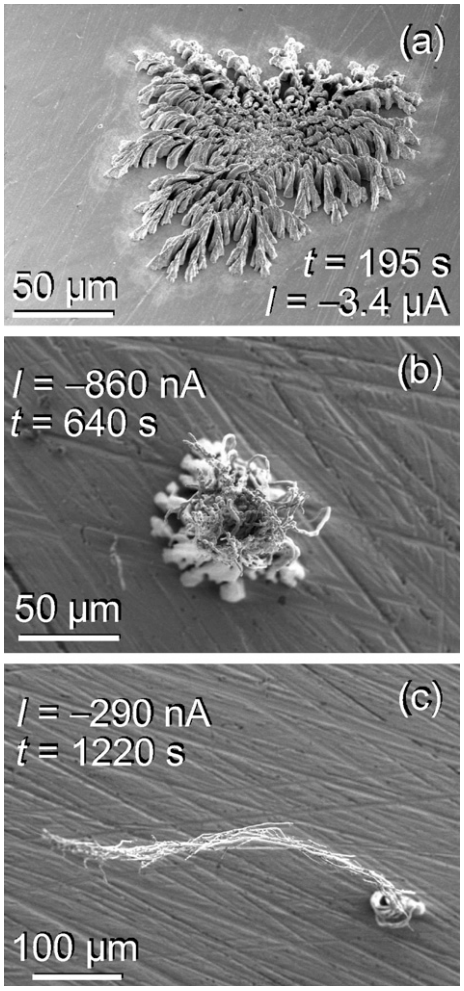

Fig. 2. HRSEM pictures: (a) dendrite: $I = -3.4$ μA, $\theta = 308$ °C, $t = 195$ s, Ø working electrode = 25 μm, (b) transition dendrite–whisker: $I = -860$ nA, $\theta = 305$ °C, $t = 640$ s, Ø working electrode = 25 μm, (c) whisker: $I = -290$ nA, $\theta = 305$ °C, $t = 1220$ s, Ø working electrode = 25 μm.

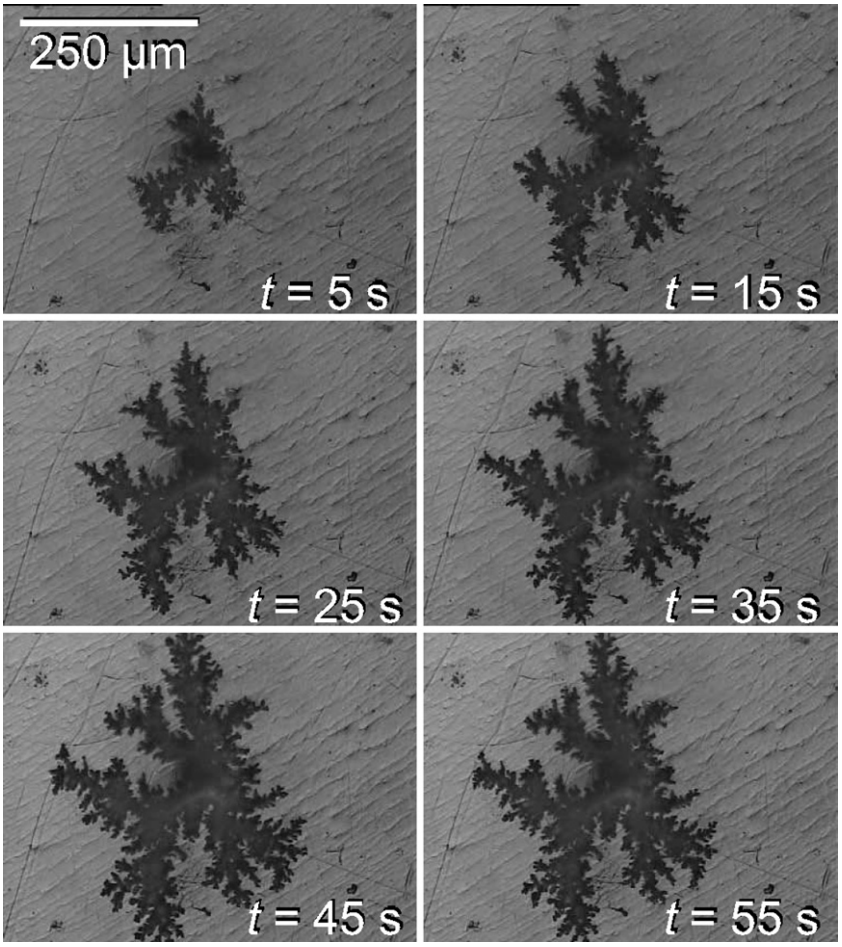

Fig. 3. Sequence of optical pictures taken during dendrite growth on silver bromide surface ($I=-57$ µA, $\theta=322$ °C, Ø working electrode=25 µm).

range of about $U_{WR}=-15$ mV was measured. The reason for this lateral thermovoltage is twofold: Firstly, both microelectrodes have different diameters and therefore suffer from a different heat loss by thermal conduction. Secondly, the reference electrode is placed near the colder edge of the electrolyte, whereas the working electrode is placed at the center of the electrolyte (cf. Fig. 1). However, assuming stationary thermal conditions during each experiment the thermovoltages can be considered as being constant. In order to obtain the net-cathodic overvoltage, the thermovoltage has to be subtracted as a constant off-set.

The deposition of silver at microelectrodes led to two different morphologies: depending on the applied current and electrode diameter a transition from dendrite to whisker growth occurred (cf. Fig. 2). The volume of the cathodic silver deposit can be calculated according to Faraday's laws, as the current is

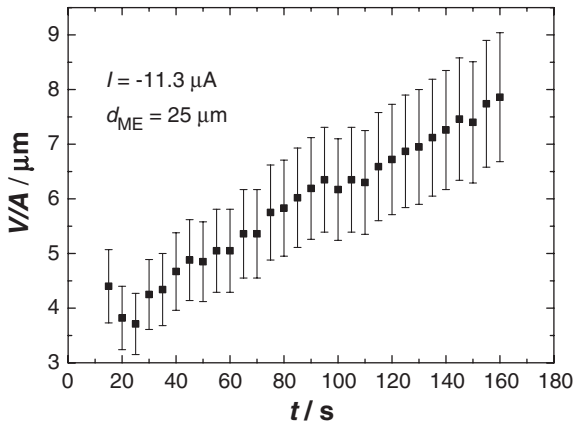

Fig. 4. Time dependent ratio between volume and interface area of a dendrite; $I=-11.3$ µA, $\theta=322$ °C.

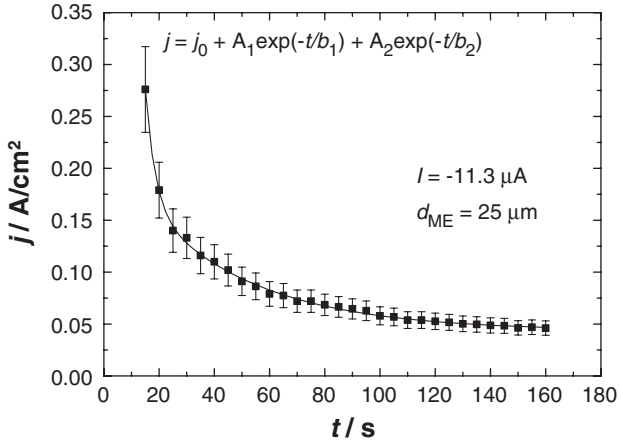

Fig. 5. Time dependence of current density during dendrite growth, $I=-11.3$ µA, $\theta=322$ °C, $j_0=(4.4\pm1.3)\cdot10^{-2}$ A/cm^2, $A_1=(7.1\pm2.3)$ A/cm^2, $b_1=(3.6\pm0.3)$ s, $A_2=(0.174\pm0.008)$ A/cm^2, $b_2=(40.2\pm2.2)$ s.

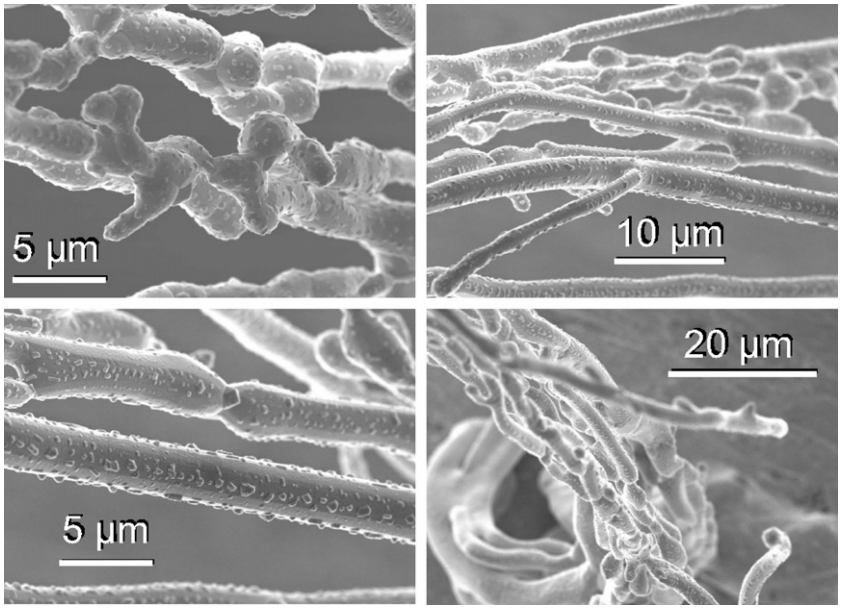

Fig. 6. HRSEM pictures of various sections of the whisker in Fig. 2(c): $I=-290$ nA, $\theta=305$ °C, $t=1220$ s, Ø working electrode=25 µm.

exclusively ionic. Thus, the time integral yields the amount of deposited silver.

3.1. Dendrite growth

The area of the deposit was determined from optical micrographs. The ratio of the deposit volume and the interface area V/A (i.e. the mean height) always increased with time, following an almost linear relation (cf. Figs. 3 and 4), but the aspect ratio is very low. However, the almost linear increase of V/A with time indicates that the growth vertical to the surface is always dominating.

During a typical long time experiment ($t=25.4$ h) at a current of 10 µA the dendrite covered a surface of 0.13 mm^2 at $t=22$ min ($j=1.1\cdot10^{-2}$ A/cm^2) and of 1.68 mm^2 at $t=25.4$ h ($j=7.4\cdot10^{-4}$ A/cm^2). Due to the increasing interface area during dendrite growth the current density always decayed exponentially.

The experimental data are best described by a double exponential fit function, see Fig. 5. We have yet no physical explanation for this specific dependence.

3.2. Whisker growth

During experiments with currents lower than 500 nA the silver deposition occurred only perpendicular to the surface in the form of whiskers. Dendrite growth parallel to the surface was not observed. The whiskers were not straight and uniform in diameter, they were often twinned or multitwinned and partially fused together in bundles. Due to the experimental difficulties of separating and preparing single whiskers without damage, we have not yet obtained crystallographic information on the whisker structure. The individual whiskers in the bundles were polygonal and covered with small crystallites, presumably of silver. The diameters of the whiskers were in the range of 1 to 10 µm (cf. Figs. 2(c) and 6).

In most cases the whisker adhered better to the microelectrode tip rather than to the silver bromide surface when the microelectrode was detached after the experiment. Thus, it was possible to document the morphological change of the electrolyte surface at the site of whisker growth (cf. Fig. 7).

We observed two different changes of the surface: either the whiskers did not grow into the electrolyte and the surface was only changed slightly, or the whiskers grew into the electrolyte and left holes after removal (cf. Fig. 7). We found no systematical correlation between this behaviour and the experimental conditions within our data.

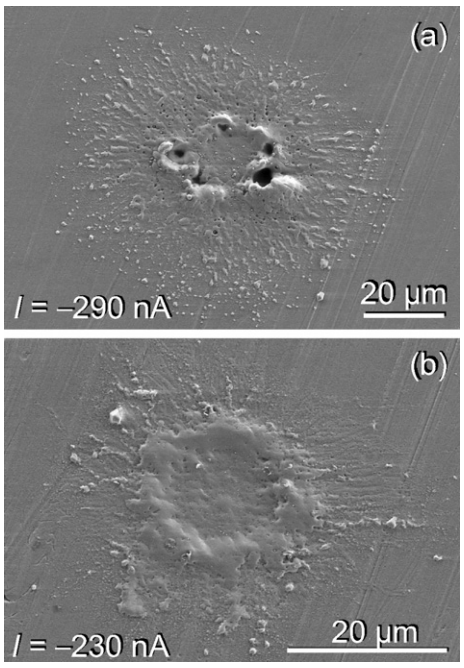

Fig. 7. HRSEM pictures of area of whisker growth after removal of whisker: (a) $I=-290$ nA, $\theta=308$ °C, Ø working electrode=25 µm, (b) $I=-230$ nA, $\theta=306$ °C, Ø working electrode=25 µm.

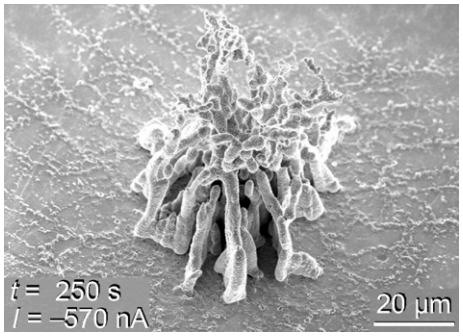

Fig. 8. HRSEM picture of the transition between whisker and dendrite growth: $I=-570$ nA, $\theta=308$ °C, $t=250$ s.

3.3. Transition whisker–dendrite growth

The transition between whisker and dendrite growth is gradual, and the contact area of a dendrite–whisker deposit with silver bromide always increased with time (cf. Figs. 2(b) and 8). In the case of a microelectrode with a diameter of 25 μm, currents greater than about 3 μA caused dendrite growth, currents smaller than about 0.5 μA led to whisker growth.

The voltage drop U_{WR} during the growth of dendrites or whiskers exhibits a characteristic difference. During whisker growth the absolute value of the voltage U_{WR} is increasing after the microelectrode is applied to the electrolyte until it reaches a constant value. During dendrite growth the absolute value of the voltage U_{WR} is decreasing until it reaches a constant value (cf. Fig. 9).

4. Discussion

As described in a previous report [7], the deposition of silver at spatially extended cathodes leads to the growth of silver whiskers between the electrolyte and the cathode. In contrast, the cathodic deposition of silver on microelectrodes leads to two different growth modes, either of dendrite- or whisker-type, depending on the experimental conditions. Assuming that the size of the cathode and the distribution of the electric field influence the growth mode, two aspects have to be taken into account:

(i) The electric field distribution at point contacts is different compared to extended planar electrodes (equipotential planes are parallel to the electrode surface, current lines are perpendicular). Assuming a hemispherical electrode geometry the equipotential planes are hemispherical and the current lines are radial (perpendicular to the equipotential lines). This is only slightly changed in the case of circular electrode geometry.

(ii) Depending on sample preparation, a highly conducting surface layer as described by Fleig at al. [11] for silver chloride may be present. Such a surface layer would cause a more homogeneous distribution of field lines, but also a significant surface current.

Both effects together cause a higher current parallel to the surface of the solid electrolyte around the point electrode. Hence, deposition of silver parallel to the surface of the electrolyte starting at the microelectrode takes place, resulting in the growth of dendrites. Therefore, whisker growth appears to be possible only if the applied current (i. e. voltage) is low enough or if we can neglect current lines parallel to the surface due to an appropriate electrode design.

The explanation why the growth rate of dendrites parallel to the surface decreases with time can also be ascribed to the distribution of the electric field. Due to the increasing area which is covered with silver the configuration of the cathode changes from a point contact to an extended electrode. Thus, the components of the current lines parallel to the surface become smaller with increasing area of the cathode. A further clue for the dependence of the morphology on the condition of the electrolyte surface is described by Spangenberg et al. in a report on “electromechanical writing on silver ion conductors” [8]. The cathodic silver deposition occurs preferentially in mechanically prestructured scratches on the electrolyte surface. The authors assume that the deposition is related to the higher surface energy in such scratches, which can result in enhanced nucleation rates.

We have yet no explanation for the difference in the time behaviour of the voltage U_{WR} during whisker and dendrite growth. We can exclude a voltage drop along the growing whisker due to the high electronic conductivity of silver metal. It may be possible that the heat radiation of the whisker bundles is greater than the heat radiation of the microelectrode (due to a greater ratio of surface to volume), thus leading to an enhanced local cooling resulting in an increase of the thermovoltage.

The observed holes in the electrolyte surface after the mechanical removal of a grown whisker correspond well with the observations of Rohnke et al. [7]. They describe three different types of whisker roots which are all grown into the solid electrolyte. It is not clear whether this fact has to be explained by plastic deformation of the relatively soft silver bromide single crystal at temperatures around $\theta=300$ °C or if it is directly related to the nucleation process.

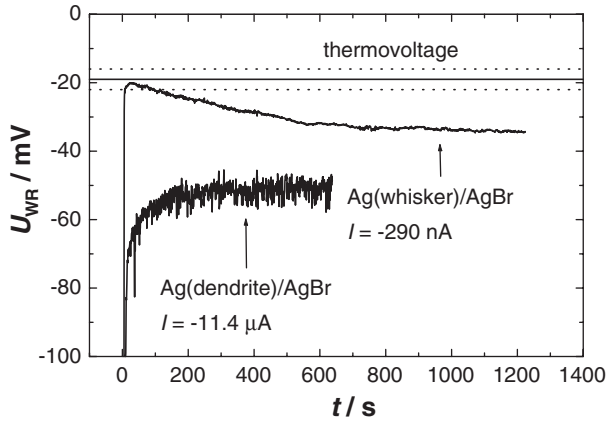

Fig. 9. Time dependence of voltage during dendrite growth: $I=-11.4$ μA, $\theta=305$ °C, Ø working electrode=100 μm, and whisker growth; $I=-290$ nA, $\theta=315$ °C, Ø working electrode=25 μm (– thermovoltage,...margin of error).

As mentioned above Ohachi and Taniguchi [5] and Corish and O'Briain [6] reported on the growth of silver whiskers on silver chalcogenides. The growth method of their whiskers is also different, as they produced whiskers by supersaturation. Thus, the place of whisker growth could not be controlled by an electrode process.

The cathodic deposition process of silver as performed by Spangenberg et al. [1,8] on silver chloride is very similar to our approach, as they used microelectrodes as well. Due to the fact that silver chloride and bromide are virtually chemical "twins", it is possible to compare their results with our observations.

In any case, it is necessary to control the experimental parameters for a defined dendrite or whisker growth precisely, including electrode geometry and surface preparation. It will also be instructive to measure the emf of whiskers and dendrites at different states of growth versus a reference electrode. Size effects influence the emf especially on the nanoscale and also lead to additional influences on the morphology, as discussed in detail by Schroeder et al. [9].

5. Conclusion

The morphology of cathodically deposited silver on solid silver ion conductors depends strongly on the experimental parameters, such as electrode geometry, applied current and surface condition. Planar extended electrodes lead to growth of silver whisker arrays [7]. At microelectrodes the morphology depends on the applied current. Dendritic growth always occurred at higher currents ($I > 3$ μA), while whisker bundle growth occurred at lower currents ($I < 0.5$ μA). Thus, there is a change in morphology depending on the applied current. We assume that the electric field distribution at the microelectrode is responsible for the different growth modes.

Acknowledgements

This study was funded by the DFG (Deutsche Forschungsgemeinschaft) within the projects Ja648/6-1 and 6-2. Financial support by the FCI (Fonds der Chemischen Industrie) is also gratefully acknowledged.

References

[1] A. Spangenberg, dissertation, Max-Planck-Institut für Festkörperforschung, Stuttgart 2001.
[2] J. Janek, professorial dissertation, University Hannover, 1997.
[3] G. Schulz, diploma thesis, University Hannover, 1991.
[4] S. Majoni, dissertation, University Hannover, 1995.
[5] T. Ohachi, I. Taniguchi, J. Cryst. Growth 24/25 (1974) 362.
[6] J. Corish, D. O'Briain, J. Cryst. Growth 13/14 (1972) 62.
[7] M. Rohnke, T. Best, J. Janek, J. Solid State Electrochem. 9 (4) (2005) 239.
[8] A. Spangenberg, J. Fleig, J. Maier, Adv. Mater. 13 (2001) 1466.
[9] A. Schroeder, J. Fleig, H. Drings, R. Wuerschum, J. Maier, W. Sitte, Solid State Ion. 173 (2004) 95.
[10] L. Patrick, W. Lawson, J. Chem. Phys. 22 (9) (1954) 1492.
[11] J. Fleig, F. Noll, J. Maier, Ber. Bunsenges. Phys. Chem. 100 (1996) 607.

2.1.3 Supplementary Information

In the previous article (chapter 2.1.2 on page 27) only the current densities and the diameters of the microelectrodes were altered, the remaining conditions were kept constant. In proceeding experiments the temperature as additional parameter has been varied, too. At first the changes in morphology of dendrites will be presented, at second the changes in the morphology of whiskers. Both observations will then briefly be discussed.

Changes in Morphology of Dendrites with Temperature

Dendrites which were deposited at the same temperature but with different currents are very similar in morphology. Thus, it is impossible to decide by the morphology of the dendrites depicted in fig. (2.1) a) and b) whether they were deposited with different currents. The same can be said for the dendrites depicted in fig. (2.1) c), they resemble each other. But the difference between the dendrites at the left side which were deposited at a temperature of $\theta = 275$ °C and the dendrites at the right side which were deposited at a temperature of $\theta = 175$ °C is evident. At the higher temperature the dendrite shape is "rounder" and shows less sharpe tips.

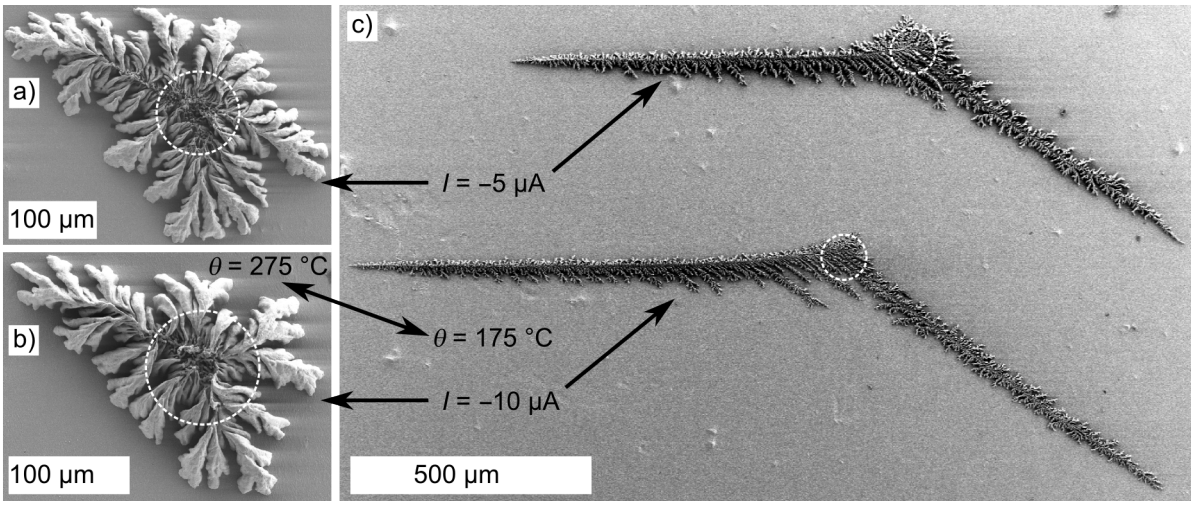

Figure 2.1: SEM images of dendrites deposited under different conditions: a) and b) Dendrites deposited at a temperature of $\theta = 275$ °C with different currents (a) $I = -5$ µA, b) $I = -10$ µA); c) Dendrites deposited at a temperature of $\theta = 175$ °C with different currents (above $I = -5$ µA, below $I = -10$ µA). The morphology is governed mainly by the temperature and not by the current density. The white dotted circles show the position of the microelectrode during deposition (d(Ag-microelectrode) = 100 µm, $t \approx 600$ s).

The reason why dendrites deposited at the same temperature but with different cur-

rents are so alike is relatively simple. During the growth of the dendrite the contact area between electrolyte and dendrite increases. Thus, the electrochemical active area also increases and the current density decreases. Taking the dendrite deposited with the higher applied current as starting point, it will reach at a certain time the same value of current density as the dendrite deposited with a lower applied current.

Comparing the dendrites deposited at different temperatures in fig. (2.1) the change from a more "isotropic" morphology at higher temperatures to an "anisotropic" morphology with preferential growth in two distinct directions at lower temperatures is apparent. Taking a closer look at dendrites deposited at lower temperatures reveals even more dramatic changes in the morphology, compared to dendrites deposited at higher temperatures. It can clearly be seen that the dendrites consist of whiskers which are connected to each other, see fig. (2.2) on page 39. The whiskers had diameters in the order of a few hundreds of nanometers, see fig. (2.2) b)-d). Thus, it is evident that the temperature plays a greater role on the resulting morphology than the current, i. e. the current density. At these lower temperatures of about 150 ℃ to 175 ℃ the voltage drop measured between the microelectrode and the counter electrode is about one order of magnitude higher than at temperatures around 275 ℃ to 300 ℃. Thus, the voltage drop is in the order of several hundreds of millivolts instead of several tens of millivolts, cf. results presented in the previous article [Peppler2006b] in chapter 2.1.2 on page 27.

Schroeder reported on a similar effect upon the cathodic deposition of silver at microelectrodes on silver chloride single crystals. But, instead of temperature the applied bias voltage was changed. Applying low bias voltages dendrites with "isotropic" morphology were deposited, with increasing bias voltages the morphology became increasingly "anisotropic" [Schroeder2004, cf. chapter 5.2.1].

Changes in Morphology of Whiskers with Temperature

Comparing whiskers deposited at different temperatures a change from a rather "isotropic" morphology with whisker diameters in the order of a few micrometers, see fig. (2.3) a) and b) on page 40, to a filigrane network of whiskers with diameters in the order of several hundreds of nanometers, see fig. (2.3) c) and d), is apparent. Thus, for the growth of whiskers in general terms the same change in morphology is observed as for dendrites.

The whiskers preferred to adhere to the microelectrode during lift-off (as already mentioned in the previous article [Peppler2006b] in chapter 2.1.2 in section 3.2 "Whisker growth"). Thus, the whiskers depicted in fig. 2.3 were mechanically stressed and deformed before they were investigated in the SEM. Especially the filigrane networks of the whiskers deposited at low temperature, cf. fig. 2.3 c) and d) on page 40 suffered from mechanical strain. Looking at the time series of images taken during the growth of a whisker network at $\theta = 150$ ℃, cf. fig. (2.4) on page 41, the morphology looked in the first seconds like one of the dendrites depicted in figs. (2.1) c) and (2.2) a). After this initial dendritic growth along the surface the growth changed to an increase of height, i. e. into the growth of a whisker network. The growth along the surface ceased when

growth in height started.

Disscussion of the Change in Morphology

Several parameters depend on the temperature. For instance, the bulk conductivity of the electrolyte decreases with decreasing temperature, and the surface energy increases slightly with decreasing temperature. Thus, the resistance between microelectrode and electrolyte increases with a decrease in temperature. Microelectrodes can be treated as constriction resistances, hence with decreasing bulk conductivity the bulk (or spreading) resistance increases according to equation (2.1) [Fleig2003].

$$R_{\mathrm{spr}} = \frac{1}{2 \cdot d_{\mathrm{ME}} \cdot \sigma_{\mathrm{bulk}}} \tag{2.1}$$

R_{spr} = spreading resistance
d_{ME} = diameter of microelectrode
σ_{bulk} = bulk conductivity of electrolyte

Thus, the overvoltage at a given current increases with decreasing temperature, as it has been observed. According to the classical approach of Volmer and Weber for liquid systems the nucleation rate for cathodic metal deposition depends on the surface energy of the nucleus and the overpotential [Budevski1996, chapter 4.2].

$$J = A_{\mathrm{3D}} \cdot \exp\left(-\frac{4 \cdot B \cdot V_{\mathrm{m}}^2 \cdot \sigma^3}{27 \cdot (z \cdot e \cdot |\eta|)^2 \cdot k \cdot T}\right) \tag{2.2}$$

J = rate of nucleation
A_{3D} = preexponential factor for 3-dimensional nucleation
B = constant depending on geometry (e. g. $B = 36\pi$ for a sphere)
V_{m} = volume occupied by one atom in the crystal lattice
σ = average specific surface energy of nucleus
η = overvoltage

The influence on the nucleation rate caused by the increase of the surface energy of silver can be neglected with respect to the increase of the overvoltage. Starting at the melting point of silver the surface energy increases only from 1.046 J/m^2 to 1.302 J/m^2 at room temperature [Giber1982], thus a decrease of only 100 °C implies only a minimal change. Even when the surface energy goes with the power of three into equation (2.2) the resulting factor is only about 1.3 for an increase of surface energy by 0.1 J/m^2. The change of one order of magnitude of the overvoltage results in a factor of about 100, because the overvoltage goes in with the power of two. Thus, the nucleation rate increases with decreasing temperature. The consequence is the observed "isotropic" growth at higher temperatures, where the growth of initially formed nucleii is favored compared to

the formation of new nucleii. During the "anisotropic" growth at lower temperatures the formation of new nucleii is favored. The reason for the preferential growth in two distinct directions might be related to the growth along designated crystallographic directions of the silver bromide single crystal. Especially the fact that on the same crystal always the same two distinct directions were observed supports this hypothesis, see fig. (2.1) c) on page 35. But the orientation of the employed single crystals was unknown, thus there is no information in which crystallographic directions the growth occured. The attempt to obtain the orientation of silver bromide single crystals by electron backscatter diffraction (EBSD) failed, because of the sensitivity of the silver bromide to the electron beam of the electron microscope.

It was not possible to grow single whiskers using this procedure. In order to obtain a single whisker it is probably necessary to further reduce the size of the microelectrode and enhance the resolution of the observation field. Then it might be possible to obtain a single whisker by contacting one silver nucleus with the tip of a "nanoelectrode" and let only this nucleus grow, see also outlook in chapter 3.2.

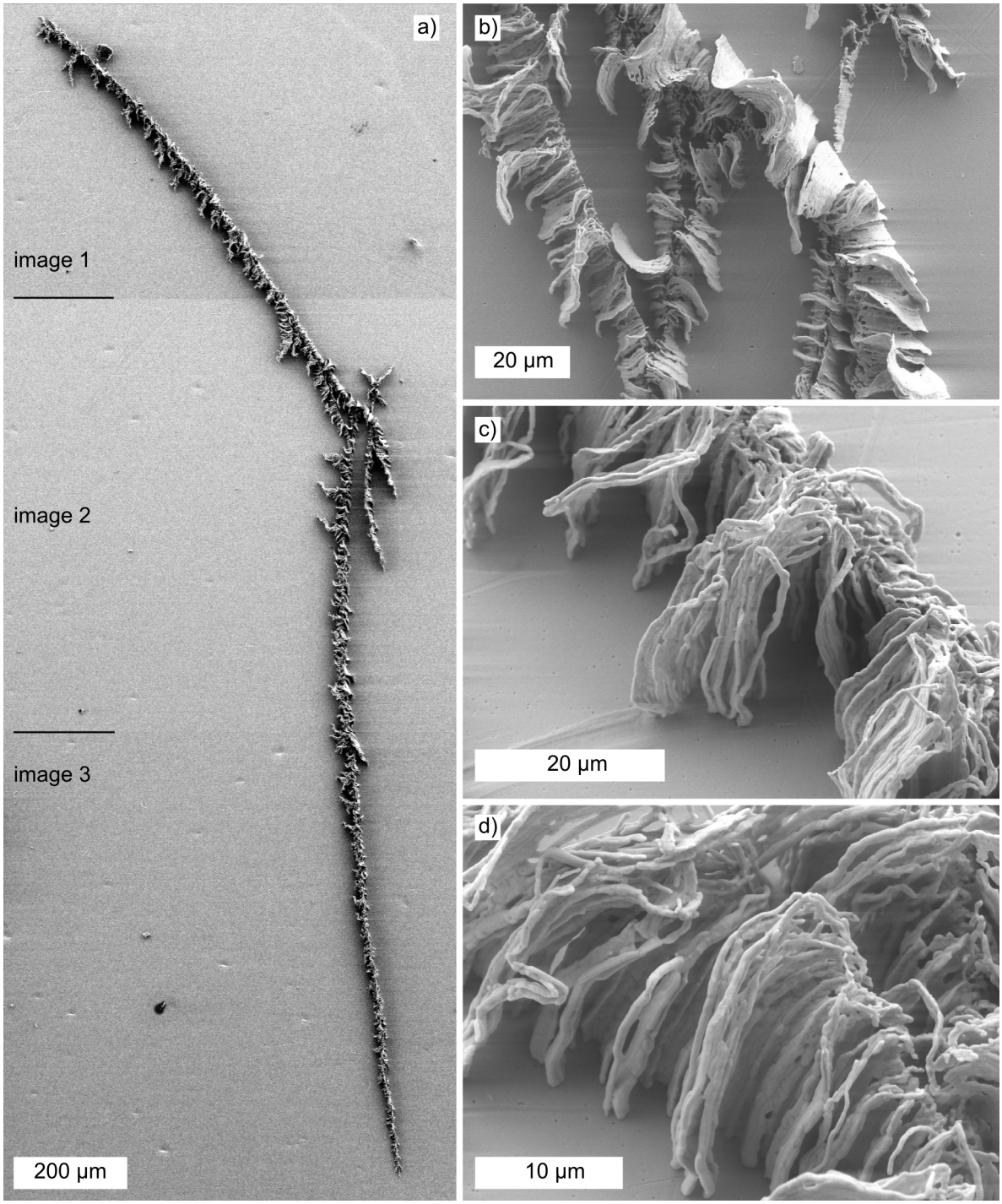

Figure 2.2: SEM images of a dendrite deposited at low temperature: a) Mosaic of three SEM images, b - d) magnifications of a) (d(Ag-microelectrode) = 25 µm, θ = 150 °C, $I = -4.9$ µA, t = 295 s).

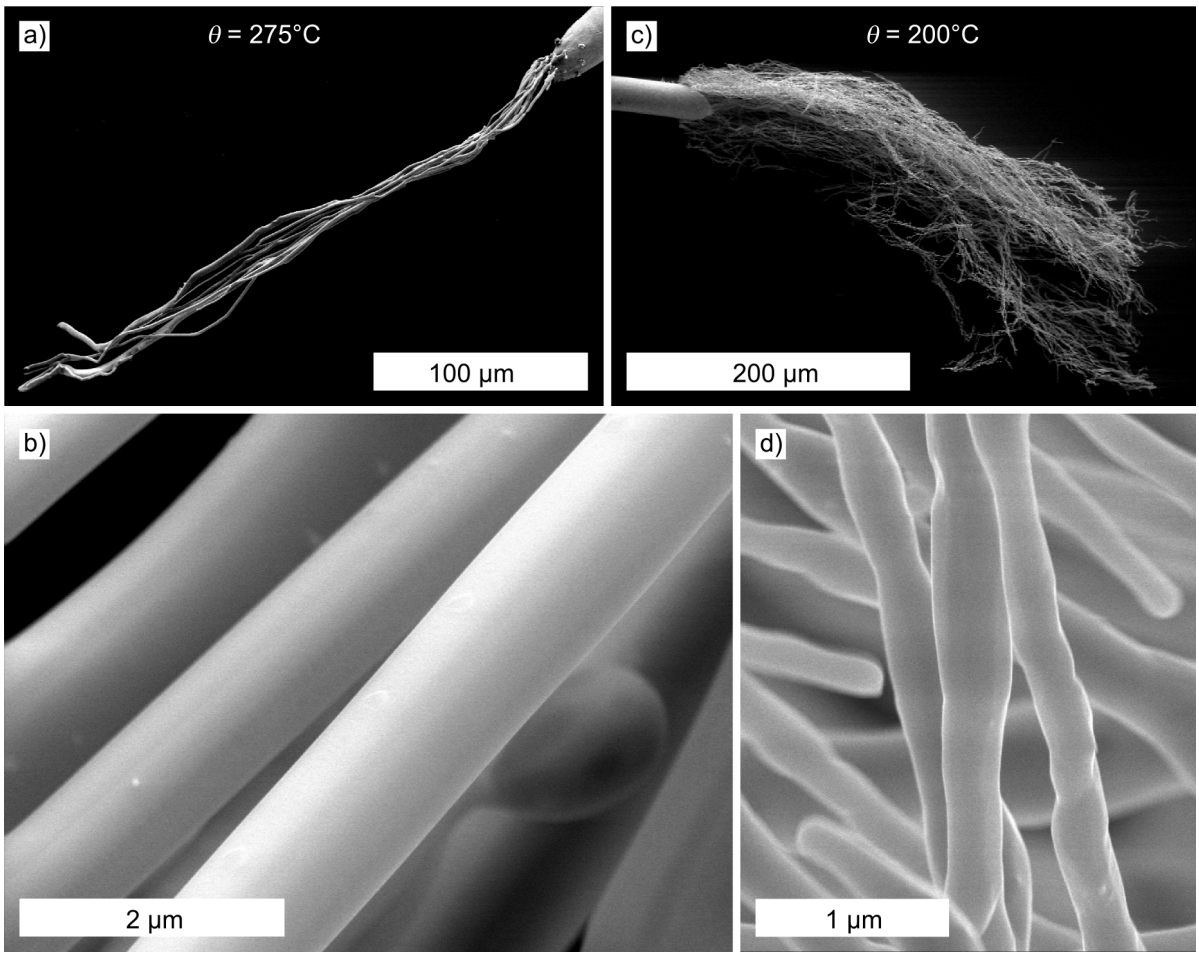

Figure 2.3: SEM images of whiskers which adhered to the microelectrode: a) d(Ag-microelectrode) = 25 µm, θ = 275 °C, I = −0.24 µA, t = 340 s, b) magnification of a), c) d(Ag-microelectrode) = 25 µm, θ = 200 °C, I = −0.48 µA, t ≈ 300 s, d) magnification of c).

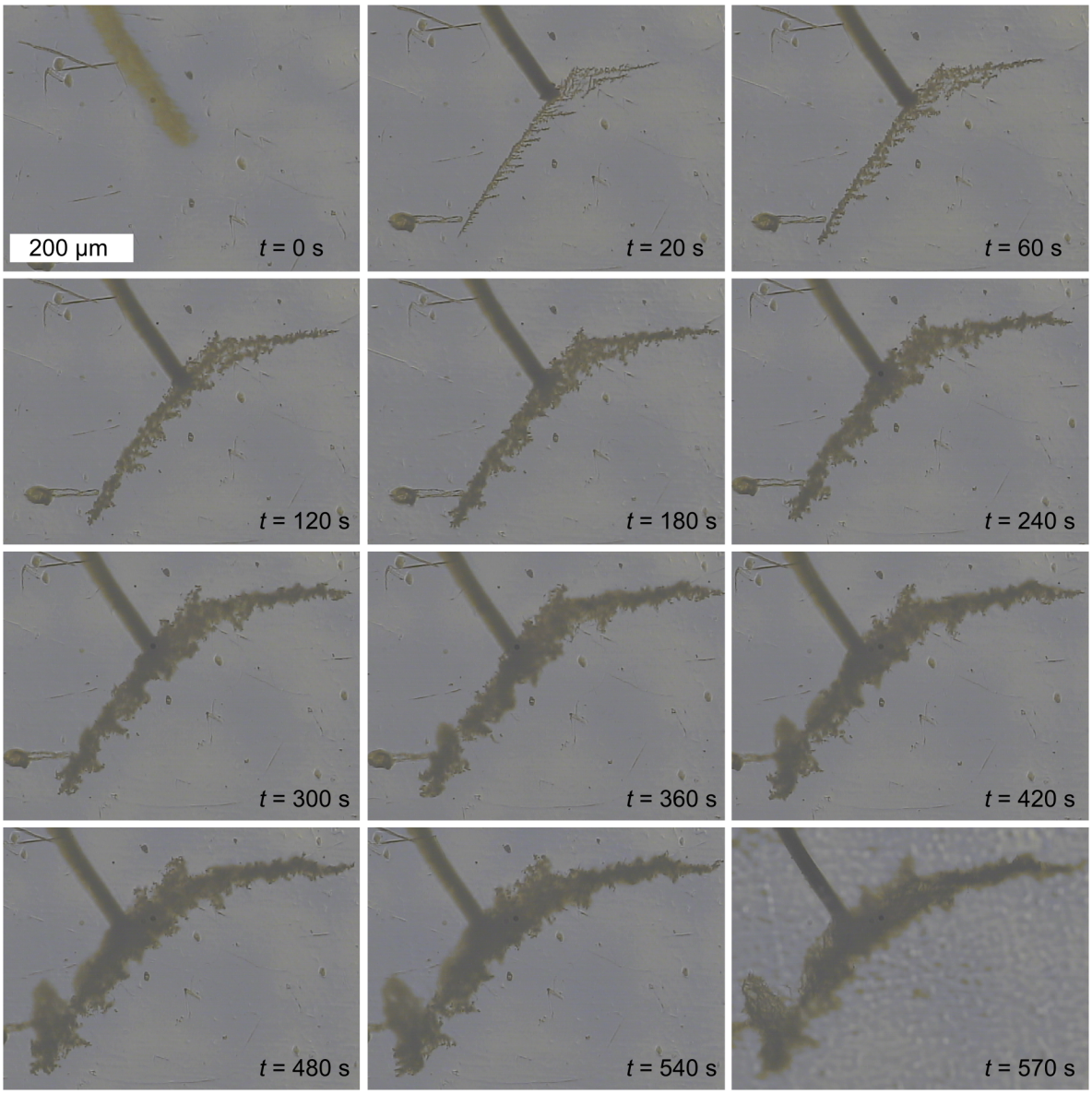

Figure 2.4: Time series of pictures taken with an optical microscope during the growth of a filigrane network of whiskers. At first dendritic growth occurred, but ceased after a few seconds. Then growth into height started without further growth along the surface. (d(Ag-microelectrode) = 25 µm, θ = 150 °C, I = −0.25 µA)

2.2 Stability of as-deposited Metal Particles in external Electric Fields

Besides the thermodynamic and kinetic stability of as-deposited metal structures on solid electrolytes, the stability in external electric fields has to be considered, too. Thinking of possible applications of solid state ionics in current and future devices for e. g. data storage (cf. article [Peppler2009] in chapter 3.1.1 on page 59), the behavior of metal particles on solid electrolytes in external electric fields is an important issue.

2.2.1 Article: Field driven Migration of Bipolar Metal Particles on Solid Electrolytes [Peppler2008]

The following article is based on a study project, experiments were carried out under my close supervision by Christian Reitz, an undergraduate student of materials science. Preliminary work leading to these investigations and also final work has been done by myself. The article was written by myself and co-edited by Prof. Jürgen Janek.

Reprinted with permission from K. Peppler, C. Reitz and J. Janek, Applied Physics Letters, Vol. 93, Page 074104, American Institute of Physics.

Synopsis

A silver particle, which was electronically but not ionically isolated on a silver bromide single crystal surface (in this case a dendrite deposited prior to the experiment), was exposed to an external electric field. The field was generated by the application of a voltage between two planar silver electrodes on the same electrolyte surface with the particle in the middle. Thus, the particle was polarized and became a bipolar electrode. Hence, silver was dissolved at the anodic side of the particle. The remaining electrons migrated in the field to the cathodic side of the particle where they discharged silver ions, i. e. silver deposition took place. Thus, the silver particle move towards the external anode. Interestingly a new kind of morphology occured at the cathodic side of the particle. The deposition took place in the form of a silver film, which has never been reported before in literature.

Field-driven migration of bipolar metal particles on solid electrolytes

Klaus Peppler, Christian Reitz, and Jürgen Janek[a)]
Institute of Physical Chemistry, Justus Liebig University, Heinrich-Buff-Ring 58, 35392 Giessen, Germany

(Received 10 March 2008; accepted 23 July 2008; published online 22 August 2008)

A metal particle, which is not electronically contacted but is electrically contacted by a purely cation conducting solid electrolyte, is driven into the direction of the anode when an external electric field is applied. The particle behaves as a bipolar electrode. During the field-driven movement, the metal particle changes its morphology and spreads across the surface. This process is studied *in situ* with an optical microscope and *ex situ* with a scanning electron microscope. It is discussed as an example of morphological instabilities in solid state transport. © *2008 American Institute of Physics*. [DOI: 10.1063/1.2973042]

Growth and dissolution at electrodes are fundamental kinetic processes in electrochemistry. They occur at interfaces between a phase with predominant ionic conduction and a phase with predominant electronic conduction. Here we report on the field-driven movement of metal particles that are not directly electronically connected with an external circuit but are electrically contacted by a solid electrolyte. In the case of batteries, a loose electrode particle inside the electrolyte represents such bipolar arrangement that might lead to an undesired local electronic short-circuit and resistance degradation.[1,2] In the case of mixed conducting resistive switching systems, it leads to a desired growth of conductive paths.[3–5]

We used a setup as depicted in Fig. 1 for the *in situ* observation of field-driven migration of silver metal particles on a solid electrolyte, in our case, a silver bromide single crystal (AgBr), with an optical microscope. In order to attain a sufficiently high silver ion conductivity, the sample was heated to a temperature of about 570 K. At the beginning of each experiment, a small amount of silver with dendritic morphology was deposited on the AgBr surface with a microelectrode as cathode on the top side of the electrolyte and a silver foil as counter electrode at the bottom, as described in Ref. 6. After the microelectrode was removed, two silver electrodes were placed on the electrolyte [Figs. 1(a) and 1(b)]. To improve contact between the electrolyte and the electrodes, silver was electrodeposited under the electrodes prior to the experiments. Finally the bottom counter electrode was removed and the sample was placed on an alumina disk.

The deposition of silver in form of dendrites on the surface can be explained by a morphological stability analysis.[7–10] Any convexity at the silver cathode, i.e., the AgBr|Ag(−) interface, increases the local electric field and thus the silver ion flux to its tip. As a consequence, the boundary at the tip moves faster than the surrounding boundary and the interface is morphologically unstable. A prediction of the exact morphology is not possible.

By applying voltage to the electrodes, the silver particle is polarized and becomes a bipolar electrode. The sequence in Fig. 2 (see also online animation in Ref. 11) shows the migration of such bipolar dendrite on AgBr. The dendrite was dissolved at its anodic side and grew at its cathodic side, giving the semblance of a silver film moving toward the anode. The deposition of silver at the cathodic side of the dendrite is caused by the higher gradient of the potential $\nabla\varphi(y_2)$ compared to the one without dendrite $\nabla\varphi(y_1)$ [see Fig. 1(c)]. In the given example, the increase in $\nabla\varphi(y_2)$ along the roughly 60 μm wide silver dendrite is about 3.5 V/m. Compared to the applied field of about 200 V/m, this is roughly 1.5%, and with the growing silver film the gradient also increases. At the end of the experiment (Fig. 3), the increase was about 20 V/m (9%). Despite the increase in the driving force, the speed of the advancing silver film was

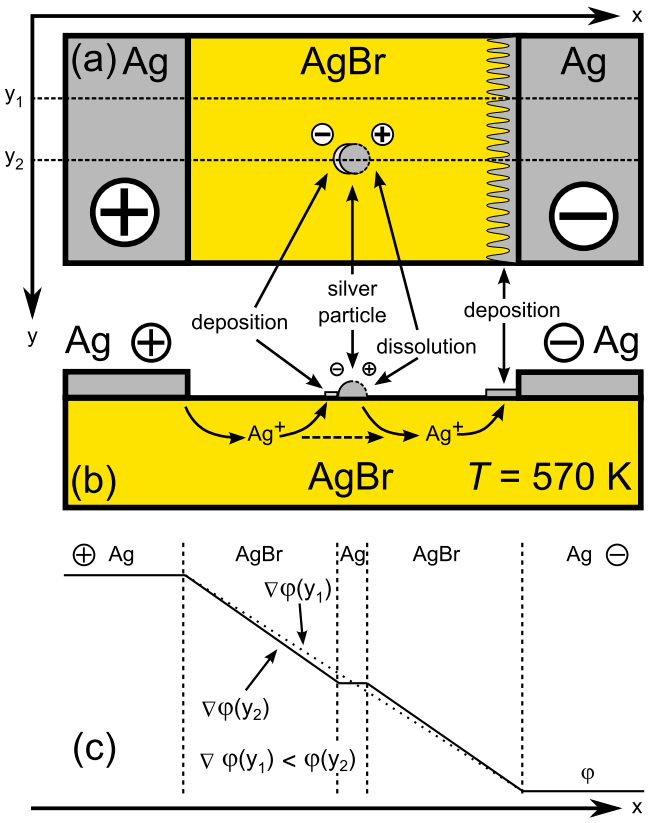

FIG. 1. (Color online) Sketch of setup. Two silver foils at the left and right sides on top of a AgBr single crystal act as electrodes ($d \approx 3.5$ mm). During polarization, the anode is dissolved and silver is deposited at the cathode. A silver particle between the electrodes becomes a bipolar electrode and is accordingly dissolved at its anodic side while silver is deposited at its cathodic side. (a) Top view, (b) side view, and (c) the schematic potential curve.

[a)]Electronic mail: juergen.janek@chemie.uni-giessen.de.

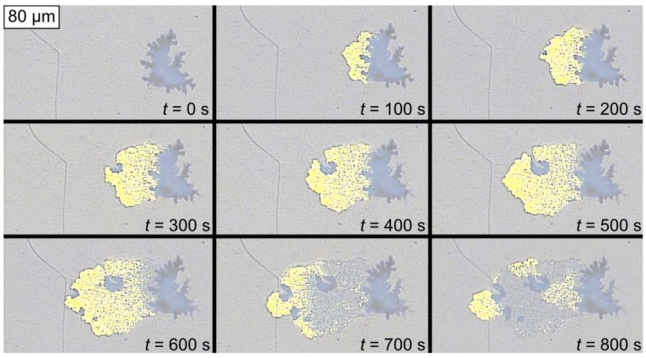

FIG. 2. (Color online) Sequence of optical pictures. The cathode was at the right side and the anode was at the left side. The polarized dendrite was dissolved at its anodic side (right) and silver was deposited at its cathodic side (left), $U=750$ mV, $d\approx 3.6$ mm, and $E\approx 200$ V/m [animation online (Ref. 11)].

constant, being approximately 0.22 ± 0.1 μm/s. Utilizing galvanostatic conditions, the migration speed correlated with the variation in the potential applied by the galvanostate. When the contact between the dendrite and the "moving" silver film was broken, the isolated film itself became bipolar, too, and dissolved at its anodic side, moving independently and leading to oscillatory behavior. Formations of dendritelike structures were also observed. By inspecting the migrated dendrite *ex situ*, the dissolution of the dendrite at its anodic side is evident [see Fig. 3(a)]. The initially formed silver film lost its coherence during the experiment [see Fig. 2]. After the experiment, the freshly formed silver film was fully disintegrated [see Fig. 3(b)]. Whereas the growth of dendrites and whiskers on solid electrolytes is a long known phenomenon,[12–15] this electrochemical migration of thin silver films on solid electrolytes has not been reported before.

In order to observe this migration, a specific preparation of the AgBr surface was necessary. When the surface of the AgBr single crystal was merely polished with a fine emery paper, experiments typically led to the fast growth of silver from the cathode to the anode. In Fig. 4 a sequence of pictures taken during the polarization shows such overgrowth from the cathode. The start of the migration of the dendrite in the electric field can also be seen. Obviously the mechanical treatment of the AgBr single crystal surface with emery paper created disordered regions, and the growth of dendrites on the surface is enhanced. Fleig *et al.*[16] investigated the

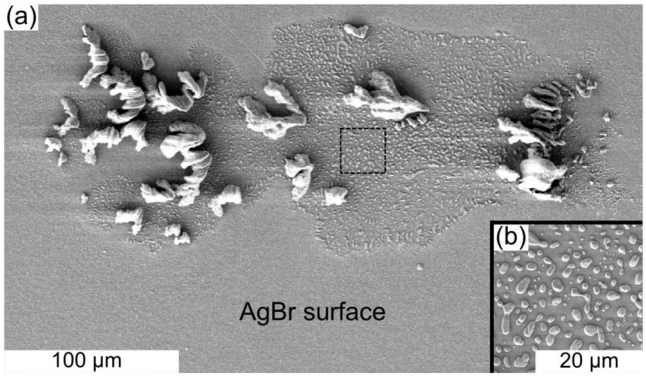

FIG. 3. High scanning electron microscope (HSEM) pictures of the same experiment as in Fig. 2. (a) The dissolution of the dendrite at its anodic side (right) and deposition of silver at its cathodic side (left) can be seen clearly. (b) Magnification of the disintegrated silver film.

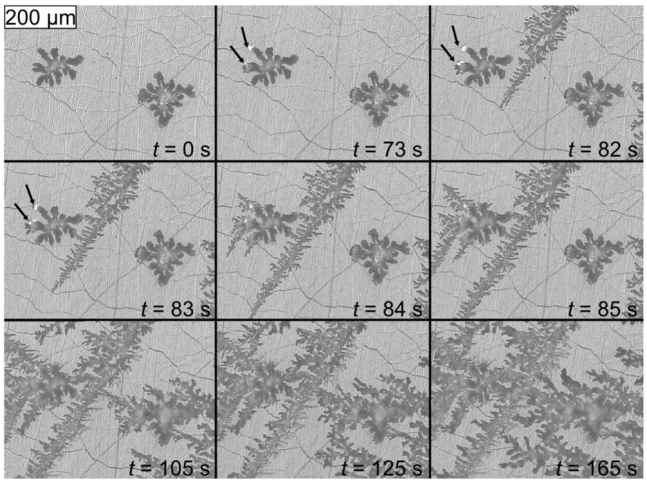

FIG. 4. Sequence of optical pictures. Overgrowth of two dendrites with silver growing at the cathode. The cathode was located at the right side and the anode was at the left side. Arrows: beginning of the migration of the dendrite, $U=480$ mV, $d\approx 3.5$ mm, and $E\approx 140$ V/m.

surface conductivity of silver chloride single crystals. He reported an enhanced silver ion conductivity of disordered surfaces and concluded that the enhancement is due to highly conductive paths along grain boundaries and/or dislocations in polycrystalline surface regions. Macroscopic electrodes are not sensitive enough to measure the effect of such a surface region because the major contribution arises from the bulk. Only a setup with a microelectrode in contact with the surface layer shows enough sensitivity.

To suppress the fast overgrowth of the surface from the cathode, we treated the polished single crystals for several minutes with $1M$ $Na_2S_3O_3$ solution to remove the disordered surface region. To further suppress the overgrowth, a barrier in form of a several micrometers deep and wide scratch parallel to the cathode was created with a scalpel. The scratch represents a region with enhanced ionic conductivity due to introduced dislocations and/or grain boundaries. Thus, the energy for the nucleation of silver is lower at this scratch in comparison to the etched electrolyte surface.[12] When a cathodic dendrite reaches this scratch, silver is now deposited primarily in this scratch.

Ex situ investigation showed that the silver formed a continuous dentritic structure at the cathode [Fig. 5(b)], whereas at the anode, this structure was partly dissolved

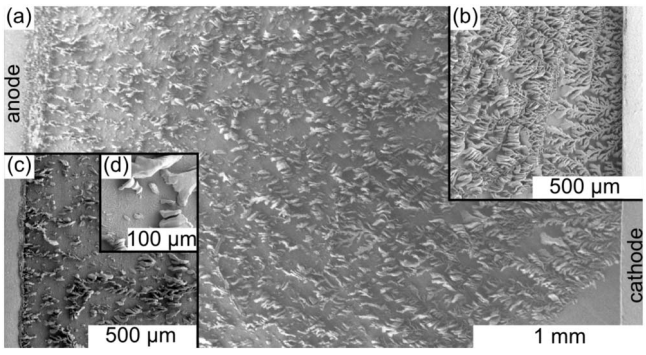

FIG. 5. HSEM pictures of the same experiment as in Fig. 4 ($t=1140$ s). (a) The whole surface of the electrolyte was covered by silver with dendritic morphology. (b) Magnification at cathode: continuous dendritelike silver structure. (c) Magnification at anode: partly dissolved dendritelike structure. (d) Magnification of (c).

[Figs. 5(c) and 5(d)]. The growth of silver did not stop when the anode was reached by dendrites, and the silver was continuously redissolved locally. During the overgrowth currents were in the regime of several 100 μA corresponding to the resistance of the electrolyte of a few kilohms. After short-circuiting, the currents went up to several 100 mA.

We assume that at the time of contact, i.e., the short-circuiting between cathode and anode, the freshly formed silver path is disconnected by dissolution at its weakest point because of high current densities. Several possible mechanisms are discussed in the literature (see Ref. 3). Thus, the anodic part of the grown silver dendrite was (partly) redissolved while the cathodic part grew continuously. Using current limitation during the overgrowth, it was possible to maintain the grown silver structure because the dissolution due to high current densities was prevented. These structures exhibited resistances of a few ohms and were stable up to currents of 750–1500 mA where dissolution took place.

In conclusion, by applying a voltage between two silver electrodes placed on a solid electrolyte surface, two different effects were observed. First is the well known short-circuiting of the electrodes by the growth of dendritic silver structures on the surface of the electrolyte starting at the cathode. Second is the migration of electronically noncontacted silver metal on the electrolyte surface. The first effect is comparable to the switching in ionic/mixed conducting resistive switching systems and serves as an easy to observe model system for the formation and dissolution of electrical conducting paths between electrodes. The second effect may be related to a possible short-circuiting of batteries by formation of filaments starting at loose electrode particles in the electrolyte. The observed spatial and temporal instabilities are closely related to the effects observed at extended electrodes.[17,18]

This study was funded by the DFG within the Projects Ja648/6–1 and 6–2. Financial support by the FCI is also gratefully acknowledged.

[1] M. Dolle, L. Sannier, B. Beaudoin, M. Trentin, and J.-M. Tarascon, Electrochem. Solid-State Lett. **5**, A286 (2002).
[2] M. Rosso, C. Brissot, A. Teyssot, M. Dolle, L. Sannier, R. Bouchet, S. Lascaud, and J.-M. Tarascon, Electrochim. Acta **51**, 5334 (2006).
[3] X. Guo, C. Schindler, S. Menzel, and R. Waser, Appl. Phys. Lett. **91**, 133513 (2007).
[4] C. Liang, K. Terabe, T. Hasegawa, and M. Aono, Nanotechnology **18**, 485202 (2007).
[5] K. Terabe, T. Hasegawa, T. Nakayama, and M. Aono, Nature (London) **433**, 47 (2005).
[6] K. Peppler and J. Janek, Solid State Ionics **177**, 1643 (2006).
[7] S. Schimschal-Thölke, H. Schmalzried, and M. Martin, Phys. Chem. Chem. Phys. **99**, 1 (1995).
[8] S. Schimschal-Thölke, H. Schmalzried, and M. Martin, Phys. Chem. Chem. Phys. **99**, 7 (1995).
[9] M. Martin, P. Tigelmann, S. Schimschal-Thölke, and G. Schulz, Solid State Ionics **75**, 219 (1995).
[10] H. Schmalzried, *Chemical Kinetics of Solids* (VCH, Weinheim, Germany, 1995).
[11] See EPAPS Document No E-APPLAB-93-067833 for an animated version of Fig. 2. For more information on EPAPS, see http://www.aip.org/pubservs/epaps.html.
[12] A. Spangenberg, J. Fleig, and J. Maier, Adv. Mater. (Weinheim, Ger.) **13**, 1466 (2001).
[13] J. Corish and C. O'Briain, J. Cryst. Growth **13–14**, 62 (1972).
[14] T. Ohachi and I. Taniguchi, J. Cryst. Growth **13–14**, 191 (1972).
[15] M. Rohnke, T. Best, and J. Janek, J. Solid State Electrochem. **9**, 239 (2005).
[16] J. Fleig, F. Noll, and J. Maier, Ber. Bunsenges. Phys. Chem. **100**, 607 (1996).
[17] J. Janek, Solid State Ionics **131**, 129 (2000).
[18] M. Vennekamp and J. Janek, Phys. Chem. Chem. Phys. **7**, 666 (2005).

2.3 The System Ag-Microelectrode|embedded-Ag_2S

The attempt to obtain a single whisker by the cathodic deposition at microelectrodes on silver bromide failed, and it was only possible to grow several whiskers in parallel, cf. chapter 2.1 on page 27. In order to produce a single whisker another procedure was employed. The electrolyte was spatially confined in a template with straight continuous cylindrical pores (resembling a perforated plate). But it was not possible to fill the pores with silver bromide within acceptable time. Hence, the solid electrolyte was changed to silver sulfide, because an easy to execute chemical reaction suffices to fill the pores, see below.

2.3.1 Article: Templated assisted Solid State Growth of Silver Micro- and Nanowires [Peppler2007]

The following article is based on own experimental research and was written by myself and co-edited by Prof. Jürgen Janek. It was published in a special issue of the journal "Electrochimica Acta" based on an oral presentation given at the "6th International Symposium on Electrochemical Micro- and Nanosystem Technology" (22nd-25th August 2006 in Bonn, Germany).

Synopsis

The article consists of two major parts. In the first part the filling mechanism of the pores of the employed templates with silver sulfide is described. As templates porous silicon with pore diameters in the order of a few micrometers and porous alumina membranes with pore diameters in the order of several hundreds of nanometers were used. In the second part the cathodic deposition of silver wires is presented. The diameters of the deposited silver wires equaled the diameter of the pores of the employed template.

Available online at www.sciencedirect.com
ScienceDirect
Electrochimica Acta 53 (2007) 319–323
ELECTROCHIMICA Acta
www.elsevier.com/locate/electacta

Template assisted solid state electrochemical growth of silver micro- and nanowires

Klaus Peppler, Jürgen Janek *

Institute of Physical Chemistry, Justus-Liebig-University, Heinrich-Buff-Ring 58, 35392 Giessen, Germany

Received 4 October 2006; received in revised form 19 December 2006; accepted 19 December 2006
Available online 23 January 2007

Abstract

We report on a template based solid state electrochemical method for fabricating silver nanowires with predefined diameter, depending only on the pore diameter of the template. As templates we used porous silicon with pore diameters in the μm range and porous alumina with pore diameters in the nm range. The template pores were filled with silver sulfide (a mixed silver cation and electronic conductor) by direct chemical reaction of silver and sulfur. The filled template was then placed between a silver foil as anode (bottom side) and a microelectrode (top side) as cathode. An array of small cylindrical transference cells with diameters in the range of either micro- or nanometers was thus obtained. By applying a cathodic voltage to the microelectrode silver in the form of either micro- or nanowires was deposited at about 150 °C. The growth rate is controllable by the electric current.

Keywords: Microwire; Nanowire; Electrodeposition; Template; Solid electrolyte

1. Introduction

The application of porous membranes with channel like pores as templates for the electrochemical growth of micro- and nanowires is a common approach. Various materials have already been deposited in pores of, e.g. porous alumina (mostly metals [1–6], but also binary compounds like silver chalcogenides [7,8]), or in pores of polymeres [9]. All reported examples have in common that the pores are filled by electrodeposition or by chemical reduction from a liquid solution. It is finally neccessary to remove the template by etching in order to obtain free-standing micro- or nanowires. Nanowire arrays in which all wires are straight and have the same diameter and length, controlled by the pore diameter and the thickness of the porous membrane, have been obtained this way.

Here, we describe a process which allows the continuous growth of few individual or arrays of silver micro- and nanowires without limitation of length. It is well known that on solid silver ion conductors (e.g. AgBr, AgCl) or mixed ionic and electronic conductors (e.g. Ag_2S) it is possible to grow silver whiskers (i.e. thin fiber like crystals), either by chemical supersaturation [10,11] or by cathodic electrodeposition [12]. These whiskers have diameters in the order of micrometers. In the present approach, we combine the cathodic gowth of metal fibers with template directed growth. Thus, the process is based on the cathodic deposition of metal on a cation-conducting solid electrolyte.

2. Experimental

2.1. Materials and preparation

As silicon templates we used porous membranes with pore diameters of 1.2 and 5.2 μm, respectively, with a thickness of 450 μm. Porous alumina membranes with a thickness of 50 μm were purchased from Whatman International Ltd. The average pore diameter was given as 200 nm, but varied in the range from 150 to 350 nm according to own HRSEM (high resolution scanning electron microscopy, LEO Gemini 982) studies. In order to fill the pores with silver sulfide a membrane was placed between two silver sulfide (Aldrich 99.9%) films, and this stack was put on a silver foil. On the top film sulfur powder was spread in a thin layer. The whole assembly was then heated on a heating

* Corresponding author. Tel.: +49 6419934500; fax: +49 6419934509.
E-mail address: juergen.janek@phys.chemie.uni-giessen.de (J. Janek).
URL: http://www.chemie.uni-giessen.de/home/janek (J. Janek).

0013-4686/$ – see front matter © 2007 Elsevier Ltd. All rights reserved.
doi:10.1016/j.electacta.2006.12.054

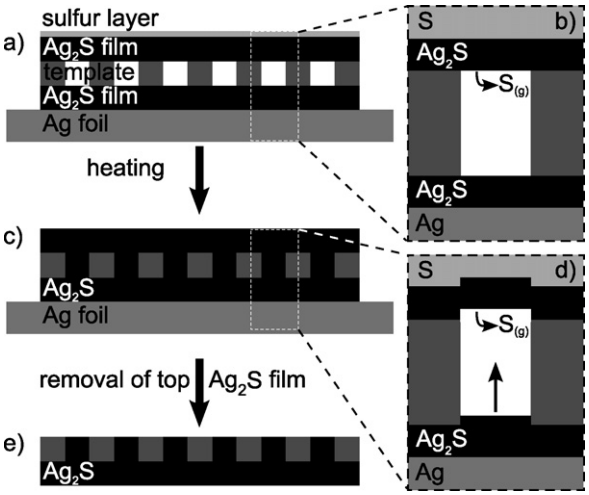

Fig. 1. Sketch of reactive pore filling: (a) initial assembly for pore filling of a template sandwiched between two silver sulfide films and a sulfur layer on top. (b) Single pore at initial state of filling process, after heating sulfur is set free into the pore at the bottom side of the top silver sulfide film. (c) After heating the pores of the membrane have been filled with silver sulfide, but are still covered with silver sulfide on top. (d) Single pore during filling. The bottom silver sulfide film grows at the cost of the top film. (e) After removal of the silver sulfide on top the pores are freely accessible.

stage above the melting point of sulfur ($T \simeq 140$–$160\,^{\circ}C$). The silver was oxidized by the liquid sulfur indirectly via the mixed-conducting silver sulfide, resulting finally in silver sulfide-filled pores (see Figs. 1 and 2). After removing the top silver sulfide layer the filled pores were freely accessible from the top side (see Figs. 3b and 4c). The mechanism of the pore filling is based on chemical diffusion in the chemical potential gradient of the components in the nonstoichiometric silver sulfide (see Fig. 2), i.e. on unidirectional growth of a mixed-conducting compound by a simple tarnishing reaction. The silver reservoir at the bottom keeps the chemical potential of silver at the highest possible

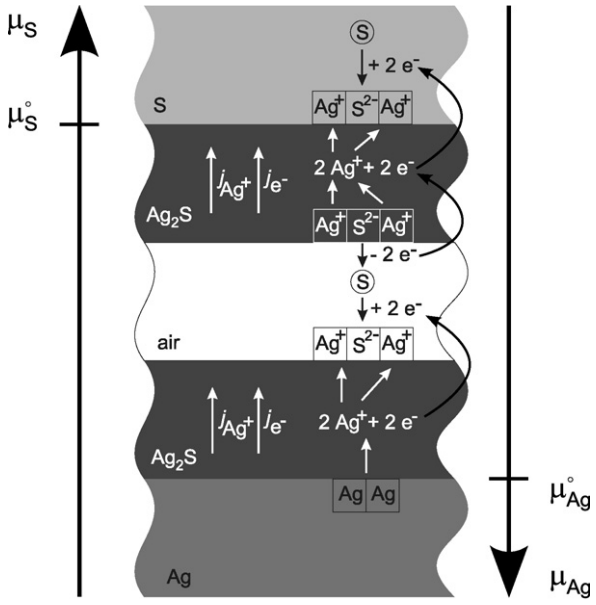

Fig. 2. Mechanism of pore filling (for details see text).

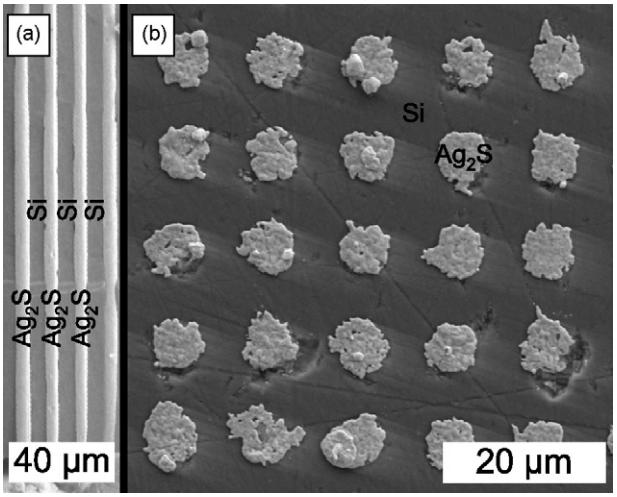

Fig. 3. HRSEM pictures of porous silicon filled with silver sulfide: (a) cross section and (b) top view.

value, i.e. to $\mu^{\circ}_{Ag}(T)$. The sulfur reservoir on top fixes the silver potential in the top silver sulfide film to the lowest possible value. This creates a chemical potential gradient, which causes a flux of silver in upper direction. The bottom film is growing despite the air gap (i.e. the pore), as the sulfur equilibration pressure above its surface is lower than the sulfur vapour pressure of the top film. A flux of sulfur arises, which causes the growth of the bottom film and the dissolution of the top film. The bottom film grows at the cost of the top film. And due to the dissolution of the bottom side of the upper silver sulfide this film can easily be removed. In the case of porous alumina as template no further preparation of the surface is required, whereas the porous silicon based samples were additionally polished. HRSEM pictures of cross sections of the filled template showed that the pores were completely filled with silver sulfide (see Figs. 3a and 4a and b).

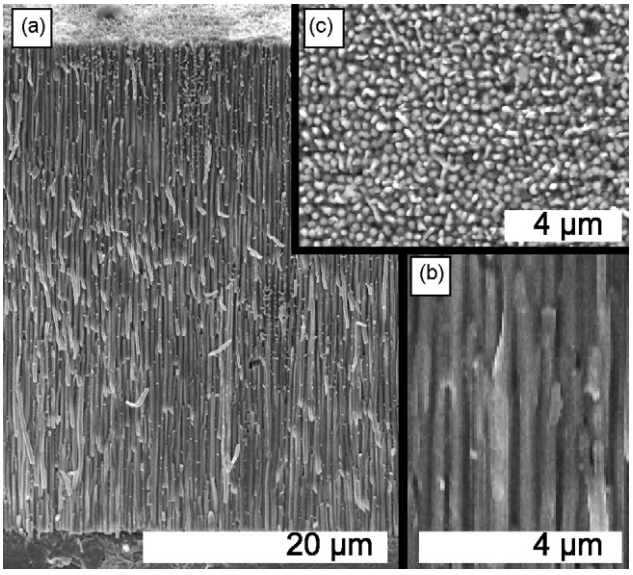

Fig. 4. HRSEM pictures of porous alumina filled with silver sulfide: (a) cross section, (b) magnification of (a), and (c) top view.

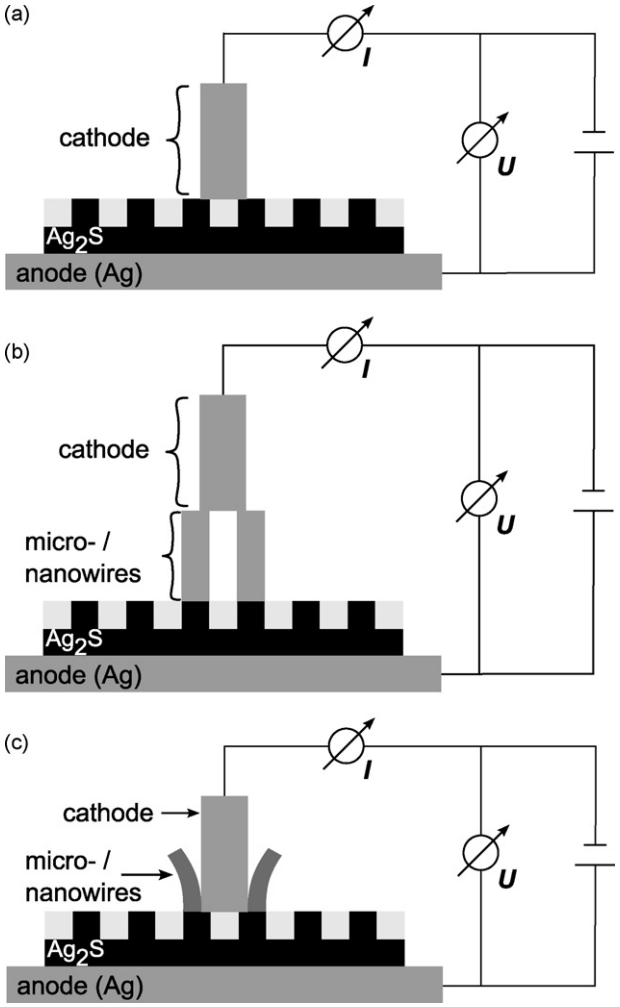

Fig. 5. Sketch of electrodeposition of silver micro- or nanowires: (a) experimental setup before deposition; consisting of a microelectrode as cathode; templated solid electrolye and anode. (b) In case of a flexible silver wire as microelectrode the microelectrode is lifted up by the growing silver micro- or nanowires. (c) In case of a rigid tungsten needle as microelectrode the silver is deposited at the edges of the microelectrode.

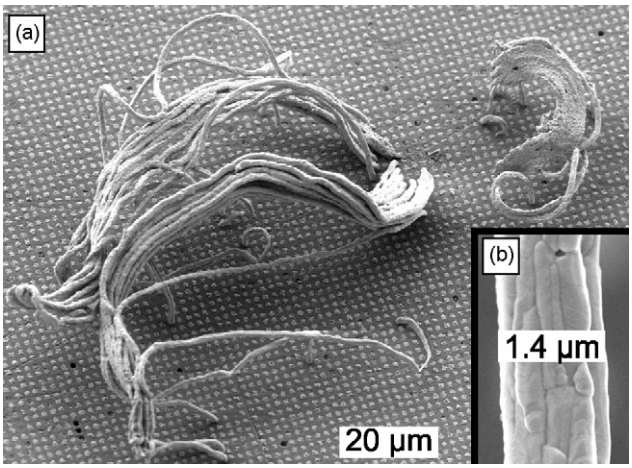

Fig. 6. HRSEM pictures of silver microwires on porous silicon: (a) bunch of silver microwires (W-needle as ME with tip-Ø of 2 µm, $I = -10$ µA, $t = 940$ s, $T \simeq 150$ °C). (b) The microwires show the same diameter (about 1.4 µm) as the pores of the used porous silicon membrane (1.2 µm).

2.2. Experimental setup

The filled template, prepared as mentioned above, was placed on a silver foil (anode), with the initial silver sulfide film on the bottom side. In order to acquire as few as possible micro- or nanowires we used microelectrodes as cathodes. Thus, the filled pores were contacted from the top side with a silver microelectrode in a modified PM8 probe station from SUSS Micro Tec (see Fig. 5a) (a detailed description of the whole experimental setup can be found in Ref. [13a]). As microelectrodes we used silver wires with a diameter of 25 µm and tungsten needles with a tip diameter of 2 µm. The whole sample was heated on a heating stage up to about $T \simeq 150$ °C. The temperature was measured with two thermocouples, one on the top side of the sample (at the height of the cathode) another at the height of the anode. In order to achieve a constant growth rate of the nanowires we applied galvanostatic conditions. Cathodic currents of a few microamperes caused the deposition of silver either as micro- or nanowires at the microelectrode, depending on the used template

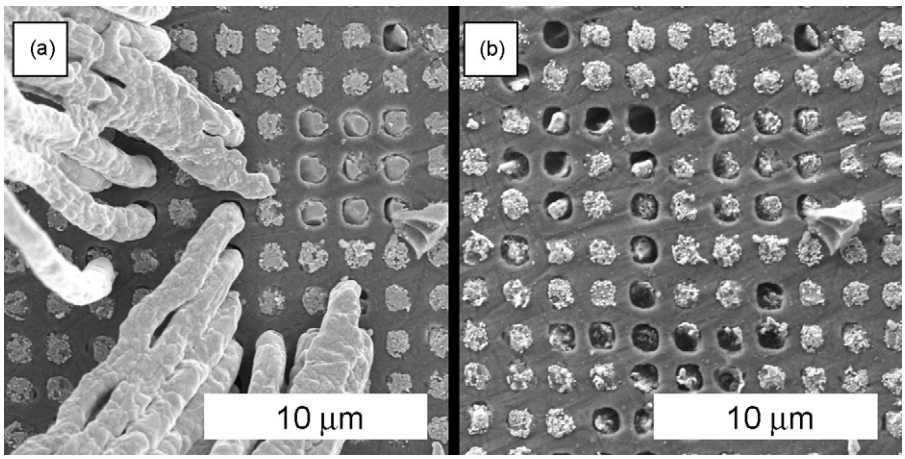

Fig. 7. HRSEM pictures of silver microwires on porous silicon: (a) magnification of Fig. 6. (b) Same place after the mechanical removal of the microwires. Pores are still filled with silver sulfide (proven with EDX, not depicted), hence no deposition into the pores occurred.

(see Fig. 5b and c). The current densities given in the following correspond to the current divided by the easily accessible cross sectional area of the microelectrodes. These apparent current densities are not necessarily equal to the current densities at the interfaces of the growing metal wires toward silver sulfide. On average we assume that the real current densities at these interfaces are higher than the apparent current density of the microelectrode, as only a few micro- or nanowires are contacted.

3. Results

Depending on the employed template we obtained silver micro- or nanowires. In Fig. 6a, a HRSEM micrograph of a bunch of silver microwires on porous silicon is shown. As a rigid tungsten needle was used as microelectrode, the deposition occurs at the edges of the electrode (see Fig. 5c). The deposited microwires have the same diameter as the pores of the porous silicon template (see Fig. 6b). After the mechanical removal of the silver microwires EDX analysis showed exclusively silver sulfide (see Fig. 7), thus deposition of silver into the pores was not observed. In Fig. 8a, a HRSEM picture of a bunch of silver nanowires on porous alumina can be seen. In this case, a flexible silver wire was used as microelectrode, and it was lifted up by the growing nanowires. The microelectrode itself was lifted off after the experiment and is not depicted. In Fig. 9, a bunch of silver nanowires is shown, which has been deposited using a rigid tungsten needle as microelectrode (again the microelectrode has been lifted off after the experiment). The difference of the appearance compared to the silver deposit at a flexible microelectrode is clearly visible.

The diameter of the silver nanowires corresponds well with the pore diameter of the used porous alumina membrane (see Fig. 8). As can be seen in Fig. 8b and c, the deposited silver nanowires are fused together and twinned or multi-twinned. One reason might be the relatively high current density of about 50 mA/cm^2 with respect to the cross sectional area of the microelectrode. The free-standing micro- and nanowires are not straight but often bend and form coils, in particular with increasing length. The measured overvoltage during deposition is very low, in the order of only a few mV (see Fig. 10). Here, it has to be taken into account that the temperature difference of approximately 5 °C between the cathode and the anode always led to a non-negligible thermovoltage, which makes quantitative statements on the small overvoltages very difficult (see

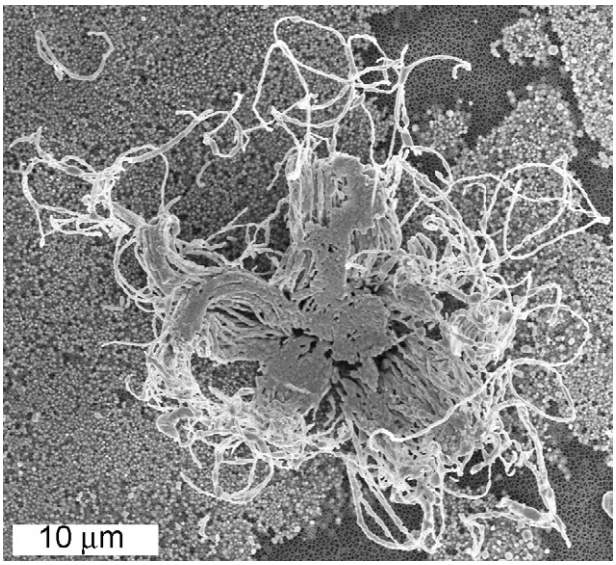

Fig. 9. HRSEM pictures of silver nanowires on porous alumina: bunch of silver nanowires which is attached to the electrolyte (W-needle as ME with tip-Ø of 2 µm, $I = -0.5$ µA, $t = 610$ s, $T \simeq 150$ °C).

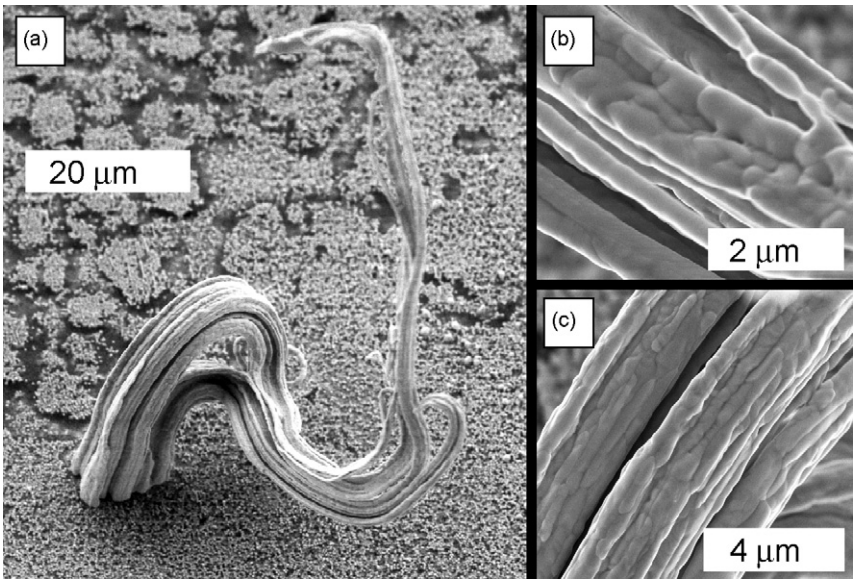

Fig. 8. HRSEM pictures of silver nanowires on porous alumina: (a) bunch of silver nanowires which is attached to the electrolyte (Ag-wire as ME with Ø of 25 µm, $I = -0.25$ µA, $t = 6000$ s, $T \simeq 150$ °C). (b and c) Magnifications of (a), nanowires have the same diameter (about 250 nm) as the pores of the applied porous alumina membrane.

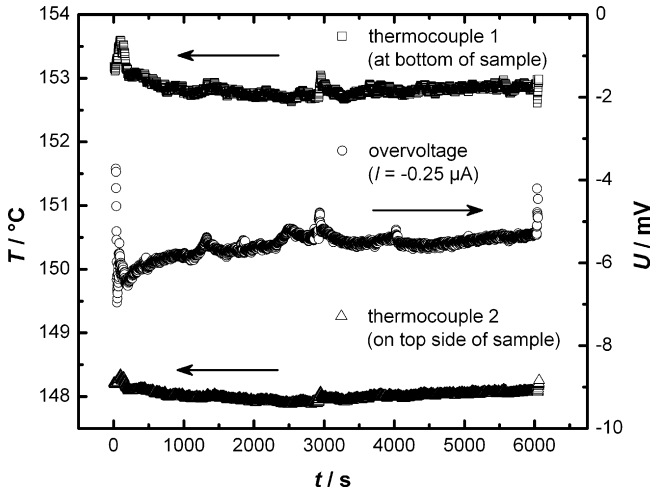

Fig. 10. Temperature and potential transient for the silver deposition of the nanowires shown in Fig. 8. The overvoltage is only a few mV. But a certain contribution is generated by a thermovoltage due to the temperature difference (approximately 5 °C) between the cathode (microelectrode) and the anode.

[13b] for a description of the thermodynamic properties of silver sulfide).

4. Discussion and conclusions

With the approach described here it is possible to grow micro- and nanowires with defined diameter and length, depending only on the applied current and the growth time. The obtained wires are not straight but bend and coil up, as they are free standing. This is a major difference to all growth processes in porous templates with liquid electrolytes, where the length of the wires is restricted by the length of the pores. Up to now the wires show a relatively poor crystallinity compared to single crystalline whiskers growing on free surfaces of solid electrolytes. We attribute this to the high current densities which we used. In order to obtain micro- and nanowires with a better crystallinity the growth rate will have to be decreased, i.e. the flux density of the silver ions has to be decreased. Even then the growth rate does not correspond 1:1 to the electric current, as silver sulfide is a mixed conductor with a relatively high electronic transference number. The ratio of the transference numbers for electrons and silver ions in the employed nonstoichiometric Ag_2S depends on the temperature and the phase composition [14,15], but once silver sulfide is in contact with silver metal, it equilibrates with the chemical potential of silver metal. And thus, the electronic transference number is at maximum. As a consequence, the growing wires do not only conduct the current required for the growth process, rather they also have to conduct a considerable leakage current caused by the electronic transference of the sulfide. In a more advanced growth cell, this electronic contribution will be filtered by a solid electrolyte film between the silver anode and the silver sulfide, allowing a 1:1 faradaic control of the growth. Anode instabilities may then occur, but do not influence the growth process [16–18].

We believe that our approach is a promising and easy way for the electrochemical synthesis of single or multiple micro- or nanowires with defined diameters in a continuous process. We used porous silicon and porous alumina membranes as templates for the cation conductor (i.e. a mixed ionic and electronic conductor). In essence, we fabricated electrochemical micro- and nanotransference cells for the continuous growth of metal micro- and nanowires. And in principle there is no restriction for the length of the micro- and nanowires, as the length depends only on the applied current and the time. There is also no restriction to the diameter of the wires, once the necessary porous template is available and can be filled with the solid electrolyte. Silver works very well, as good silver-conducting materials are available that can be grown at moderate temperatures. We expect that copper wires can also be grown from templated copper sulfide. Other systems may work, the availablity of stable cation-conducting solid electrolytes will be the bottle-neck.

Acknowledgements

This study was funded by the DFG (Deutsche Forschungsgemeinschaft) within the projects Ja648/6-1 and 6-2. Financial support by the FCI (Fonds der Chemischen Industrie) is also gratefully acknowledged. We wish to thank Dr. Volker Lehmann from Infineon Technologies for the supply with porous silicon.

References

[1] G. Sauer, G. Brehm, S. Schneider, K. Nielsch, R.B. Wehrspohn, J. Choi, H. Hofmeister, U. Gösele, J. Appl. Phys. 91 (5) (2002) 3243.
[2] J. Choi, G. Sauer, K. Nielsch, R.B. Wehrspohn, U. Gösele, Chem. Mater. 15 (2003) 776.
[3] Z. Hu, T. Xu, R. Liu, H. Li, Mater. Sci. Eng. A 371 (2004) 236.
[4] W. Wu, J.B. DiMaria, H.G. Yoo, S. Pan, L.J. Rothberg, Y. Zang, Appl. Phys. Lett. 84 (6) (2003) 966.
[5] H. Masuda, A. Abe, M. Nakao, A. Yokoo, T. Tamamura, K. Nishio, Adv. Mater. 15 (2) (2003) 161.
[6] K. Nielsch, R.B. Wehrspohn, J. Barthel, J. Kirschner, S.F. Fischer, H. Kronmüller, T. Schweinböck, D. Weiss, U. Gösele, J. Magn. Magn. Mater. 249 (2002) 234.
[7] R. Chen, D. Xu, G. Guo, L. Gui, J. Electrochem. Soc. 150 (3) (2003) G183.
[8] C. Liang, K. Terabe, T. Hasegawa, R. Negishi, T. Tamura, M. Aono, Small 1 (10) (2005) 971.
[9] J. Liu, J.L. Duan, M.E. Toimil-Molares, S. Karim, T.W. Cornelius, D. Dobrev, H.J. Yao, Y.M. Sun, M.D. Hou, D. Mo, Z.G. Wang, R. Neumann, Nanotechnology 17 (2006) 1922.
[10] J. Corish, C.D. O'Briain, J. Cryst. Growth 13/14 (1972) 62.
[11] T. Ohashi, I. Taniguchi, J. Cryst. Growth 24/25 (1974) 362.
[12] M. Rohnke, T. Best, J. Janek, J. Solid State Electr. 9 (4) (2005) 239.
[13] (a) K. Peppler, J. Janek, Solid State Ionics 177 (2006) 1643;
(b) C. Korte, J. Janek, J. Phys. Chem. Solids 58 (1997) 623.
[14] P. Junod, Helv. Phys. Acta 32 (1959) 567.
[15] N. Valverde, Z. Phys. Chem. Neue Fol. 70 (1970) 128.
[16] J. Janek, S. Majoni, Ber. Bunsenges. Phys. Chem. 99 (1995) 14.
[17] S. Majoni, J. Janek, Ber. Bunsenges. Phys. Chem. 102 (1998) 756.
[18] J. Janek, Solid State Ionics 101 (1997) 721 (Proc. ISRS 1996, Hamburg).

2.3.2 Supplementary Information

In the previous article [Peppler2007] in chapter 2.3.1 a possible method to suppress the electronic transference of the silver sulfide is mentioned in section 4 "Discussion and conclusions". It was suggested that between anode and silver sulfide a layer of silver bromide should hinder the transport of electrons, because silver bromide is nearly a pure cation conductor. Thus, the transference cell is assembled as follows $(-)Ag|Ag_2S|AgBr|Ag(+)$, see fig. (2.5) a) on page 58. At the interface $Ag_2S|AgBr$ the silver bromide can only provide silver cations, but as the cathode is directly connected to the silver sulfide a part of the silver cations is discharged by the still present electronic current through the silver sulfide, see fig. (2.5) b). In consequence a new layer of silver between the silver sulfide and the silver bromide is deposited. Thus, after an initial time the transference cell changes to $(-)Ag|Ag_2S|Ag|AgBr|Ag(+)$. The newly formed layer of silver between the silver bromide and the silver sulfide grows continuously. At the Ag|AgBr interface silver ions are provided and discharged by an electronic current through the silver sulfide and the silver layer. At the $Ag_2S|Ag$ interface silver is partially dissolved to provide silver cations for the ionic part of the current through the silver sulfide. At the cathode $((-)Ag|Ag_2S)$ the silver ions are consecutively discharged. Thus the silver layer is an interconnector, acting as cathode at the Ag|AgBr interface and anode at the $Ag_2S|Ag$ interface. As a consequence it is not possible to suppress the electronic flow in the silver sulfide by inserting a pure cation conductor between the anode and the silver sulfide, a mixed ionic electronic conductor. The authors were misled upon their first assumption.

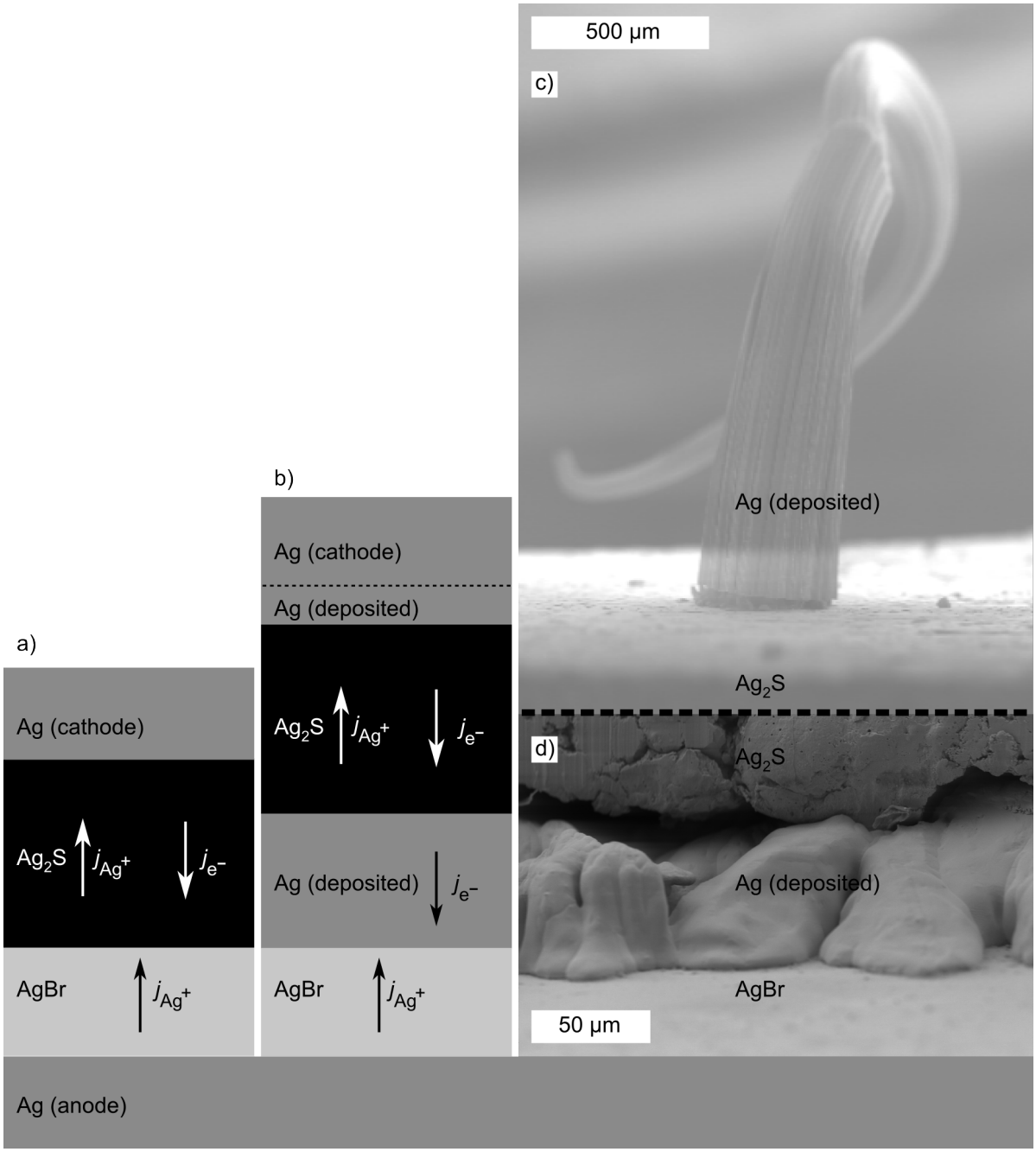

Figure 2.5: Employment of AgBr as "electron filter" (description see text): a) Sketch of experiment befor start. b) Sketch of experiment after a certain time. c) and d) Mosaic of SEM images after experiment. (d(Ag-microelectrode) = 250 µm, $\theta \approx 275$ °C, $I = -99.5$ µA, $t \approx 18$ h)

3 Classification, Outlook & Summary

3.1 Classification

In order to classify the data from own investigations and compare it with the present knowledge in the field the manuscript in chapter (3.1.1) was prepared.

3.1.1 Manuscript: Electrodeposition of Metals on Solid Electrolytes [Peppler2009]

The following article is a manuscript which needs some final editing. It is intended to be submitted as a perspective, a special article format of the journal "*Physical Chemistry Chemical Physics*" for topical reviews. It was a written by myself and co-edited by Prof. Jürgen Janek.

Synopsis

The manuscript is divided in two major parts. In the first part fundamental aspects of cathodic metal deposition are discussed, like proper reference electrode positioning, suitable cation conducting solid electrolytes, comparison of liquid and solid electrochemistry. In this part the present work on cathodic metal deposition (cf. chapters 2.1 and 2.3) is compared to other related work on this topic, as well as the stability of metal deposits in external electric fields (cf. chapter 2.2). In the second part the impact of fundamental aspects of cathodic metal deposition on current and futur applications is discussed. For future memory and switching devices different attempts are followed, one is the switching between a high and a low resistive state. Systems exploiting the growth of filaments by cathodic deposition in or on solid electrolytes are investigated and thus closely related. Currently the employment of lithium metal electrodes for lithium secondary batteries is thoroughly investigated. But the growth of dendrites and whiskers upon cycling is a known failure mechanism reducing the lifetime by shortening of the cell. The nanostructuring/-printing with the aid of solid electrochemical deposition and dissolution methodes and the growth of whiskers as failure mechanism in electric and electronic devices is shortly discussed.

Electrodeposition of metals on solid electrolytes

Klaus Peppler and Jürgen Janek

Institute of Physical Chemistry, Justus-Liebig-University,
Heinrich-Buff-Ring 58, 35392 Giessen, Germany
E-mail: juergen.janek@phys.chemie.uni-giessen.de

Electrochemical metal deposition in *liquid* electrolytes is used in modern technology for surface modification or nanostructuring. It can be considered as one of the key electrochemical processes which motivated numerous experimental and theoretical studies. The deposition of a metal from a *solid* electrolyte is by far less intensively studied and understood, mainly due to less prominent technological applications. Recently, the deposition of metals on solid electrolytes attracts much more interest, driven by new applications. Examples are presented and the current understanding of the mechanisms is briefly summarized, highlighting the need for further systematic studies.

1 Introduction

In this paper we address a classical electrochemical subject, i. e. electrodeposition, but in an environment that is much less studied than the conventional liquid electrolyte. Electrodeposition on *solid* electrolytes is today a subject of growing interest – mostly due to applications in nanotechnology and energy technology. Processes at electrodes in liquid electrolytes were intensively studied [1, 2, 3] in the last 150 years and are still investigated today. The driving force behind these investigations was – and still is – of course mainly the (electro-) galvanization of metals with smooth metal films. In contrast, the investigation of processes at electrodes in or on solid electrolytes just started some 30 to 40 years ago, but still is in its infancy, so that in many cases the microscopic mechanisms are yet not understood.
We focus on reversible metal electrodes, i. e. on electrodes which allow both anodic and cathodic currents at low overvoltages. These are represented by electrodes of the type Me|MeX with MeX being a cation-conducting electrolyte. Raleigh [4, 5] coined the expression "parent metal electrode" for this type of electrode, but we will rather use the expression *reversible metal electrode* in order to distinguish it from the blocking type of metal electrode Me|AX. Both anodic and cathodic processes at reversible metal electrodes may be considered as the simplest electrode reactions to deal with. The proper understanding of their characteristics and their mechanisms is of upmost importance for the improvement and optimization of electrochemical devices. As is shown below in some details, metal electrodeposition on solid electrolytes relies on a number of fundamental physico-chemical phenomena that are by far not fully understood: Heterogeneoues nucleation, morphological development under the influence of local electrical fields (and perhaps

also mechanical strain fields) and charge transfer at a solid|solid interface. The influence of size effects (nano-scaling) adds to these three phenomena and leads to interesting consequences, as is also shown below.
Besides these fundamental aspects, electrodeposition on solid electrolytes is part of advanced electrochemical technologies or may be utilized in future technologies. Maybe the most important application today is found in lithium ion batteries, where lithium electrodeposition in the form of dendrites is a failure mechanism that has to be avoided. Interestingly, reversible lithium metal electrodes form an important element of new types of batteries, and therefore are intensively studied [6, 7, 8]. Other recent applications which still are in the state of exploration are solid state electrochemical switching and memory devices [9, 10]. Solid state imprinting or structuring is another recent development [11, 12, 13].
In the following (section 2) we firstly summarize briefly the most important fundamental aspects: Solid electrolytes as substrate materials, morphology of electrodeposits, kinetics of electrodeposition and size effects. Recent examples follow in section 3. In section 4, we summarize and give an outlook on possible future developments.

2 Fundamental Aspects

2.1 Electrochemical cells for the study of metal deposition on solid electrolytes

From the phenomenological point of view the cell arrangement for the study of electrode processes on a solid electrolyte does not differ from cells with liquid electrolytes: A three electrode arrangement is required in order to exclude processes at the counter electrode. As the electrolyte is solid, all three electrodes cannot be "emersed" in the electrolyte but rather have to be attached to surfaces of the solid electrolyte. The reference electrode (RE) in the case of cation-conducting solid electrolyte (SE) is usually made from the parent metal of the electrolyte in the form of a thin wire. Whereas it is usually no problem to place both working (WE) and counter electrode (CE) at opposite ends of the electrolyte, the proper positioning of the reference electrode requires care. Due to the problem of RE positioning often a two-electrode cell is used. In order to reduce the IR drop the WE is then made much smaller than the CE, see fig. (1). The position/geometry of the reference electrode is crucial in order to obtain accurate measurements. In the literature WE, CE and RE geometries as depicted in fig. (1) (a)-(c) are described to be the best arrangements [14, 15, 16, 17]. It is advantageous when WE and CE are symmetrically placed. It is important that the RE is not placed too close to the other electrodes and the RE should be smaller in geometry. If a pseudo RE (RE placed on the same surface as WE/CE, cf. fig. (1) (c)) is placed too close, nonuniform current densities causes "area" (instead of "point") RE to average different potentials [15]. In fig. (1) (d) a setup with only two electrodes is shown. Here, the WE is a microelectrode, thus the voltage drop at the much larger CE is often negligible compared to the overpotential of a microelectrode. A RE is therefore not necessary to get rid of the influence of the CE. [18], cf. also section 2.4.3 about constriction resistances.
A major problem in all types of cell is the mechanical boundary condition of the experiment. The deposition of the metal phase leads to serious compressive stress at the WE interface. Once

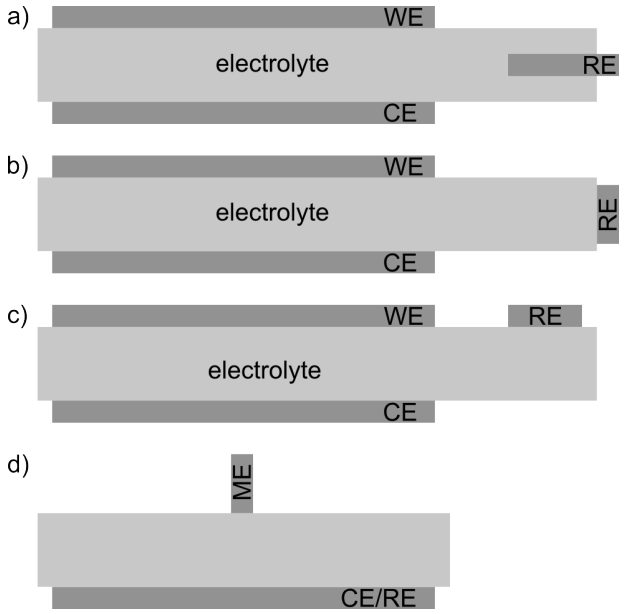

Figure 1: Proper positioning of reference electrodes (RE), explanation see text. (a) and (b) "Real" RE, (c) "Pseudo" RE, (d) Microelectrode as WE, no RE needed.

the electrode is fixed to its position, the growing metal deposit may exert such strong stress as to grow into the electrolyte and destroy it. In any case the I-U characteristics will be strongly influenced, and experiments my suffer from poor quantitative reproducibility.
The next paragraphs will in fact show that the mechanical boundary conditions play a major role for the deposition process.

2.2 Cation conducting solid electrolytes

In contrast to liquid electrolytes where in case of aqueous solutions only a suitable salt is needed to obtain an electrolyte with respective ionic conductivity, only relatively few crystalline materials exist with adequate ionic conductivity at moderate temperatures. There is also only a limited number of cations for which solid conductors are known: H^+ [19], Li^+ [20], Na^+ [21], K^+ [22], Ag^+ [23, 24, 25, 26, 27], Cu^+ [28], (Pb^{2+}, Ba^{2+}). β-alumina exhibits good ionic conductivity for hydrogen, lithium, sodium, potassium and silver. Divalent cations are mobile in β-alumina, but the electrochemical properties are mostly not satisfactory. The best investigated solid ion conductors are silver, copper and lithium ion conductors. Well known silver ion conductors are the silver halides AgX (X = Cl, Br, I), which exhibit an almost pure cationic conductivity at temperatures higher than 100 ℃ to 150 ℃. An excellent ion conductor even at room temperature is $RbAg_4I_5$, showing structural disorder in the silver sublattice. The silver chalckogenides Ag_2S and Ag_2Se are mixed ionic and electronic conductors (MIEC). Like for silver, the copper halides and chalkogenides are conductive for copper ions. The improvement of ionic conductivity of the binary compunds by mixing them with dopands has been intensively investigated.
Solid lithium ion conductors can be subdivided into crystalline and glassy phases. Among the best crystalline lithium ion conductors are e. g. garnets like $Li_5La_3M_2O_{12}$ (M = Nb, Ta) [29].

For a review of crystalline solid lithium ion conductors see Robertson et al. [20]. Glassy lithium ion conductors are e. g. LiPON and Li_2S-P_2S_5.
Another difference compared to liquid electrolytes is that in purely cationic conductive solids only cations are mobile, i. e. the cationic transference number is close to one because anions are locally bound while the electronic conductivity is negligibly small. There are also some solid electrolytes with an additional electronic conductivity, too. For a detailed survey about solid state ionics see the review by Knauth and Tuller [30].

2.3 Morphologies

Beyond the initial step of nucleation the growth mode of an electrodeposit is of primary interest, i. e. the morphological development of the growing metal. Morphology has always been an important aspect in electrodeposition in general: Technologically, perfectly flat surfaces of deposited films are desired. From the fundamental point of view, electrodeposition in liquid electrolytes is the archetype for a morphogologically unstable system. Therefore, the control of the surface morphology of electrodeposits has always been an important practical and theoretical subject. Besides planar and rough/curved, two different types of morphologies occur – *whiskers* and *dendrites*. For clarity we will define these terms – which are unfortunately not used uniformly throughout the literature: According to the IUPAC Gold Book dendrites show a "crystalline morphology produced by skeletal growth, leading to a 'tree-like' appearance" [31]. Dendrites may be fractal, but this is not a necessary condition. Without a clear proof for fractal character, tree-like deposits should simply be considered as dendrites. There is yet no generally agreed definition for whiskers, but it is reasonable to define whiskers as filament- or fiber-type forms without branching. Whiskers may be single crystals, but this is not a necessary prerequisite. In most cases whiskers are straight, but they can also be bend as long as they do not branch, see fig. (2). The diameter of whiskers can vary from root to tip, i. e. they can be tapered. In case of lithium batteries with lithium metal as electrode material Huggins [32] (cf. Chapters 7.3.3 and 7.3.4) states that filamentary growth "is often mistakenly confused with dendrite formation". According to him the formation of dendrites and filaments is based on two different mechanisms. Dendrite formation is due to the inherent morphological instability of flat interfaces on a microscopic scale. Thus, in an electric field a local protuberance will grow fastern than the rest of the interface during recharge. But the formation of filaments is also possible, i. e. growth without branching, i. e. whisker formation. Additionally, the growth of filaments can also be caused by imperfect reaction product layers. Such reaction product layers are present when lithium metal electrode and electrolyte (in most cases an organic electrolyte) are not stabele in the presence of each other. These reaction product layers are known as *solid electrolyte interfaces* (SEI). Thus, at regions with reduced impedance (i. e. thin SEI) the formation of deleterious filamentary growth upon recharge occurs. But, the term *filament* is also not clearly defined. In case of resistive switching devices (see section 3.1) the fast formation of filaments is essential for the change between two different resistance states. There, filaments are presumed to grow along dislocation lines in the lattice of a solid insulator or electrolyte in case of 3D cell arrangements [9, 10]. In case of 2D cell arrangements, the growth of dendrites on the electrolyte surface is observed. Additional information about the development of morphological instabilities in solids can be found in references [33, 34, 35, 36].

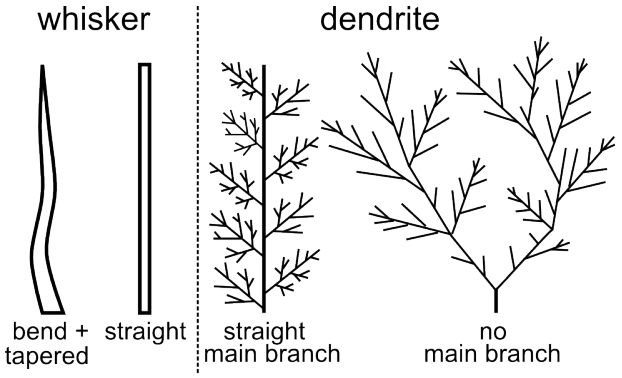

Figure 2: Classification of whiskers and dendrites.

2.3.1 Liquid Electrolytes

From electrodeposition in liquid electrolytes it is a well known fact that growth occurs rather in the form of whiskers and dendrites than in the form of planar and smooth surfaces. Numerous works on the electrodeposition of various metals in the form of dendrites and whiskers can be found, e. g. for silver [37, 38, 39, 40, 41, 42, 43, 44, 45], copper [46, 47, 48, 49, 50, 51, 52], iron [53], or zinc [54, 55, 56]. A theoretical interpretation for the growth of these ramified structures (fractal trees, dendrites) has been given by Witten and Sander [57] who developed a model of diffusion limited aggregation (DLA) for electrodeposition. Recently, Bicelli et al. reviewed the nanostructural aspects of metal electrodeposition in liquid electrolytes [58]. As we restrict ourselves to solid|solid interfaces we refer the reader to the available literature.

2.3.2 Metal Electrodeposition on Solid Electrolytes

Only a small number of studies on the morphology of electrodeposits on solid electrolytes has been published: Knauth et al. [59] observed the growth of fractal copper dendrites in a coplanar electrode arrangement, see fig. (3) (a). The authors mention that the phenomenon of formation of ramified structures is less documented for solid electrolytes, because the ion mobility at ambient temperatures is generally lower than in liquid solutions. Therefore, they used thin microcrystalline CuBr films with enhanced conductivity due to fast grain boundary transport. In fact, the ionic conductivity of solid electrolytes is usually lower than the conductivity of liquid electrolytes. This will only quantitatively influence the growth kinetics under a given external voltage but not the occurrence of instability.
Kozicki et al. [60] reported on the growth of silver dendrites on Ag-doped germanium chalcogenide glasses in a similar cell arrangement. Peppler et al. [61] made comparable obervations at electrodes placed on AgBr single crystal surfaces. Silver dendrites grew from the cathode towards the anode. In all three studies with similar coplanar electrode configurations the same growth morphology occurred, regardless of the microstructure of the electrolyte (microcrystalline, glassy and single crystalline). Thus, diffusion limited aggregation (DLA) occurs independent of the electrolyte microstructure and is thus a general phenomenon during metal growth on solid electrolytes.
In contrast, recent work based on the cathodic deposition of silver on silver halogenides with per-

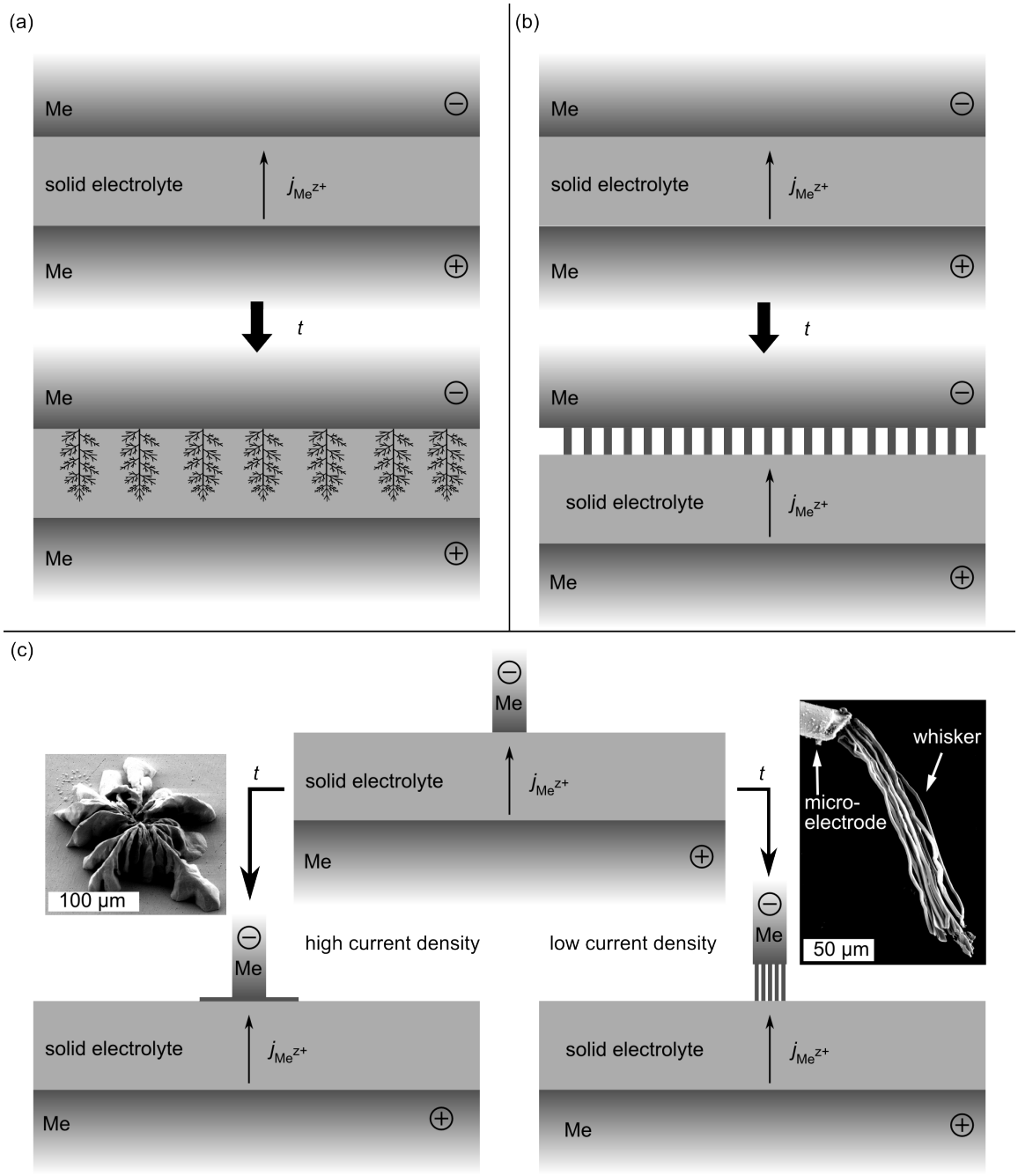

Figure 3: Sketch of observed morphologies: (a) Top view of dendritic growth on the surface of a solid electrolyte (2D cell arrangement). (b) Cross section of the growth of whisker arrays (3D cell arrangment). (c) Cross section of electrodeposition at microelectrodes. Left HRSEM picture: Silver dendrite deposited on AgBr at a temperature of $\vartheta \simeq 275$ ℃ ($I = -5$ µA, $t = 640$ s). Right HRSEM picture: Silver whiskers deposited at a temperature of $\vartheta \simeq 275$ ℃ ($I = -0.5$ µA, $t = 300$ s).

pendicular electrode alignment lead to the deposition of both whiskers and dendrites. Rohnke et al. [62] reported the growth of silver whisker arrays at laterally extended planar cathodes on silver bromide single crystals. After deposition the electrolyte and the electrode surface were separated by the growing whisker array, see fig. (3) (b). The whiskers had diameters in the micrometer regime. The authors could also show that the silver whisker growth takes place at the Ag-whisker|AgBr interface rather than by surface diffusion. The whisker density in the order of $2 \cdot 10^6$ cm^{-2} agreed well with typical dislocation densities in ionic crystals and thus supports the hypothesis that the growth of whiskers starts at points of emergence of dislocations.
It was also found that growth of dendrites instead of whisker arrays occured, once the contact between the laterally extended electrode and the electrolyte was bad, i. e. consisted only of a few point contacts.
Interestingly, Spangenberg et al. [63, 64] reported only dendritic morphology of silver electrodeposits on AgCl single crystal surfaces at microelectrodes as cathodes, see fig. (3)(c). Peppler and Janek [65] observed the same bahavior for AgBr single crystal surfaces, but also observed the growth of silver whisker bunches at low current densities, see fig. (3) (c).
Irrespective of the specific morphology all reported cases show that electrodeposition on solid electrolytes appears to be always morphologically unstable, i. e. dendrite and whisker growth is the normal case. The growth of extended and surface covering metal films have yet not been reported. Being trivial, it is nevertheless worth mentioning that the normal mode of growth in the direction of the anode is not observed under normal conditions, as the solid electrolyte is mechanically rigid. Only in extreme conditions, i. e. strong electric fields and high mechanical pressure on the electrodes, (filamentary) metal growth within the electrolyte may occur, of course finally leading to a short-circuit of the cell.
This leads to the question how parameters like temperature, current density, applied voltage, electrode geometry, etc. influence the morphology of the metal deposition on solid electrolytes.

2.3.3 A case study: Silver deposition on AgBr

In the past years Peppler and Janek made a systematic study of cathodic silver deposition at microelectrodes, attempting to identify the experimental conditions for whisker or dendrite growth. They identified both temperature and current density as key parameters, see also fig. (3) (c).
At temperatures of $\vartheta \simeq 275$ ℃ the dendrites were rather compact and the whiskers had diameters in the order of several micrometers. This morphologies changed drastically when the temperatures was decreased below 220 ℃. [65]

Deposition of Silver Dendrites at Microelectrodes At temperatures of $\vartheta \simeq 150$ ℃ a clear preference for the growth of dendrites in two crystallographic directions occurred. The angle between those two directions is about 150°, see fig. (4) (a). Even if the sample was rotated and a new microelectrode was used the dendritic growth took place in the same directions. Thus, an influence of the interface between microelectrode and electrolyte and any external field on the preference of the growth direction could be excluded. It was not possible to determine in which crystallographic direction of the silver bromide the growth took place, because of unknown orientation of the used single crystal. A determination of the crystal orientation by electron backscatter diffraction (EBSD) failed because of the sensitivity of the AgBr towards the electron

beam. The cathodic overpotential was in the range of several tens of mV. Closer inspection of the dendrite reveald that it was not a compact structure like at higher temperatures (cf. fig. (3) (c)) but that it consisted of several whiskers aligned together, see fig. (4) (c). Schroeder [66] reported a similar behavior on silver chloride surfaces.

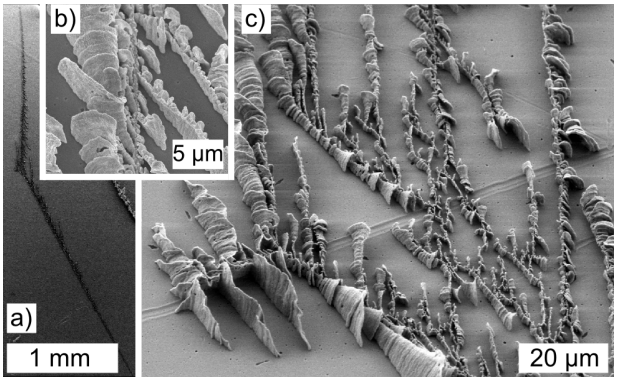

Figure 4: HRSEM pictures: (a) Dendrite deposited on AgBr at a temperature of $\vartheta \simeq 150$ ℃ ($I = -5$ µA, $t = 1{,}5$ min), (b) and (c) magnifications of (a).

Deposition of Silver Whiskers at Microelectrodes The diameters of whiskers deposited at temperatures of $\vartheta \simeq 220$ ℃ were not longer in the order of several micrometers but in the order of several 100 nanometers, see fig. (5). Furthermore, the growth was not longer limited under or close around the electrode. Initially, a filigrane dendrite grew on the surface which showed the same preferential growth in two crystallographic directions as described above. After a short time lateral growth on the surface stopped and only growth into height occured in form of filigrane silver whiskers which formed a structure like a tangled ball of wool. During lift-off of the microelectrode this silver whisker bunch was stressed and deformed, resulting in the appearance of spun sugar, see fig. (5) (a). The overvoltage was higher compared to the growth of whiskers at higher temperatures, but still in the range of some tens of mV.

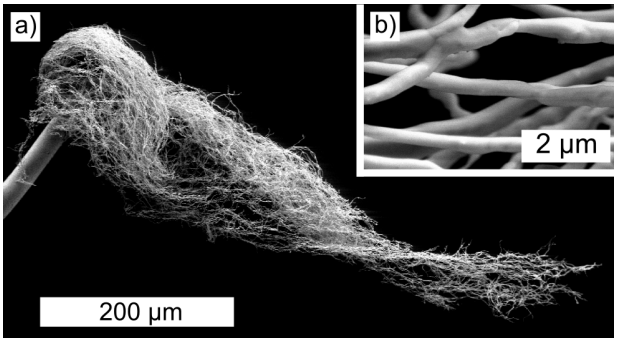

Figure 5: HRSEM pictures: (a) Silver whiskers deposited at a temperature of $\vartheta \simeq 220$ ℃ which adhered to the microelectrode at liftoff ($I = -0.5$ µA, $t = 630$ s), (b) magnification of (a).

In essence, the morphology of metal electrodeposits on a solid electrolyte depends strongly on the geometric boundary conditions, as these control the local current densities and the electric field. Generally, high current densities lead to dendritic growth. In simple terms, dendritic growth increases the electroactive interface and therefore leads to a decrease of the local curent densities and the related overvoltage. Low current densities lead to whisker-type growth, provided that the mechanical boundary conditions allow the growth of extended filamentary deposits.
There will be a number of second order effects, e. g. the influence of the surface properties or non-equilibrium defects in the electrolyte. Their influence on the electrodeposition process has yet not been demonstrated, as even the exact reproduction of the geometric boundary conditions is not simple. Without progress in well defined model experiments with geometrically and microstructurally well defined systems, advances beyond the current state of knowledge have not to be expected.

2.3.4 Stability in External Electric Fields

An interesting question with implications for a number of applications concerns the stability of metal deposits in contact with electrolytes under the influence of electric fields – in particular once the deposit has lost contact to the electrode. This experimental situation of a metal particle which is not directly electronically contacted to one of the electrodes but contacted ionically via the electrolyte is usually denoted as a bipolar electrode. And as is discussed in the following, a bipolar parent metal electrode is intrinsically morphologically unstable.
Both Marshall et al. [56] and Bradley et al. [67] studied bipolar electrodes in liquid electrolytes. They reported on the behavior of two metal discs in a water which are not electronically connected to an external circuit. The discs were aligned with an externally applied electric field, thus polarisation leads to opposite charging of the both faces of the discs, i. e. the now bipolar discs show an anodic and a cathodic side, see fig. (6) (a). As the aqueous environment was free of metal ions, deposition occured after a short time during which metal ions dissolved at the disc closest to the cathode and moved toward the disc closest to the anode. The deposition took place in the form of dendrites with a directed growth from one disc to the other, and the growth ceased immediately when the gap was closed.
A similar effect is observed if a parent metal particle is contacted with a solid electrolyte. Peppler et al. observed the morphological development of silver dendrites on AgBr single crystal surfaces [61] exposed to an external electric field. The silver dendrite is only ionically contacted by a silver electrolyte, and by polarising the electrolyte the dendrite becomes a bipolar electrode. Thus, dissolution took place at the anodic side of the particle (the side directed towards the external cathode) and deposition of silver at the cathodic side, see fig. (6) (b). As described in more detail in [61] the bipolar electrode spreads fast along the electrolyte surface in the form of a thin silver surface film, thus shortening the distance to the anode. Silver deposition at the cathode takes place simultaneously, see fig. (3) (b).
Interestingly, Nielsen and Jacobsen [68, 69] observed morphological changees of Pt, Pd and Ag microelectrodes on YSZ single crystals under cathodic polarization. As YSZ is a pure oxygen ion conductor, the mechanism of this migration is not clear yet. Nielsen and Jacobsen discusss gas phase transport along the polarized metal electrode as a possible mechanism.
In summary, we have to conclude that a parent metal which is in contact with an ion-conducting

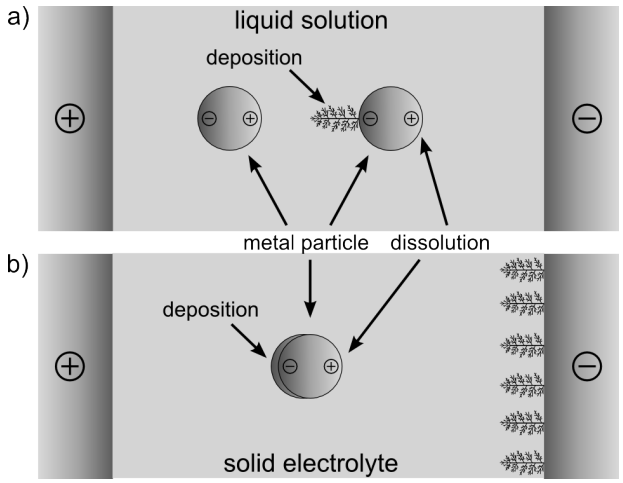

Figure 6: Field driven migration of metal particles: (a) Setup for bipolar electrode processes used by Bradley [67] and Marschall [56] for aqueous solutions, (b) Setup for bipolar electrochemistry on a solid electrolyte surface [61].

phase, and which is exposed to electric polarisation by the electrolyte, becomes a bipolar electrode. In other terms we may consider the metal particle as an electronic short-circuit of the surrounding electrolyte phase. Depending on the current along this short-circuit the particle will grow at its cathodic side and dissolve at its anodic side. This bipolar effect is a general phenomenon and should always be taken into account if micro- or nanostructured metal assemblies are exposed to electrolye environments – being solid or liquid. In section (3.1) we will see that the bipolar electrode effect plays an important role for the mechamism of electrochemical memory devices.

2.4 Kinetics of electrodeposition on solid electrolytes

There ist yet no comprehensive treatment of the mechanism of cathodic metal deposition available. As in every electrode process, the crucial step is the charge transfer across the phase boundary which in the present case has to be described as the jump of a metal ion from the electrolyte lattice towards the metal surface. Nucleation and crystallization of the metal follow. This sequence has been well analyzed for liquid electrolytes in the past (see e. g. the book by Budevski, Staikov and Lorenz [1]). The same analysis for the solid|solid interface is complicated by mechanical effects: The electrolyte is rigid, and metal deposition causes severe mechanical stress. Either the growing metal nuclei separate electrode and electrolyte, cf. fig. (7), or they deform both phases plastically, thereby introducing serious damage to the lattices.
In contrast to liquid electrolytes solid electrolytes cannot adapt to rough electrode surfaces, and in reality the solid electrolyte surface is rough, too. As already pointed out early by Rickert [72, 73] this leads to a very small number of electrochemically active interface sites and to laterally highly inhomogeneous electrode processes. As shown in the previous paragraph, dendrite formation may start from these few interface sites and will lead to a continuously changing active contact area. Qualitatively we may adopt the terrace-ledge-kink model for the

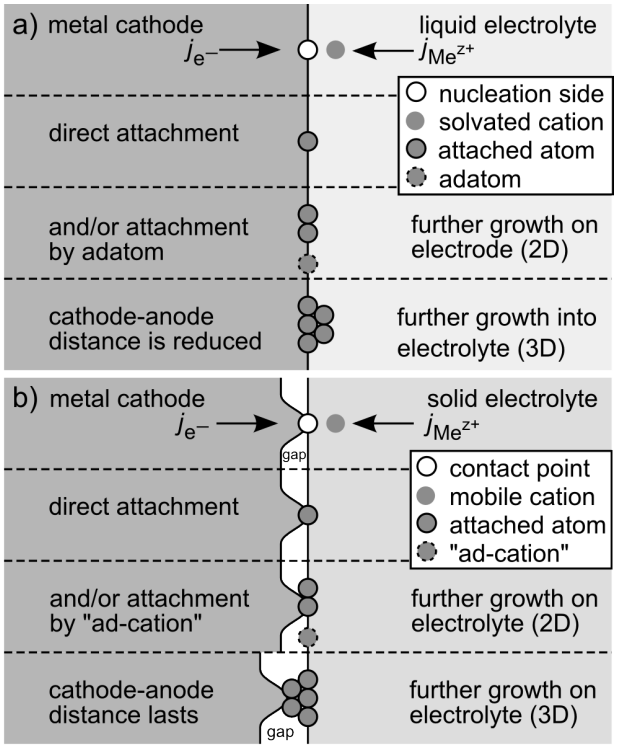

Figure 7: Aspects of electrodeposition at solid|liquid and solid|solid interfaces (a) Solid|liquid: Ions from the solution are discharged at the cathode surface but may still be mobile on the surface as adatoms (b) Solid|solid: Ions from the solid electrolyte can only be discharged at contact points between cathode and electrolyte when the electrolyte is a pure cation conductor. Maybe ad-cations on the electrolyte surface exist [70, 71].

description of the microscopic steps during deposition or dissolution, but due to missing experimental verifiction this is of limited value. Even simple metal deposition leads to complicated kinetics, because metal nucleation takes place only at designated sites. As a consequence, it is virtually impossible to determine current densities across a solid|solid electrode. Usually the current density is given as an apparent current density, dividing the measured current simply by the geometric area of the electrode rather than by the true contact area. Therefore, current densities at solid|solid interfaces are mostly underestimated.

2.4.1 Electrocrystallization

The anodic dissolution of metals into solid electrolytes, i. e. the nucleation of pores in a metal electrode, has been studied in more detail than the cathodic deposition, cf. [74, 75, 76]. The reason for the stronger interest in the dissolution process is its participation in corrosion and tarnishing. During the formation of tarnishing surface layers by corrosive attack the kinetics of the inner interface between metal and growing film plays a crucial role for the overall kinetics and morphological development.
The electrodeposition of metals at solid|liquid interfaces has been investigated intensively during

the last decades, and detailed survey can be found in [1, 77, 78, 79, 80, 81, 82, 83]. The development of new in situ methods in electrochemistry like optical spectroscopies (linear and non-linear), X-ray diffraction and scanning probe microscopy has led to "an atomistic view of electrochemistry" [84].

Concerning the formation of specific microstructures, there is common agreement that powdery electrodeposition occurs only under the condition of current limitation, i. e. the current must exceed the diffusion limiting current, and that it starts only after a initial transient time (i. e. the time needed to deplete cations at the cathode to zero concentration). The limiting current and transition time depend on electrolyte concentration, supporting electrolyte concentration, temperature, etc. Surface inhomogeneities of the cathode have to be considered, too. Surface inhomogeneities of different dimensionality significantly influence the kinetics of metal deposition and the time dependent surface morphology. The competition between growth and nucleation determines grain size and microstructure of the deposit [1].

In the early years of liquid state electrochemistry most results suffered from irreproducibility because clean and structurally well defined surfaces were not available. This was partly solved by the development of the dropping mercury electrode (DME), where the surface is constantly renewed and free of defects. A second important step was the introduction of flame-annealing of metal electrodes, thus offering crystalline surfaces with well defined and orientated facets. Being critical, solid state electrochemistry has still to overcome the equivalent experimental difficulties: The influence of impurities or of crystallographic orientation has been rarely addressed, as usually the influence of mechanical effects is much stronger. This leads directly to the major problem – the control of the mechanical conditions. Progress will only be achieved once electrodes are applied under controlled mechanical force.

Armstrong et al. [85, 86] found for solid electrolytes that "the magnitude of current increased markedly with applied pressure" (i. e. mechanical load). They also had the problem that the current "at constant pressure (i. e. mechanical load) varied from one experiment to another". These two factors still are the main factors for the lack of reproducible data from solid|solid interfaces. In the 1970s first monographs on solid state electrochemistry where published [72, 73], but their emphasis was mainly on the transport properties of the solid electrolytes, in most cases the interface between the electrode and the solid electrolyte is only briefly addressed [36, 87]. It has also to be kept in mind that under high mechanical load the solid electrolyte might become plastic [74] and strongly disordered. But there are also solid|solid interfaces which exhibit large current densities at very low overpotentials. There are several contributions [74, 88, 89, 90, 91, 92] which report on high exchange current densities at the interface Ag-whisker|α-Ag_2S with low overvoltages. In general, literature concerning the kinetics of ion transfer from a solid electrolyte to a solid electrode is still scarce. Armstrong et al. [85, 86] investigated the deposition of silver from $RbAg_4I_5$ on silver, platinum, pyrolytic graphite and vitreous carbon as cathodes. They always found a nucleation and growth of discrete centers. Bazan et al. investigated the kinetics of silver and copper(I) ion transfer at Ag|AgI [70] and Cu|CuI [71] interfaces. They proposed a two step mechanism for the ion transfer, (i) ion transfer from the crystal lattice of the electrolyte to the electrolyte surface, (ii) incorporation into the metall. In a further step they investigated the nucleation and growth of copper on glassy carbon electrodes [93]. From their measurements they proposed a 3-dimensional growth for high current densities (> 24 mA/cm^2) and a 2-dimensional growth for low current densities (< 24 mA/cm^2). Spangenberg et al. [63, 64] reported on the in situ observation of electrodeposition of silver on

silver chloride at microelectrodes by optical microscopy. They introduced mechanical scratches on silver chloride single crystals and subsequently positioned the microelectrode in the scratch and applied negative voltages for a few seconds. This resulted in the filling of the scratches. They assumed that the higher surface energy in such scratches leads to enhanced nucleation rates. If they applied the voltages longer as necessary to fill the scratches, they observed the growth of silver dendrites or fractal-like structures on the silver chloride surface. This behavior was also observed by Peppler and Janek on silver bromide surfaces [65]. Ostapenko [94, 95] investigated the anodic dissolution and cathodic deposition of copper at solid $Cu_4RbCl_3I_2$|Cu interfaces. He assumed an instantaneous formation and 3-dimensional growth of copper nuclei in accordance with his data.
In conclusion, our current understanding of the initial stages of nucleation and crystallization at the solid|solid interface is still poor. The adaption of concepts developed for liquid electrolytes is generally not possible due to the different mechanical boundary conditions at solid|liquid and solid|solid interfaces, cf. fig. (7). Systematic experimental studies of model systems with geometrically well defined microelectrodes under controlled mechanical conditions and STM experiments are required in order to obtain reliable quantitative data. Up to now there have been only a few attempts of this kind. [96, 97, 98, 99]
Summarizing, only isolated investigations on the metal deposition at solid|solid interfaces exist. A comprehensive description is missing and because of the scarce data not yet in sight.

2.4.2 Mechanical effects

Mechanical contacts between electrodes and solid electrolytes are not as perfect as with liquid electrolytes [100]. Occasionally pores develop at the anode due to dissolution of the electrode metal and/or decomposition of the electrolyte. In some systems cathodically growing crystallites separate the electrolyte from the electrode metal. This results in a considerable decrease of the electrode area. The nature of the deposition mechanism and the resulting structure is affected by solid electrolytes. The higher viscosity of a solid electrolyte impedes the growth into the electrolyte to a large extent. Therefore, deposits tend to grow on the surfaces, on the side surfaces when macroscopic electrodes are used, and on the top surface when microscopic electrodes are applied. The electrolyte surface influences the morphology of the growing deposit due to its crystallographic orientation and surface structure including adsorbates. The kinetics of metal deposition on solid electrolytes is further complicated by the structural integrity of the interface. Certainly, it will make a difference wether the interface is coherent, semi coherent or incoherent. The fabrication of (semi-)coherent interfaces is associated with experimental effort, therefore often incoherent interfaces are investigated. Even if a coherent interface has been prepared prior to experiments it can change into an incoherent interface during electrodeposition. Whereas in fluid systems only hydrostatic pressure is present, in solid systems strong inhomogeneous force interaction is a problem depending on elastic and plastic deformation of the electrode and the electrolyte. Thus, data are normally not well reproducible.

2.4.3 Constriction resistance

Due to the surface roughness of solid electrolyte and electrode the apparent (or geometrical) contact area is always lager than the load bearing contact area. Thus, the contact area can in some cases be regarded as an array of point contacts. In case of point contacts at nearly

reversible solid|solid electrodes the potential drop occurs in a small volume of the electrolyte around this point contact. The relation between constriction resistance and local conductivity depends on the electrode geometry. For hemispherical point contacts equation (1) is valid and for circular point contacts equation (2).

$$R_{\text{hemi}} = \frac{1}{\pi \cdot \sigma_{\text{bulk}} \cdot d_{\text{geo}}} \tag{1}$$

$$R_{\text{circ}} = \frac{1}{2 \cdot \sigma_{\text{bulk}} \cdot d_{\text{geo}}} \tag{2}$$

with
R_{hemi} = Constriction resistance of hemispherical contact
R_{circ} = Constriction resistance of circular contact
σ_{bulk} = bulk conductivity of electrolyte
d_{geo} = geometric diameter of point contact

Thus, the temperature dependence of constriction resistances is in inverse proportion to the temperature dependence of the electrolyte conductivity. In a contribution about "rough electrodes in solid and liquid electrochemistry" Fleig and Maier [101] showed that the difference of the contact area between a rough electrode and liquid respective solid electrolyte changes the impedance drastically. In case of such a solid|liquid interface only one semicircle appears which can be described by one parallel RC element. The values of R and C differ only slightly compared to values of a smooth electrode. In case of such a solid|solid interface two semicircles appear which can be described by two parallel RC elements in series. The high frequency semicircle is independent of contact geometry and enables the calculation of bulk parameters (e. g. σ_{bulk}). The additional low frequency semicircle is a consequence of the imperfect contact. This so called constriction resistance can also be used to make local conductivity measurements on solid electrolytes with microelectrodes, i. e. single point contacts [97, 102].

2.5 Size Effects

It is known that different physical and chemical properties arise when a critical size is reached. For most cases this applies only to dimensions in the regime below about 100 nm.

2.5.1 Thermodynamic Stability - Electrochemical Ostwald Ripening

Schroeder et al. [66, 103, 104] reported an excess emf of a few mV in a solid state transference cell of the type nano-Ag|$RbAg_4I_5$|micro-Ag, which declines over time. This excess emf is caused by the difference in the chemical potential of nanocrystalline silver and microcrystalline silver due to surface energy. Single nanoparticles with slightly different sizes possess different chemical potentials, too. If these metal nanoparticles are indirectly ionically connected by a pure ion conductor and electronically by a current collector, the smaller particles with the higher chemical potential are dissolved and the bigger particles grow, see fig. (8) (a). The electrons propagate along the current collector and the metal ions through the solid electrolyte. During this ripening process the difference of the chemical potentials of the (former) nanocrystalline

and the (still) microcrystalline silver declines and thus, the excess emf. If the metal nanoparticles are indirectly connected by a mixed electronic and ionic conductor, the flux of electrons and metal ions takes place in the same material, see fig. (8) (b). Knauth [105] reported on an excess emf in the solid state transference cell nano-Ag|AgI|micro-Ag. He stated that the cell reaction is the transfer of silver from the nanocrystalline to the microcrystalline electrode. Thus, single metal nano particles indirectly in contact with microcrystalline parent metals over a mixed conductor should be unstable too, at least when the electrolyte is thin, see fig. (8) (c). This electrochemical Ostwald ripening is a very important fact which has to be taken into account not only for fundamental research but also for the ongoing miniaturization of solid electrochemical devices. It limits the time and temperature of operation of nanocrystalline devices.

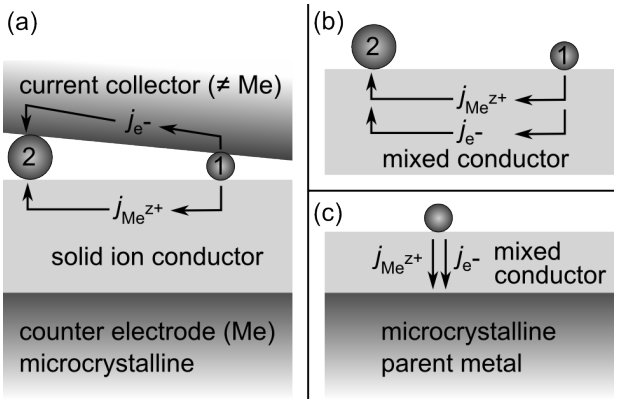

Figure 8: Electrochemical Ostwald Ripening: (a) Transference cells with nano particles as one electrode (i. e. nanocrystalline electrode) and microcrystalline counter electrode show an excess emf, which declines with time, because the larger particles (2) grow at the cost of the smaller ones (1) (according to [103, 104]). (b) Isolated nanoparticles on a mixed conductor do not need external electronic contacts for ripening. (c) Isolated nano particles on mixed conductors in contact with microcrystalline parent metal are unstable, too.

3 Current and Future Applications

3.1 Memories and Switching Devices

Terabe et al. [106, 107] constructed a "quantized conductance atomic switch" based on silver sulfide (a MIEC) as solid electrolyte. The switch is based on the formation of an one nm thick silver particle by a tunneling current between an electrolyte and a platinum wire (on state) and the dissolution of this particle (off state). Because of the low tunnel current only small particles are initially formed. Considering electrochemical Ostwald ripening the stability of this particles with time is in question especially when the counter electrode is macro- or microcrystalline silver with a lower chemical potential of silver, see fig. (8) (c). There are also several contributions about resistive switching [9, 10, 44, 108, 109]. Resistive switching is the reversible switching between a low and a high resistance state. In case of cation conducting

materials the switching to a low resistance state is attributed to the electrochemical formation of thin metallic filaments between the electrodes, thus the electrodes are short-circuited. In order to obtain stable connections it is also necessary to use current compliance during the formation. Thus, the destruction of the filament is prevented due to high current densities at the time of contact with the anode. Switching back into the high resistance state necessarily involves the (at least partially) dissolution of this filament. By reversing the voltage between the electrodes the electronic current through the filament is reversed, too. Thus, the dissolution cannot be explained by simple re-oxidation of the deposited filament. There are still several mechanisms under discussion, for example blasting by Joule heating (like a fuse) or electromigration due to high current densities. Guo et al. [44] proposed that the curvature of a formed silver bridge (i. e. a filament) in combination with its diameter is responsible for the dissolution. Compared to the (parent metal) electrode the curvature of the filament is much higher and the diameter much smaller. Thus, the chemical potential of the silver bridge is higher, favoring the dissolution. Employing numerical field simulation they calculated that the major voltage drop occurs near the neck of the silver bridge i. e. the point with highest curvature and smallest diameter of the filament. Thus, the filament is dissolved at this point (further dissolution now is due to electrochemical re-oxidation of the metallic filament). This means, that the morphology of the initially formed filament is important for the subsequent dissolution. Longe time data storage can only be guaranteed when the initially formed filament does not change its morphology to much. There is the possibility that due to the difference in the chemical potentials either the connection is lost, or later a dissolution might not be possible anymore, because of an augmented silver bridge. Because of the repeated switching between on and off state a degradation of the cell must be considered, too. For the research in the field of non-silicon based devices for data storage and processing it is important to find an understanding of mechanism of (parent) metal deposition on solid electrolytes [9].

3.2 Lithium Secondary Batteries

For current and future technologies such as e. g. transportation of people and cargo, mobile devices etc. the storage of energy is a major issue. Lithium based rechargeable batteries are one possible solution for energy storage, but there are still some shortcomings which prevent employment for many applications, for instance the time of charging, especially for electric cars, life time, i. e. number of charging discharging cycles.
Batteries are based on complex interactions between anode, electrolyte and cathode. Lithium ion conducting electrolytes can be subdivided in different classes, i. e. liquid electrolytes, polymers, glasses and crystalline compounds. Up today lithium secondary batteries with liquid electrolytes are employed in devices such as laptops and mobile phones. But for possible future applications research concerning all solid state lithium secondary batteries is gaining more and more importance, as well as the employment of lithium metal as anode material instead of intercalation compounds because of higher capacities and voltages. Thus, there is plenty of room to further enhance the performance by the investigation of various materials and material combinations for anode, electrolyte and cathode.

3.2.1 Dendritic Growth (ex situ)

The employment of lithium as anode material in contact with liquid electrolytes has the advantage of high capacity, but on the cost of some serious problems. The problems are:

- surface passivation of lithium (SEI formation)
- internal shortening due to lithium deposition between electrodes during charging (in literature this phenomenon is called either dendritic or filamentary growth, cf. subsection 2.3)
- low charging/discharging rates
- limited number of cycles
- thermal runaway (which can lead to explosion) due to misuse

There are only comparatively few papers which combine the investigation of battery cycling and morphological development of lithium electrodes. Aurbach et al. [110] investigated "the correlation between charge/discharge rates and morphology, surface chemistry and performance of lithium electrodes" with ex situ methods like scanning electron microscopy (SEM), energy dispersive X-ray spectroscopy (EDX) and Fourier transform infrared spectroscopy (FTIR) after different cycling steps and rates. They showed that the lifetime (number of cycles) could be enhanced when prior to normal cycling the cell was cycled with a special combination of high discharging and low charging rates. With this pretreatment the surface chemistry of lithium was changed, a native film of Li_2O and $LiCO_3$ on the lithium electrode was removed and replaced by a protective layer of solvent reduction products (SEI). The electrolyte system was $LiAsF_6$/tributylamine (stabilizer)/1,3-dioxolane. They concluded that this protective layer induced an uniform lithium deposition, thus preventing the formation of 'dendrites'. In a following contribution Aurbach et al. [111] concluded that the formation of polydioxolane, which is an elastomere, is responsible for the good cohesion on the lithium surface. The major factor that limits battery cylce life is depletion of solution due to reactions with deposited lithium [111]. Gireaud et al. [112] performed 'lithium metal stripping/plating mechanism studies'. They investigated deposition and dissolution of different lithium surfaces in EC/DMC-$LiPF_6$ and EC-$LiPF_6$ electrolytes and used pristine lithium foil surfaces as shipped by manufacturers, polished surfaces and lithium thin films prepared by pulsed laser deposition (PLD). As expected the deposition of lithium on smooth surfaces is free of dendritic growth, but this effect cannot be extended upon cycling where the initially smooth surfaces are destroyed when the inner lithium microstructure emerges upon dissolution. They concluded that dendritic growth models have to take into account the lithium surface state as additional key parameter.

3.2.2 Dendritic Growth (in situ)

In order to expand knowledge on the mechanism of dendritic growth the next obvious step was the in situ investigation. Brissot et al. [113, 114, 115] made investigations under in situ observation with optical microscopes. They observed growth of dendrites and determined concentration gradients by optical methodes. The experimental efforts were relative low and lack of high local resolution. The cell geometry is very different from those of actual batteries, in principle it resembled the geometry shown in fig. (3) (a). Hence it is not surprising to

observe the growth of dentrites from cathode to anode. Dollé et al. [116] reported on the in situ observation of the cycling of a Li|polymer-LiTFSI|$Li_xV_2O_5$ battery in a SEM. They observed the delamination of the lithium electrode and the polymer during charging due to the growth of 'dendrites', i. e. filaments. This separation of electrode and solid electrolyte is comparable to the growth of silver whisker arrays as described by Rohnke et al. [62], see fig. (3) (b). It is noteworthy that this growth of silver whisker arrays still occured under mechanical load. Dollé et al. [116] observed the growth of a 'dendrite' (i. e. a filament) through the electrolyte between two lithium electrodes, too. This short circuiting resulted in a breakdown of the voltage under galvanostatic conditions. But after some time the voltage returned back to the inital voltage. They attributed this behavior to the function of the 'dendrite' as a fuse which blasted due to high currents. In a following contribution about "dendrite short-circuit and fuse effect on Li|polymer|Li cells" Rosso et al. [117] enlarged this thesis. To obtain even more detailed information about the different interfaces Brazier et al. [118] employed transmission electron microscopy (TEM) on nanobatteries. They did not achieve in situ TEM oberservation yet, but they are in the course of manufacturing. Because of the necessary nanoscale dimension of the cells the question arises if the obtained data will be comparable with micro-/macroscale cells. Nevertheless, in situ TEM observations will give valuable information about the formation of 'dendrites'.

3.2.3 Therory

Monroe and Newman [119, 120] presented two models for dendrite growth in lithium|polymer systems. One is based on electrochemical considerations and tip curvature (i. e. surface energy) of the growing dendrites [119], another is based on linear eleasticity theory (i. e. shear moduli and Poisson's ratios of lithium and polymer) [120]. With the first model they could explain why low current densities (i. e. current densities below 75 % of limiting current) are favorable to reduce growth of dendrites and they also showed that the surface energy has only a minor impact on growth of dendrites. In the second model they deduced that at shear moduli of electrolytes lower than twice the shear modulus of the lithium electrode the electrode is instable, i. e. growth of 'dendrites' takes place. At shear moduli of electrolytes twice as high as the shear modulus of the lithium electrode the electrode is stable, i. e. no growth of 'dendrites' takes place. A shear modulus which is at least twice as high as the shear modulus of lithium is three or more orders of magnitude higher than those achieved by commonly researched polymers [120]. Their model also predicts that stability is more difficult to achieve when the separator is compressible. Both models are simplified and thus give only qualitative results. The greatest drawback of both models is the neglect of adhesion between the electrolyte and the lithium electrode, as they pointed out themself [120]. But delamination of electrolyte is a commonly observed problem at lithium electrodes, as mentioned before [116]. 'Dendritic' growth is a multifaceted problem.

3.2.4 All Solid State Cells

Besides liquid and polymer based electrolytes (which cannot be counted as real solid electrolytes) solid electrolytes are gaining importance. Solid electrolytes are especially favorable for lithium batteries in integrated circuits. The reason is the fabrication of silicon chips by lithographic methodes in connection with coating and ion implantation which is still connected with coating of wafers by solid materials. Dudney and co-workers [121, 122] produced thin-film

lithium batteries with a capacity loss of only 0.05 % per cycle at discharge rates of 1.5 mA/cm^2. The batteries were of the type Li|LiPON|$LiCoO_2$, LiPON denotes glassy lithium phosphorous oxynitride. This batteries have long shelf times, can be cycled over 1000 times and show low self-discharge. Interestingly, batteries where the lithium anode was made during the first charging, i. e. by electroplating on the current collector, showed a higher capacity loss. Liu et al. [123] reported for Li|LiPON|TiO_2 batteries a good capacity retention over cycling, too. They investigated also the influence of battery preparation and found that when all preparation steps were carried out without breaking vacuum and inert gas atmosphere, batteries showed better cyclabilities and lower interface resistances. Thus, the preparation of the interface, i. e. microscopic structure and/or impurities, influences the metal deposition and dissolution process. But, a detailed morphological investigation of the lithium|electrolyte interface is missing. For instance, the Ag-whisker|α-Ag_2S (high temperature modification) interface exhibits high exchange current densities and low overvoltages [124, 89]. It would by highly interesting to know if this is also the case in batteries with a Li|LiPON interface and thus is responsible for the good performance of this batteries.

3.2.5 Conclusions

All given examples regarding lithium batteries have in common that the structure of the interface between lithium anode and electrolyte (beneath other factors) influences the performance of the battery. Regardless of the type of electrolyte, i. e. liquid, polymer or solid, the growth of 'dendrites' (filaments) during charging is one of the main problems. In case of liquid and (soft) polymer electrolytes this growth leads to the shortening of the cell and thus limits the lifetime, i. e. number of cycles. In case of solid electrolytes this growth leads to delamination, this effect is observed at polymer electrolytes, too. Data on the growth of 'dendrites' during charging of lithium batteries with lithum anodes is still scarce. Especially the relationship between results from standard investigations like cycling, cyclovoltammetry and electrochemical impedance spectroscopy (EIS) and the morphological development of the battery is still missing in most cases. Clearly the reason is the problem of transport from glove box to electron microscope without contamination by oxygen and moisture, i. e. destruction of sample. But in order to understand and improve lithium batteries there is probably no other way.

3.3 Nanostructuring /-printing

3.3.1 Liquid electrolyte

Employing liquid electrolytes the micro- or nanostructuring of a metal surface (i. e. workpiece or counter electrode) can be achieved by using a microelectrode (i. e. worktool or working electrode). In most cases the workpiece electrode is part of an AFM, STM or SECM equipment. Depending on the polarization the workpiece surface can be dissolved or metal can be deposited from the worktool electrode. Schuster et al. [125, 126, 127] showed that with ultrashort voltage pulses in the order of ns (i. e. far from equilibrium) it is possible to modify the surface locally on the nm scale. It is also possible to use microelectrodes in order to machine a workpiece with micrometer precision [128].

3.3.2 Solid electrolyte

In case of solid electrolytes it is not possible to machine a workpiece metal electrode with a worktool metal electrode because of the high viscosity of the electrolyte. Instead the solid electrolyte has to be used as the worktool. It is possible to dissolve the metal workpiece into the solid electrolyte or to deposit metal on the workpiece from the solid electrolyte. For instance, Kawada et al. [12] used metal|β-alumina worktools with pyramidal shape with µm scale in order to create pyramidal holes in silver metal. Hsu et al. [13] patterned silver sulfide with a FIB and used this stamp to convey the structure on silver by dissolution of the silver. It was possible to create structures in the submicrometer regime. Terabe et al. [11, 106] used silver sulfide as functional STM tip. Depending on polarization silver is either deposited or (re-)dissolved at the apex of the silver sulfide tip by the tunneling current. They found that small amounts of silver (10 nm wide and 0.2 nm high) were deposited continuously on the sample (i. e. a silicon wafer) from the silver sulfide tip upon line scanning (negative bias at sample, i. e. deposition of silver at apex of silver sulfide tip). They assumed high-field evaporation responsible for the silver deposition on the sample. Kamada et al. [129] used a Ag|Ag-β"-alumina microelectrode (diameter about 10 µm) as silver ion source in order to dope an alkali silcate glass with silver. By connecting the microelectrode to a microstage they could draw pattern of silver into the glass. Lee et al. [130] used a conductive AFM tip to electrodeposit silver structures on $RbAg_4I_5$ (a silver ion super conductor). The counter electrode was a silver film. Thus, their setup resembled the configuration depicted in fig. (3) (c). They achieved structures with sub 100 nm features.

3.3.3 Conclusions

With the exception of the nano stamp of Hsu et al. [13] all electrochemical techniques mentioned in this section have in common that the structuring was achieved by sequential methodes, for both liquid and solid based approaches. Thus, they are not suitable to replace the today employed methode of lithography, because they are to slow. Regarding the structuring by the way of metal electrodeposition it is questionable if a reproducible large-area structuring is feasible under commercial conditions. For the near future electrochemical micro- and nanostructuring methodes might be used for special applications but they will not be relevant for large-scale production.

3.4 Failure Mechanism in Electric and Electronic Devices

In some cases electric devices are coated with silver either as corrosion protection or in order to guarantee good electric contact between two connectors. In environments which contain hydrogen sulfide, like in paper mills or in purification plants, the growth of whiskers was observed [131]. This growth often leads to shortening with neighboured devices. The reason for the growth of silver whiskers can easily be explained. The hydrogen sulfide leads to the corrosion of silver, i. e. the formation of silver sulfide, a MIEC. Especially at devices which are warm or hot because of joule heating due to high current flows, the formation of silver sulfide is promoted. The generated heat by the current flow causes also a gradient in temperature from inside to outside which consecutively causes a gradient in the chemical potential of silver over the silver sulfide. If the driving force of the chemical potential gradient is high enough

nucleation of silver takes place leading to the growth of whiskers and thus to the shortening. The growth of whiskers in electronic devices is a known cause of failure, but is based on a totally different mechanism. In this case the growth is due to electromigration [132], the ballistic impact of charge carriers on the atom cores in the conductor path.

4 Summary

In contrast to liquid electrochemistry where electrodeposition is an important process in refining surfaces, e. g. for corrosion protection, the electrodeposition from solid electrolytes does not have such a significant usage. But as shown above, the electrodeposition of metals at solid|solid interfaces is an important process in many different applications. But compared to electrodeposition of metals at solid|liquid interfaces the underlying mechanisms are less well understood. Typically theory developed for solid|liquid systems is used and adapted to solid|solid electrodes. Astonishingly this works very well, depending on the investigated phenomenon. But there are also phenomena which do not occur at solid|liquid interfaces only at solid|solid interfaces. For instance, at solid|liquid interfaces no contact problems (due to geometrical and/or mechanical reasons) occur between rigid electrode and fluid electrolyte. In case of solid|solid interfaces the contact between rigid electrode and rigid electrolyte depends strongly on the applied mechanical load. Janek and Majoni [75, 76] reported on periodic phenomena during anodic dissolution of silver into solid α-AgI. They observed a regular or an irregular oscillation of the cell voltage under galvanostatic conditions, depending on applied mechanical load. They concluded, that during silver dissolution vacancies in the silver electrode accumulated to pores, leading to a decrease of contact area. Hence, the overall resistance increased as well causing an increase in voltage. If more and more pores were formed the walls became thinner and thinner until the structured collapsed under the mechanical pressure. Thus, increasing instantaneously the contact area and causing a drop in voltage. Then the process beginns again, thus the oscillation can be explained. At the cathodic side such oscillationg phenomena are not very likely. After the formation of crystallites and an inital growth of this crystallites the electrode and the electrolyte are separated. Thus, depending on experimental conditions either fruther growth of the initially formed crystallites is possible or additional nucleation at the edges of the growing crystallites. In the first case the growth of whiskers is observed [62, 65, 116, 117, 133], in the second case the growth of dendrites [59, 61, 63, 64, 65, 66, 114]. Thus, the contact area between solid electrolyte and solid electrode either remains more or less constant after a short time or grows continiously. Well, there are certain phenomena in solid|solid systems at anode and cathode which hinder the collection of reproducible i. e. quantitative data in the first place. It is necessary to investigate suitable model systems with defined interfaces (e. g. single crystalline electrode and electrolyte, coherent interface, etc.) in detail. In solid electrochemistry the match of a dropping mercury electrode from liquid electrochemistry is missing!
Unfortunately the most easy to fabricate and manageable cation conducting solid electrolytes i. e. the silver halides are rather soft with low Mohs hardness (2-3). Hence, the preparation of well defined solid|solid interfaces with soft silver halides is (nearly?) impossible. A further problem is the sensitivity of cation conducting materials to electron beams, thus *in situ* and *ex situ* investigations in SEM and TEM will always result in a local reduction by the electron beam [134].

When all this obstacles are overcome qualtitative and reproducible results concerning the metal deposition at solid|solid interfaces can be achieved. Then it might be possible to develop a (first simple) theory for metal deposition which can predict the occurence of different morphologies. And in a further development the transfer of knowledge from model interfaces to real interfaces. In short the problems concerning solid|solid interfaces are:

- preparation of well defined interfaces (coherent, semi-coherent, incoherent)
- stabel materials for electron microscopic investigations
- avoiding of contamination during preparation and transport, e. g. from glove box to electron microscope
- influence of impurities or instrinsic defects like screw dislocations
- transfer of knowledge from model interfaces to real interfaces

References

[1] E. Budevski, G. Staikov, and W. Lorenz, *Electrochemical Phase Formation and Growth*, VCH, Weinheim, 1996.

[2] J. O. Bockris and S. U. Khan, *Surface Electrochemistry*, Plenum Press, New York, 1993.

[3] A. J. Bard and L. R. Faulkner, *Electrochemical Methods – Fundamentals and Applications*, John Wiley & Sons Inc., 2nd edition ed., 2001.

[4] D. O. Raleigh In ed. W. V. Gool, *Fast Ion Transport in Solids, Solid State Batteries and Devices. Proceedings of the NATO sponsored Advanced Study Institute on Fast Ion Transport in Solids, Solid State Batteries and Devices, Belgirate, Italy, 5-15 September 1972.*, pp. 477–487. Amsterdam, North Holland Pub. Co.; New York, American Elsevier Pub. Co., 1973.

[5] D. O. Douglas O. Raleigh In ed. M. Kleitz, *Electrode Processes in Solid State Ionics - Theory and Application to Energy Conversion and Storage*, pp. 119–148. D. Reidel Publishing Company, Dordrecht, Holland, 1976.

[6] C. A. Vincent, *Solid State Ionics*, 2000, **134**, 159–167.

[7] M. S. Whittingham, *Chemical Review*, 2004, **104**, 4271–4301.

[8] M. Armand and J.-M. Tarascon, *Nature*, 2008, **451**, 652–657.

[9] R. Waser and M. Aono, *Nature Materials*, 2007, **6**, 833–840.

[10] R. Waser, R. Dittmann, G. Staikov, and K. Szot, *Advanced Materials*, 2009, **21**, 2632–2663.

[11] K. Terabe, T. Nakayama, T. Hasegawa, and M. Aono, *Applied Physics Letters*, 2002, **80**, 4009–4011.

[12] K. Kamada, M. Tokutomi, N. Enomoto, and J. Hojo, *Electrochimica Acta*, 2007, **52**, 3739–3745.

[13] K. H. Hsu, P. L. Schultz, P. M. Ferreira, and N. X. Fang, *Nano Letters*, 2007, **7**, 446–451.

[14] M. Nagata, Y. Itoh, and H. Iwahara, *Solid State Ionics*, 1994, **67**, 215–224.

[15] G. Hsieh, T. Mason, E. Garboczib, and L. Pederson, *Solid State Ionics*, 1997, **96**, 153–172.

[16] H. Hu and M. Liu, *Solid State Ionics*, 1998, **109**, 259–272.

[17] A. Hashibon, S. Raz, and I. Riess, *Solid State Ionics*, 2002, **149**, 167–176.

[18] J. Fleig, *Solid State Ionics*, 2003, **161**, 279–289.

[19] G. Alberti and M. Casciola, *Solid State Ionics*, 2001, **145**, 3–16.

[20] A. D. Robertson, A. R. West, and A. G. Ritchie, *Solid State Ionics*, 1997, **104**, 1–11.

[21] A. Essoumhi, C. Favotto, M. Mansori, and P. Satre, *Journal of Solid State Chemistry*, 2004, **177**, 4475–4481.

[22] E. I. Burmakin and G. S. Shekhtman, *Inorganic Materials*, 2008, **44**, 882–885.

[23] P. Junod, *Helvetica Physica Acta*, 1959, **32**, 567.

[24] P. Müller, *Physica Status Solidi*, 1965, **9**, K193–K197.

[25] P. Müller, *Physica Status Solidi*, 1965, **12**, 775–794.

[26] T. Takahashi, *Pure and Applied Chemistry*, 1978, **50**, 1091–1098.

[27] H. Schmalzried, *Progress in Solid State Chemistry*, 1980, **13**, 119–157.

[28] T. Takahashi, *Journal of Electroanalytical Chemistry*, 1984, **180**, 231–239.

[29] V. Thangadurai and W. Weppner, *Journal of Solid State Chemistry*, 2006, **179**, 974–984.

[30] P. Knauth and H. L. Tuller, *Journal of The American Ceramic Society*, 2002, **85**, 1654–1680.

[31] Iupac compendium of chemical terminology, electronic version, http://goldbook.iupac.org/d01588.html, 2008.

[32] R. A. Huggins, *Advances in Batteries*, Springer Verlag, Berlin, Heidelberg, New York, 2009.

[33] M. Martin, P. Tigelmann, S. Schimschal-Thölke, and G. Schulz, *Solid State Ionics*, 1995, **75**, 219–228.

[34] S. Schimschal-Thölke, H. Schmalzried, and M. Martin, *Berichte der Bunsengesellschaft: Physical Chemistry, Chemical Physics*, 1995, **99**, 1–6.

[35] S. Schimschal-Thölke, H. Schmalzried, and M. Martin, *Berichte der Bunsengesellschaft: Physical Chemistry, Chemical Physics*, 1995, **99**, 7–13.

[36] H. Schmalzried, *Chemical Kinetics of Solids*, VCH, 1995.

[37] L. Graf and W. Morgenstern, *Zeitschrift für Naturforscher*, 1955, **10a**, 345–346.

[38] W. G. Courtney, *Journal of Chemical Physics*, 1957, **27**, 1349–1356.

[39] P. B. Price and D. A. Vermilyea, *Journal of Chemical Physics*, 1958, **28**, 720–721.

[40] P. Carro, S. Ambrosolio, S. Marchiano, A. H. Creus, R. Salvarezza, and A. Arvia, *Journal of Electroanalytical Chemistry*, 1995, **369**, 183–195.

[41] F. Fourcade and T. Tzedakis, *Journal of Electroanalytical Chemistry*, 2000, **493**, 20–27.

[42] I. B. Murashova, A. P. Khramov, I. V. Zotin, Y. P. Zaikov, V. G. Zyryanov, and G. I. Murygin, *Russian Journal of Electrochemistry*, 2002, **38**, 1200–1205.

[43] X. Wen, Y.-T. Xie, M. W. C. Mak, K. Y. C. X.-Y. Li, R. Renneberg, and S. Yang, *Langmuir*, 2006, **22**, 4836–4842.

[44] X. Guo, C. Schindler, S. Menzel, and R. Waser, *Applied Physics Letters*, 2007, **91**, 133513.

[45] Z. Wang, Z. Zhao, and J. Qiu, *Journal of Physics and Chemistry of Solids*, 2008, **69**, 1296–1300.

[46] R. Brady and R. C. Ball, *Nature*, 1984, **309**, 225–229.

[47] D. B. Hibbert and J. R. Melrose, *Physical Review A*, 1988, **38**, 1036–1048.

[48] D. Barkey, F. Oberholtzer, and Q. Wu, *Physical Review Letters*, 1995, **75**, 2980–2983.

[49] F. Oberholtzer, D. Barkey, and Q. Wu, *Physical Review E*, 1998, **57**, 6955–6961.

[50] O. Devos, C. Gabrielli, L. Beitone, C. Mace, E. Ostermann, and H. Perrot, *Journal of Electroanalytical Chemistry*, 2007, **606**, 75–84.

[51] O. Devos, C. Gabrielli, L. Beitone, C. Mace, E. Ostermann, and H. Perrot, *Journal of Electroanalytical Chemistry*, 2007, **606**, 85–94.

[52] O. Devos, C. Gabrielli, L. Beitone, C. Mace, E. Ostermann, and H. Perrot, *Journal of Electroanalytical Chemistry*, 2007, **606**, 95–102.

[53] T. Hoffmann, J. Mazur, J. Nikliborc, and J. Rafalowicz, *British Journal of Applied Physics*, 1961, **12**, 635–636.

[54] D. Grier, E. Ben-Jacob, R. Clarke, and L. M. Sander, *Physical Review Letters*, 1986, **56**, 1264–1267.

[55] Y. Sawada, A. Dougherty, and J. P. Gollub, *Physical Review Letters*, 1986, **56**, 1260–1263.

[56] G. Marshall, F. Molina, and A. Soba, *Electrochimica Acta*, 2005, **50**, 3436–3445.

[57] T. A. Witten and L. M. Sander, *Physical Review B*, 1983, **27**, 5686–5697.

[58] L. P. Bicelli, B. Bozzini, C. Mele, and L. D'Urzo, *International Journal of Electrochemical Science*, 2008, **3**, 356–408.

[59] C. Lambert, P. Lauque, J.-L. Seguin, G. Albinet, M. Bendahan, J.-M. Debierre, and P. Knauth, *ChemPhysChem: A european journal of physical chemistry and chemical physics*, 2002, **3**, 107–110.

[60] M. Kozicki, M. Mitkova, and J. Aberouette, *Physica E*, 2003, **19**, 161–166.

[61] K. Peppler, C. Reitz, and J. Janek, *Applied Physics Letters*, 2008, **93**, 074104 (3 pages).

[62] M. Rohnke, T. Best, and J. Janek, *Journal of Solid State Electrochemistry*, 2005, **9**, 239–243.

[63] A. Spangenberg, J. Fleig, and J. Maier, *Advanced Materials*, 2001, **13**, 1466–1468.

[64] A. Spangenberg *Elektrochemische Untersuchungen an Silberchlorid mit Hilfe von Mikrokontakten und Rastersondenmethoden* PhD thesis, University Stuttgart, 2001.

[65] K. Peppler and J. Janek, *Solid State Ionics*, 2006, **177**, 1643–1648.

[66] A. Schroeder *Electrochemical Investigations of Silver Nanostructures* PhD thesis, Montanuniversity Leoben, 2004.

[67] J.-C. Bradley, H.-M. Chen, J. Crawford, J. Eckert, K. Ernazarova, T. Kurzeja, M. Lin, M. McGee, W. Nadler, and S. G. Stephens, *Nature*, 1997, **389**, 268–271.

[68] J. Nielsen and T. Jacobsen, *Solid State Ionics*, 2007, **178**, 1001–1009.

[69] J. Nielsen and T. Jacobsen, *Solid State Ionics*, 2007, **178**, 1769–1776.

[70] J. C. Bazan and L. E. Fasano, *Electrochimica Acta*, 1989, **34**, 309–312.

[71] J. C. Bazan and J. A. Schmidt, *Materials Chemistry and Physics*, 1990, **24**, 473–458.

[72] H. Rickert, *Einführung in die Elektrochemie fester Stoffe*, Springer Verlag, Berlin, Heidelberg, New York, 1973.

[73] H. Rickert, *Electrochemistry of Solids – An Introduction*, Springer Verlag, Berlin, Heidelberg, New York, 1982.

[74] L. Contreras and H. Rickert, *Berichte der Bunsengesellschaft: Physical Chemistry, Chemical Physics*, 1978, **82**, 292–297.

[75] J. Janek and S. Majoni, *Berichte der Bunsengesellschaft: Physical Chemistry, Chemical Physics*, 1995, **99**, 14–20.

[76] S. Majoni and J. Janek, *Berichte der Bunsengesellschaft: Physical Chemistry, Chemical Physics*, 1998, **102**, 756–762.

[77] R. Aogaki, K. Kitazawa, Y. Kose, and K. Fueki, *Electrochimica Acta*, 1980, **25**, 965–972.

[78] R. Aogaki and T. Makino, *Electrochimica Acta*, 1981, **26**, 1509–1517.

[79] J.-N. Chazalviel, *Physical Review A*, 1990, **42**, 7355.

[80] D. P. Barkey, R. H. Mueller, and C. W. Tobias, *Journal of The Electrochemical Society*, 1989, **136**, 2199–2207.

[81] D. P. Barkey, R. H. Mueller, and C. W. Tobias, *Journal of The Electrochemical Society*, 1989, **136**, 2207–2214.

[82] L.-G. Sundström and F. H. Bark, *Electrochimica Acta*, 1995, **40**, 599–614.

[83] S. Villain, P. Knauth, and G. Schwitzgebel, *Journal of Physical Chemistry B*, 1997, **101**, 7452–7454.

[84] D. Kolb, *Surface Science*, 2002, **500**, 722–740.

[85] R. D. Armstrong, T. Dickinson, H. R. Thirsk, and R. Whitfield, *Journal of Electroanalytical Chemistry*, 1971, **29**, 301–307.

[86] R. D. Armstrong, T. Dickinson, and P. M. Willis, *Electroanal Chem Inter Electrochem*, 1975, **59**, 281–293.

[87] J. Maier, *Festkörper - Fehler und Funktion – Prinzipien der Physikalischen Festkörperchemie*, Teubner Studienbücher, Stuttgart - Leibzig, 2000.

[88] J. Corish and C. O'Briain, *Journal of Crystal Growth*, 1972, **13/14**, 62–67.

[89] J. Corish and C. J. Warde, *Berichte der Bunsengesellschaft: Physical Chemistry, Chemical Physics*, 1978, **82**, 282–291.

[90] T. Ohachi and I. Taniguchi, *Journal of Crystal Growth*, 1972, **13/14**, 191–197.

[91] T. Ohachi and I. Taniguchi, *Journal of Crystal Growth*, 1974, **24/25**, 362–366.

[92] T. Ohachi *Solid State Ionics of Silver Compounds - Ionic and Electronic Properties of the High-Temperature Phase of Silver Compounds and their technological Applications* PhD thesis, Doshisha University, 1974.

[93] J. A. Schmidt, M. R. Prat, and J. C. Bazan, *Electrochimica Acta*, 1993, **38**, 577–580.

[94] G. I. Ostapenko, A. Cox, and L. A. Ostapenko, *Journal of Solid State Electrochemistry*, 2002, **6**, 245–252.

[95] G. I. Ostapenko, *Journal of Solid State Electrochemistry*, 2006, **10**, 91–95.

[96] J. Fleig and J. Maier, *Solid State Ionics*, 1996, **86-88**, 1351–1355.

[97] J. Fleig and J. Maier, *Solid State Ionics*, 1996, **85**, 9–15.

[98] J. Fleig, F. Noll, and J. Maier, *Berichte der Bunsengesellschaft: Physical Chemistry, Chemical Physics*, 1996, **100**, 607–615.

[99] J. Fleig and J. Maier, *Physical Chemistry Chemical Physics*, 1999, **1**, 3315–3320.

[100] J. Janek *Zum Ladungsdurchtritt an Phasengrenzen in Festkörpern* PhD thesis, University of Hannover, 1997.

[101] J. Fleig and J. Maier, *Solid State Ionics*, 1997, **94**, 199–207.

[102] J. Fleig and J. Maier, *Solid State Ionics*, 1996, **85**, 17–24.

[103] A. Schroeder, J. Fleig, H. Drings, R. Wuerschum, J. Maier, and W. Sitte, *Solid State Ionics*, 2004, **173**, 95–101.

[104] A. Schroeder, J. Fleig, D. Gryaznov, J. Maier, and W. Sitte, *Journal of Physical Chemistry B*, 2006, **110**, 12274–12280.

[105] P. Knauth, *Journal of Solid State Electrochemistry*, 2001, **5**, 107–111.

[106] K. Terabe, T. Nakayama, T. Hasegawa, and M. Aono, *Journal of Applied Physics*, 2002, **91**, 10110–10114.

[107] K. Terabe, T. Hasegawa, T. Nakayama, and M. Aono, *Nature*, 2005, **433**, 47–50.

[108] R. Oligschlaeger, R. Waser, R. Meyer, S. Karthäuser, and R. Dittmann, *Applied Physics Letters*, 2006, **88**, 042901.

[109] C. Liang, K. Terabe, T. Hasegawa, and M. Aono, *Nanotechnology*, 2007, **18**, 485202.

[110] D. Aurbach, I. Weissman, H. Yamin, and E. Elster, *Journal of The Electrochemical Society*, 1998, **145**, 1421–1426.

[111] D. Aurbach, E. Zinigrad, H. Teller, and P. Dan, *Journal of The Electrochemical Society*, 2000, **147**, 1274–1270.

[112] L. Gireaud, S. Grugeon, S. Laruelle, B. Yrieix, and J.-M. Tarascon, *Electrochemistry Communications*, 2006, **8**, 1639–1649.

[113] C. Brissot, M. Rosso, J.-N. Chazalviel, P. Baudry, and S. Lascaud, *Electrochimica Acta*, 1998, **43**, 1596–1574.

[114] C. Brissot, M. Rosso, J.-N. Chazalviel, and S. Lascaud, *Journal of The Electrochemical Society*, 1999, **146**, 4393–4400.

[115] A. Teyssot, R. B. Michel Rosso and, and S. Lascaud, *Solid State Ionics*, 2006, **177**, 141–143.

[116] M. Dolle, L. Sannier, B. Beaudoin, M. Trentin, and J.-M. Tarascon, *Electrochemical and Solid-State Letters*, 2002, **5**, A286–A289.

[117] M. Rosso, C. Brissot, A. Teyssot, M. Dolle, L. Sannier, J.-M. Tarascon, R. Bouchet, and S. Lascaud, *Electrochimica Acta*, 2006, **51**, 5334–5340.

[118] A. Brazier, L. Dupont, L. Dantras-Laffont, N. Kuwata, J. Kawamura, and J.-M. Tarascon, *Chemistry of Materials*, 2008, **20**, 2352–2359.

[119] C. Monroe and J. Newman, *Journal of The Electrochemical Society*, 2003, **150**, A1377–A1384.

[120] C. Monroe and J. Newman, *Journal of The Electrochemical Society*, 2005, **152**, A396–A404.

[121] J. Bates, N. Dudney, B. Neudecker, A. Ueda, and C. Evans, *Solid State Ionics*, 2000, **135**, 33–45.

[122] N. Dudney, *Materials Science and Engineering B*, 2005, **116**, 245–249.

[123] W.-Y. Liu, Z.-W. Fu, and Q.-Z. Qin, *Thin Solid Films*, 2007, **515**, 4045–4048.

[124] H. Rickert and H.-D. Wiemhöfer, *Solid State Ionics*, 1983, **11**, 257–268.

[125] R. Schuster, V. Kirchner, X. H. Xia, A. M. Bittner, and G. Ertl, *Physical Review Letters*, 1998, **80**, 5599–5602.

[126] R. Schuster, V. Kirchner, P. Allongue, and G. Ertl, *Science*, 2000, **289**, 98–101.

[127] R. Schuster and G. Ertl, Marcel Dekker, Inc., New York - Basel, 2003; chapter Electrochemical Nanostructuring of Surfaces, pp. 211–238.

[128] J. W. Schultze and A. Bressel, *Electrochimica Acta*, 2001, **47**, 3–21.

[129] K. Kamada, S. Yamashita, and Y. Matsumoto, *Journal of Materials Chemistry*, 2003, **13**, 1265–1268.

[130] M. Lee, R. O'Hayre, F. B. Prinz, and T. M. Gür, *Applied Physics Letters*, 2004, **85**, 3552–3554.

[131] B. H. Chudnovsky In *Proceedings of the 48th IEEE Holm Conference on Electrical Contacts*, pp. 140–150, 2002.

[132] P. S. Ho and T. Kwok, *Reports on Progress in Physics*, 1989, **52**, 301–348.

[133] K. Peppler and J. Janek, *Electrochimica Acta*, 2007, **53**, 319–323.

[134] H. Sone, T. Tamura, K. Miyazaki, and S. Hosaka, *Microelectronic Engineering*, 2006, **83**, 1487–1490.

3.1.2 Supplementary Classification

The main questions concerning the cathodic deposition of metals (in this work silver) on solid electrolytes are the morphology and the growth mechanism of these morphologies. The hypothesis that the growth of whiskers occurs at points where dislocations emerge at the surface of a solid electrolyte is based on the good agreement between whisker density in whisker arrays and typical dislocation densities in ionic crystals [Rohnke2005]. However, this hypothesis could neither be confirmed nor disproven in this work. But it has been shown that the morphology of the deposited silver depends strongly on experimental conditions, i. e. mainly cell geometry, temperature and current density. Previous to this work the deposition of silver at microelectrodes on solid electrolytes only in form of dendrites has been reported in literature [Spangenberg2001a, Spangenberg2001b, Schroeder2004]. In this work it has been shown that the deposition of silver at microelectrodes in form of whiskers is also possible, cf. chapter 2.1.2 on page 27. Further, the deposited dendrites consisted of whiskers which were physically connected, cf. chapter 2.1.3 on page 35. Additionally, a further morphology in form of thin silver films was observed, cf. chapter 2.2.1 on page 43. On the one hand the spectrum of known deposition morphologies was increased. And on the other hand the emergence of these different morphologies can be understood in a phenomenological way. But why these particular morphologies appear is still uncertain.

3.2 Outlook

3.2.1 Cathodic Deposition of Silver on Silver Bromide at Microelectrodes

In the present work cathodic metal deposition with the aid of the Prober Module Station PM8 from SUSS MicroTec (cf. experimental section in the article [Peppler2006b] in chapter 2.1.2 on page 27) has been carried out. Experiments still to be done with this experimental setup are detailed investigations of the "anisotropic" growth of dendrites on silver bromide single crystals with known orientations. One problem which cannot totally be solved is the temperature gradient across the sample due to the open cell assembly which is necessary in order to observe the deposition in situ. Thus, a thermovoltage is always present and has to be considered.

The major drawback of this experimental setup is the limitation of resolution due to the optical microscope. Thus, it was not possible to place the microelectrodes with high accuracy and observe the inital deposition of silver. In order to enhance the resolution and the positioning accuracy of the microelectrodes it is necessary to construct a new experimental setup. The High Resolution Scanning Electron Microscope LEO Gemini 982 existing in the Institute of Physical Chemistry of the Justus-Liebig-University provides this high resolution. Hence, a Prober Module suitable for electrochemical experiments

was purchased from Kammrath & Weiss GmbH and adapted. With this setup it should be possible to observe the cathodic deposition with high resolution. Thus, it should also be possible to observe the microstructure of whiskers without the deformation during microelectrode lift-off and preparation for SEM imaging. Additionally "microelectrodes" (with even smaller tip diameters) can be placed with an accuracy of 10 nm, because of the employment of piezo motors. First works have been carried out with this setup by Rabea Dippel during her Diploma Thesis.

3.2.2 Field driven Migration of Bipolar Metal Particles on Solid Electrolytes

It could be shown, that electronically isolated metal particles on solid parent metal electrolytes are sensitive to external electric fields. Clearly, the conducted experiments are only a beginning. Further work has to be done concerning the quality of the particles. It would be instructive to use defined particles with different sizes, geometries (circles, squares, rectangles, etc.) and thicknesses. Additionally, experiments at different temperatures and with various materials would be informative, too.

3.2.3 Template assisted Solid State Growth of Silver Micro- and Nanowires

The deposition of silver wires with predefined diameters on a template embedded electrolyte is possible. A further refinement could be the employment of templates with even smaller pore diameters in order to find out down to which diameter this method can be used. It would also be nice to embed a solid electrolyte which is a pure cation conductor, instead of the mixed ionic electronic conducting silver sulfide. Thus, the current would be converted entirely into a cation flux. In order to deposit other metals, different electrolytes with the according cation conduction have to be employed. The main problem will always be the embedding of the electrolyte because the pores of the template have to be filled completely to guarentee a continuous conduction path.

3.3 Summary

This work deals with the influence of experimental parameters on the cathodic deposition of silver on solid silver cation conductors. In order to investigate the cathodic deposition on solid electrolytes for "electrochemical micro- and nanostructuring" it is necessary to employ a relative simple model system. Hence, in this work the transference cell $(-)$Ag|AgBr(single crystal)|Ag$(+)$ in different configurations was used. The above mentioned single crystalline silver bromide as solid electrolyte has several advantages. It is stable at ambient conditions, even to irradiation with light. It exhibits only a marginal electronic conductivity, hence it is almost a pure silver cation conductor. Thus,

electronic current is converted fully into a cation current at the Ag|AgBr interface. The transference cell of the type $(-)\mathrm{Ag}|\mathrm{Ag_2S(polycrystalline)}|\mathrm{Ag}(+)$ was used for a special kind of electrolyte preparation, i. e. the embedding into a porous template material. Silver sulfide has the advantage of a relative easy fabrication which is favorable for filling pores of a template. But it is a mixed ionic and electronic conductor with a considerable deviation from stoichiometry. In equilibrium with silver (which is the case when in contact with an silver electrode at elevated temperatures) the transference number for electrons exeeds the transference number for silver cations considerably. Thus, electronic current is not converted fully into a cationic current at the $\mathrm{Ag}|\mathrm{Ag_2S}$ interface.

The present work is devided into three parts:

In chapter 2.1 (on page 27) the cathodic deposition of silver at microelectrodes on single crystalline silver bromide was dealt with. Depositions were carried out galvanostatically in order to get constant deposition rates of silver. Two different morphologies of the silver deposits were observed. At "low" current densities ($j < 0.1$ A/cm^2; $I < 0.5$ µA, d(Ag-microelectrode) = 25 µm) growth in height (perpendicular to the electrolyte surface) in form of whiskers was observed. In this case the flexible microelectrodes were pushed up by the growing whiskers. At "high" current densities ($j > 0.6$ A/cm^2; $I >$ 3.0 µA, d(Ag-microelectrode) = 25 µm) growth parallel to the electrolyte surface in form of dendrites was observed. Variation of temperature caused a considerable change in morphology. The diameters of whiskers decreased from a few micrometers to several hundreds of nanometers at a decrease of temperature from $\theta = 300$ ℃ to $\theta = 150$ ℃. Dendrites changed from an "isotropic" form to an "anisotropic" morphology with preferential growth in two directions (presumably along designated crystallographic directions of the electrolyte). These "anisotropic" dendrites consisted of whiskers connected to each other. This temperature dependence of morphology is related to the nucleation rate.

In chapter 2.2 (on page 43) the stability of as-deposited electronically isolated metal particles in external electric fields was treated. In the last years the application of solid state ionics in future memory devices has been investigated, e. g. the switching between two resistive states by cathodic metal deposition and subsequent dissolution. Thus, the stability of as-deposited metal is an issue which has to be considered. It could be shown that electronically (but not ionically) isolated silver metal particles on a solid silver cation conductor behaved as bipolar electrodes when put in an external electric field. They were dissolved at the anodic side, and silver was deposited at their cathodic side. The deposition occurred neither in form of whiskers nor dendrites, but as a thin film. This is a new kind of deposition morphology for silver on solid silver electrolytes.

In chapter 2.3 (on page 49) the deposition of silver in the form of wires with predefined diameters was reported. The cathodic deposition of silver on silver bromide at microelectrodes yielded whiskers with different diameters, depending on experimental

conditions. But in this case the diameter could not be predicted prior to the experiment. In order to obtain silver microwires (i. e. whiskers) with predefined diameters it was necessary to embed the electrolyte in a porous template with straight cylindrical pores. As templates porous silicon and porous alumina were used. The pores were filled with silver sulfide by a simple chemical reaction of silver and sulfur. Subsequent electrodeposition led to silver wires with the same diameter as the pores of the template.

Finally, this work was concluded by a classification (chapter 3.1 on page 59) and an outlook (chapter 3.2 on page 91).

References outside Articles

[Armstrong1971] Armstrong, R. D.; Dickinson, T.; Thirsk, H. R. and Whitfield, R.; The Kinetics of Silver|Silver Rubidiumiodide electrode; *Journal of Electroanalytical Chemistry*, **29** (1971) 301–307

[Armstrong1973] Armstrong, R. D.; Dickinson, T. and Willis, P. M.; The Impedance of the Pt|Ag_4RbI_5 and C|Ag_4RbI_5 Interphases at Anodic Potentials; *Journal of Electroanalytical Chemistry* **48** (1973) 47–53

[Armstrong1975] Armstrong, R. D.; Dickinson, T. and Willis, P. M.; Silver deposition from Silver Rubidium Iodide; *Electroanalytical Chemistry and Interfacial Electrochemistry* **59** (1975) 281–293

[Best2001] Best, T.; Beobachtung der Metallabscheidung aus silberionenleitenden Festelektrolyten; Master's Thesis, Justus-Liebig-University Giessen, 2001

[Budevski1996] Budevski, E.; Staikov, G. and Lorenz, W. J.; *Electrochemical Phase Formation and Growth*; VCH, Weinheim, 1996

[Corish1972] Corish, J. and O'Briain, C. D.; The Growth and Dissolution of Silver Whiskers; *Journal of Crystal Growth*, **13/14** (1972) 62–67

[Corish1978] Corish, J. and Warde, C. J.; Electrochemical Transfer across Phase Boundaries; *Berichte der Bunsengesellschaft: Physical Chemistry, Chemical Physics*, **82** (1978) 282–291

[Fleig2003] Fleig, J.; Microelectrodes in Solid State Ionics; *Solid State Ionics*, **161** (2003) 279–289

[Giber1982] Mezey, L. Z. and Giber, J.; The Surface Free Energies of solid chemical Elements: Calculation from internal Free Enthalpies of Atomization; *Japanese Journal of Applied Physics*, **21** (1982) 1569–1571

[Majoni1995] Janek, J. and Majoni, S.; Investigation of Charge Transport across the Ag|AgI-Interface: (I) Occurence of periodic Phenomena during anodic Dissolution of Silver; *Berichte der Bunsengesellschaft: Physical Chemistry, Chemical Physics*, **99** (1995) 14–20

[Ohachi1972] Ohachi, T. and Taniguchi, I.; Controlled filamentary Growth of Silver from Silver Compounds; *Journal of Crystal Growth*, **13/14** (1972) 191–197

[Ohachi1974a] Ohachi, T. and Taniguchi, I.; The Growth and Morphology of Silver Whiskers; *Journal of Crystal Growth*, **24/25** (1974) 362–366

[Ohachi1974b] Ohachi, T.; *Solid State Ionics of Silver Compounds - Ionic and Electronic Properties of the High-Temperature Phase of Silver Compounds and their technological Applications*; Ph. D. Thesis, Doshisha University, 1974

[Peppler2006a] Peppler, K.; Pölleth, M.; Meiss, S.; Rohnke, M. and Janek, J.; Electrodeposition of Metals for Micro- and Nanostructuring at Interfaces between solid, liquid and gaseous Conductors: Dendrites, Whiskers and Nanoparticles; *Zeitschrift für Physikalische Chemie*, **220** (2006) 1507–1527

[Peppler2006b] Peppler, K. and Janek, J.; Cathodic Deposition of Silver on Silver Bromide at Microelectrodes; *Solid State Ionics*, **177** (2006) 1643–1648

[Peppler2007] Peppler, K. and Janek, J.; Template assisted Solid State electrochemical Growth of Silver Micro- and Nanowires; *Electrochimica Acta*, **53** (2007) 319–323

[Peppler2008] Peppler, K.; C. Reitz, and Janek, J.; Field driven Migration of bipolar Metal Particles on Solid Electrolytes; *Applied Physics Letters*, **93** (2008) 074104 (3 pages)

[Peppler2009] Peppler, K. and Janek, J.; Electrodeposition of Metals on Solid Electrolytes; *Manuscript*, 2009

[Rohnke2005] Rohnke, M.; Best, T. and Janek, J.; Controlled electrochemical Growth of Silver Microwires; *Journal of Solid State Electrochemistry*, **9** (2005) 239–243

[Schroeder2004] Schroeder, A.; *Electrochemical Investigations of Silver Nanostructures*; Ph. D. Thesis, Montanuniversität Leoben and Max-Planck-Institut für Festkörperforschung Stuttgart, 2004

[Sickenius2003] Sickenius, B. T.; Experimentelle Untersuchungen zum Whiskerwachstum auf Silberhalogeniden; Diploma Thesis, Justus-Liebig-University Giessen, 2003.

[Spangenberg2001a] Spangenberg, A.; Fleig, J. and Maier, J.; Electrochemical Writing on Silver Ion Conductors; *Advanced Materials*, **13** (2001) 1466–1468

[Spangenberg2001b] Spangenberg, A.; *Elektrochemische Untersuchungen an Silberchlorid mit Hilfe von Mikrokontakten und Rastersondenmethoden*; Ph. D. Thesis, Universität Stuttgart and Max-Planck-Institut für Festkörperforschung Stuttgart, 2001

Appendix

List of Publications included in this Thesis

Peppler, Klaus; Janek, Jürgen:
Electrodeposition of metals on solid electrolytes.
Manuscript (2009)

Peppler, Klaus; Reitz, Christian; Janek, Jürgen:
Field driven migration of bipolar metal particles on solid electrolytes.
Applied Physics Letters **93** (2008) 074104
DOI 10.1063/1.2973042
Reprinted with permission from American Institute of Physics.

Peppler, Klaus; Janek, Jürgen:
Template assisted solid state electrochemical growth of silver micro- and nanowires.
Electrochimica Acta **53** (2007) 319–323
DOI 10.1016/j.electacta.2006.12.054
Reprinted from with permission from Elsevier.

Peppler, Klaus; Pölleth, Manuel; Meiss, Sebastian; Rohnke, Marcus; Janek, Jürgen:
Electrodeposition of Metals for Micro- and Nanostructuring at Interfaces between Solid, Liquid and Gaseous Conductors: Dendrites, Whiskers and Nanoparticles.
Zeitschrift für Physikalische Chemie **220** (2006) 1507–1527
DOI 10.1524/zpch.2006.220.10.1507
Reprinted with permission from Oldenbourg Wissenschaftsverlag.

Peppler, Klaus; Janek, Jürgen:
Cathodic deposition of silver on silver bromide at microelectrodes.
Solid State Ionics **177** (2006) 1643–1648
DOI 10.1016/j.ssi.2005.12.012
Reprinted from with permission from Elsevier.

List of Presentations

Oral Presentations

Bunsentagung 2007

17th–19th May 2007 in Graz (Austria)

Klaus Peppler and Jürgen Janek

Electrochemical Fabrication of Silver Micro- and Nanowires by Cathodic Deposition on Solid Electrolytes

Jahrestagung der GDCh-Fachgruppe Angewandte Elektrochemie 2006

9th–11th September 2006 in Bayreuth (Germany)

Klaus Peppler and Jürgen Janek

Templatunterstützte kathodische Abscheidung von Mikro- und Nanodrähten aus Festelektrolyten

6th International Symposium on Electrochemical Micro- & Nanosystems Technology

22nd–25th August 2006 in Bonn (Germany)

Klaus Peppler and Jürgen Janek

Template-assisted Solid State Electrochemical Growth of Silver Micro- and Nanowires

15th International Conference on Solid State Ionics

17th–22nd July 2005 in Baden-Baden (Germany)

Klaus Peppler, Marcus Rohnke, Jürgen Janek

Spatially Restricted Electrocrystallisation of Silver on Silver Ion Conductors

Poster Contributions

Electrochemistry - Crossing boundaries

6th–8th October 2008 in Giessen (Germany)

Klaus Peppler, Christian Reitz, Rabea Dippel and Jürgen Janek

Application of Microelectrodes in Solid State Electrochemistry: Electrodeposition of Metals

99th Bunsen Colloquium "Solid State Reactivity - From macro to nano"

In Honour of the 75th Birthday of Hermann Schmalzried

7th–9th June 2007 in Monastery Eberbach (Germany)

Klaus Peppler and Jürgen Janek

Cathodic Deposition of Silver on Silver Ion Conductors at Microelectrodes

Bunsentagung 2005

5th–7th May 2005 in Frankfurt (Germany)

Klaus Peppler, Marcus Rohnke and Jürgen Janek

Spatially restricted Electrocrystallization of Silver on Silver Ion Conductors

Bunsentagung 2004

20th–22nd May 2004 in Dresden (Germany)

Klaus Peppler, Bernd T. Sickenius, Timo Best, Marcus Rohnke and Jürgen Janek

Electrocrystallization of Silver on Silver Bromide Single Crystal Surfaces

Der Lebenslauf wurde aus der elektronischen Version der Arbeit entfernt.

The curriculum vitae was removed from the electronic version of the paper.